CHARACTERIZATION OF ATMOSPHERIC PARTICULATE MATTER AT E-WASTE LANDFILL SITE IN AGBOGBLOSHIE, ACCRA

A dissertation presented to the:
Department of NUCLEAR SCIENCES AND APPLICATIONS

SCHOOL OF NUCLEAR AND ALLIED SCIENCES

COLLEGE OF BASIC AND APPLIED SCIENCES

UNIVERSITY OF GHANA

by

Hyacinthe Ahiamadjie (ID: 10235632)
BSc (Cape Coast), 2005
MPhil (Legon), 2008

In partial fulfillment of the requirements for the degree of
DOCTOR OF PHILOSOPHY

in

APPLIED NUCLEAR PHYSICS

2017

Declaration

This thesis is the result of research work undertaken by Hyacinthe Ahiamadjie in the Department of Nuclear Sciences and Applications, School of Nuclear and Allied Sciences, University of Ghana, under the supervision of Rev. Dr Samuel Akoto-Bamford (SNAS, UG-Legon, Ghana) and Prof. Innocent Joy Kwame Aboh (NRA, Accra-Ghana).

Sign: ....

Hyacinthe Ahiamadjie
(Student)

Sign:	Sign: ....
Rev. Dr Samuel Akoto-Bamford (Supervisor)	Prof. Innocent Joy Kwame Aboh (Co-Supervisor)

This thesis is dedicated to the Almighty God and to the blessed memory of my mother Mercy Aku Dedoo . . .

Acknowledgements

First and foremost, I am most grateful to the Almighty God for bringing me this far by ordering my footsteps and for His abundant grace through these years. May His name be glorified forever. In a special way, I wish to express my sincere gratitude to all my supervisors, Rev. Dr. S.A. Bamford and Prof. I.J.K. Aboh for their support, guidance, encouragement and for believing in me. My sincere thanks go to Dr. Christian K. Nuviadenu for his help during the analysis of the samples, teaching of latex and Proof reading of my thesis. I find it appropriate to acknowledge you, Dr C.K. Nuviadenu really made my life easier. May the Lord bless you. Special thanks to my colleagues and friends and Prof. G.K. Banini (our Manager) at the Accelerator Research Center (ARC) of GAEC for their encouragements and support. I wish to single out Dr. Joseph B. Tandoh, Dr. Oscar K. Adukpo, Dr. Amos Forson, and Dr. Owiredu Gyampo for their assistance throughout the writing period. Finally I wish to express my heartfelt gratitude to my dear wife Evelyn and our children Fafali and Kekeli for lending their support and care throughout this study.

Abbreviations

ADC	Analogue-to-Digital Converter
APM	Atmospheric Particulate Matter
AQG	Air Quality Guidelines
ARC	Accelerator Research Centre
CA	Cluster Analysis
CBD	Central Business District
CFC	Charge-Frequency-Converter
DF	Deposited Fraction
EF	Enrichment Factor
EIA	Environment Impact Assessment
EMP	Environmental Management Plan
EDXRF	Energy Dispersive X-ray Fluorescence
EDPXRF	Energy Dispersive Polarised X-ray Fluorescence
EU-Dir	European Union Directorate
EPA	Environmental Protection Agency
e-waste	Electronic and Electrical Waste
GASDA	Greater Accra Scrap Dealers Association
Gmet	Ghana Meteorological Service
IBA	Ion Beam Analysis
IF	Inhalable Fraction
IAEA	International Atomic Energy Agency
LI	Legislation Instrument

NRA	Nuclear Regulatory Authority
NILU	Norwegian Institute for Air Research
INFN	National Institute of Nuclear Physics
MCA	Multichannel Analyser
NSAP	Nuclear Science and Applications
SDD	Silicon Drift Detectors
PCA	Principal Component Analysis
PIGE	Particle Induced Gamma-ray Emission
PIXE	Particle Induced X-ray Emission
PM	Particulate Matter
PMF	Positive Matrix Factorization
SFU	Stack Filter Unit
SRM	Standard Reference Material
SNAS	School Of Nuclear and Allied Sciences
UG	University of Ghana
UG	University of Gent
UK	United Kingdom
UNEP	United Nations Environment Programme
USAID	United States Agency for International Development
USEPA	United States Environmental Protection Agency
WHO	World Health Organization
XRF	X-Ray Fluorescence

Table of Contents

List of Tables

List of Figures

Physical Constants

Constant Name	Symbol	=	Constant Value (with units)
Acceleration due to gravity	g	=	$9.8m/s^2$
Universal Gas constant	R	=	$8.314kJ/K/mol$
pi	π	$= 8.314$	

Symbols

Symbol	Name	
σ	Standard deviation	
θ	Potential Temperature	
ϵ	virtual source matrix	
β	Entrainment parameter	
ρ	Density	kg/m^3

Abstract

A year-long investigation has been carried out on atmospheric particulate matter (APM). Elemental composition,mass concentration, sources contributions and their fingerprints were determined in APM samples collected, in Agbogbloshie scrap market, between May 2010 and April 2011. $PM_{2.5}$ and $PM_{102.5}$ size fractions of APM were collected 24-hourly on 47 mm diameter nuclepore filters of pore sizes 0.4 µm and 8 µm respectively, using the Gent sampler. Gravimetric analyses were carried out to determine the APM mass concentrations. The minimum, maximum and annual mean mass concentration values for $PM_{2.5}$ obtained for the sampling site throughout the period of investigation were 35.43 ($\mu g/cm^3$), 349.68 ($\mu g/cm^3$) and 88.62 ($\mu g/cm^3$) respectively. For $PM_{10-2.5}$, the minimum, maximum and annual mean mass concentration values obtained were 76.83($\mu g/cm^3$), 448.67 ($\mu g/cm^3$) and 138.31 ($\mu g/cm^3$) respectively. These measured concentration levels are all substantially higher than the WHO, USEPA, EU, JAPAN EQS, UK National Air quality objective, World Bank and Canada air quality standards. Particle Induced X-Ray Emmission (PIXE), Particle Induced Gamma Emmission (PIGE) and Energy Dispersive X-Ray Fluorescence (EDXRF) were used to determine elemental composition and concentration of the atmospheric particulate matter. The five most abundant elements in coarse fraction $PM_{102.5}$ are Si average 6545.05 (range: 261.3359950.56) ngm^{-3}, Al average 3743.25 (range: 218.9424719.25) ngm^{-3}, Fe average

2464.77 (range: 182.0818982.45) ngm^{-3} , Cl average 5918.47 (range: 587.76 15796.13) ngm^{-3}, Na average 4040.17, (range: 418.2515010.32) ngm^{-3}. In the fine fraction ($PM_{2.5}$) concentrations reordered were in the following order: Si average 5466.44 (range: 1339.9361029.16) ngm^{-3} , Al average 3073.44 (range: 888.7425389.05) ngm^{-3}, Fe average 1877.57 (range : 769.2819569.65) ngm^{-3}, Cl average 4972.86 (range: 1533.3616741.73) ngm^{-3}, Na average 3163.27 (range: 1295.1515887.22) ngm^{-3}. Enrichment Factor evaluation was first used as one of the means to separate elements in terms of natural and anthropogenic sources. PMF was employed in fingerprint and source contributions identifications, PMF resolved five sources each for both $PM_{2.5}$ and PM_{10-25}. The following sources were identified for the $PM_{2.5}$:E-waste burning (49%), Industrial activities (23%), vehicular traffic (16%), resuspended dust (7%) and sea spray (5%). In the coarse fraction, soil dust (45%),biomass burning (17%), Heavy oil burning (16%),sea spray (12%) and e-waste burning (10%) were apportioned. Natural sources (45%) were the major contributors in the coarse fraction while anthropogenic sources(88%) were the major contributors in the fine fraction. E-waste burning contributions were identified in both fractions. In this work, the following elements (Zn, As, Br, Sn, Cd, Hg, Pb) have been identified as fingerprint for e-waste burning and this source contributed 49% of the pollutants identified in the study area.

Chapter 1

Chapter 1: General Introduction

The advances in information technology and demand for electronic and electrical gadgets have increased astronomical, and however the disposal of used and obsolete equipment is becoming global issues. Since in the third world countries, disposal of e-waste has become a huge challenge, people turn to openly burn the e-waste, since we do not have any proper regulation on how to dispose of e-waste. However anytime e-waste is burned, it emits toxic fumes into the air. Air pollution occurs when solid, liquid and gaseous materials have been emitted into air environment. The emission can originate from stationary or mobile sources and can sometimes involve chemical or/and physical transformations before being returned to surfaces such as the soil, plants, trees, monuments, buildings etc...(Bandyopadhyay, 2010).

Particles exist in the environment as the suspensions in air and are commonly called aerosol. Solid particles and liquid droplets are combined in the atmosphere to form an aerosol. The aerosol particles have a very wide size range from molecular clusters of 0.001 µm to fog and dust particles as large as few hundred micrometers. Particulate Matters are always grouped into two main particulate matter size fractions: coarse $PM_{10-2.5}$ and fine $PM_{2.5}$ (PM <10 and 2.5 µm in aerodynamic diameter, respectively). The depth of PM deposition in the humans respiratory system is determined by size of the particles. Also the impact of the PM on humans depend on the size. The smaller the PM the more dangerous is to humans. The origin of the particles could be from natural process (e.g sea spray, dust etc....) or from man made processes also known as anthropogenic process (vehicle emission, emission from industry, e-waste burning, waste incineration etc....). Aerosol particles in the atmosphere are caused by wide range of sources and have diverse compositions and characteristics. As a result,the effects of aerosol particles on the environment and humans are many and varied. Some of the effect could just be a nuisance like dust deposited on clean surface to serious climatic effect like environmental degradation, acid rains, impact on climate, impact on humans and animal health. The fine particles are more hazardous, it is due to the size and morphology. Thus $PM_{2.5}$:

- can easily traveled over long distances far away from the pollution sources
- can easily be inhaled and deposited in the lower part of the human respiratory tract
- have a larger surface area per unit mass and hence higher ability to absorb gas molecules and transport them to any part of the respiratory system to catalyze chemical and biochemical reactions
- consist of large soluble fraction

The coarse fraction includes particles greater than 2.5 µm which are usually released directly into the atmosphere by mechanical processes or from natural sources. $PM_{10-2.5}$ can not be transported beyond our upper part of the human respiratory tract (the nose and throat), it is impossible for $PM_{10-2.5}$ to reach the lungs (Hinds, 2012) (Smolders et al., 2008). Particle size is one of the most important parameter in characterizing the physical behaviour of particulate matter. The size of a particle affects many of its properties such as volume, mass and settling velocity. Size also influences a particles transport, deposition and migration through the environment. Also concentration of particulate matter dependent on these factors: weather patterns, wind, stability (vertical movement of air), turbulence, precipitation, topography, and smokestack height and temperature of gases toxic (Hinds, 2012) (Smolders et al., 2008).

1.1 What is the current situation of air pollution in Ghana?

Since the establishment of the Environmental Protection Council in 1974, government of Ghana has been working very hard to achieve air quality management strategy for Ghana. Government of Ghana has made it a general requirement by law, for new businesses to provide an environment impact assessment (EIA) and for the existing ones to provide environmental management plan (EMP). National environmental standards to serve as guideline for compliance have also been introduced. For some specific sources however additional legislation have been put in place to control their emission. Government of Ghana has approved a legislation instrument LI 1732 to ban the activities of leaded gasoline in the system since January 2004. The Environmental Protection Agency of Ghana has been doing a lot of collaborated research works with the United States Agencies in charge of environmental issues, In march 2005 and December 2008 results were found that emissions from vehicles exhaust, uncontrolled burning of waste (domestic and industrial), industrial emission sources, domestic cooking, commercial activities and wind-blown dust are the major contributors to the air quality. A lot of studies have been conducted by both researchers and students on issues pertaining to air in Ghana (Aboh et al., 2009) (Atiemo et al., 2012) (Ofosu et al.,) (Ofosu et al., 2012). Despite various legislative mechanisms being in place and with all these researches, we are still not able to have regular and systematic air quality monitoring for air quality assessment because our information on the concentrations as well as the characteristics of atmospheric particulate matter is still not enough to do extensive work. Some works have been done on the PM_{10} particulate in some major cities in Ghana by the Environmental Protection Authority of Ghana (EPA-Ghana),but that of fine particulate there is no records because air quality standard for $PM_{2.5}$ has not been established in Ghana.

1.2 Problem statement

E-waste burning is one of the major processes in the exploitation of e-waste at the landfill sites. Consequently contribution of e-waste burning to air pollution has become one of the most serious environmental concerns in most cities throughout the world especially in developing countries (Diaz-Barriga, 2013) (Needhidasan et al., 2014) (Modak, 2010) (Samson, 2009). Ewaste particulate matter is on the rise in sub-Saharan Africa. Rise in the e-waste burning at Agbogbloshie has led to emission of air borne particulate matter into the ambient environment. A lot of works have been done in other media of pollution such as soil, water etc.... Nevertheless no data on environmental pollution impact of e-waste burning on ambient air quality. No comprehensive study on the nature of atmospheric particulate matter (APM), their concentration levels and sources of emission. In the absent of such data no effective management and mitigation procedures can be implemented. In order to assess and to lessen the impacts of e-waste particulate matter pollution, any program aimed at regulating the levels of particles in the urban atmosphere through generating knowledge on the size distribution, chemical composition and sources of aerosol particles.

1.3 Current situation at Agbogloshie

The Agbogbloshie scrap yard, as shown in figure 1.1, is located on a flat ground along the side of the Odaw River, and of the Korle Lagoon in Accra. Agbogbloshie has two major recycling sites. The main recycling site is close to the South Industrial area at bank of the Odaw River. The other recycling site is located north of the Korle lagoon. Agbogbloshie scrap yard is adjacent to the food market, a market where onion, tomato and yam are sold to the growing urban population of Accra. Proximate to the scrap yard are also food joints. Apart from these, there are also other informal activities proliferating near the scrap yard including women selling used clothes. There are also artisans who use metallic materials from the scrap to make coal pots cooking and grilling pots etc. These activities are flourishing along the road connecting Agbogbloshie to the Central Business District. The growing tendencies of the informal activities nearby the scrap yard have led to overcrowding and traffic jams in Agbogbloshie. The Agbogbloshie scrap yard is also adjacent to some large formal industrial enterprises such as brewing, paint manufacturing, engineering etc. There are some banking institutions Merchant Bank, Eco bank and micro finance institutions operating in the area close to the scrap yard. The two major recycling sites are in close proximity to the slum (popularly called Sodom and Gomorra) which serves as dwelling place for the e-waste workers and other traders in the area. The slum is known to be the largest and the most notorious slum in Ghana housing about 79,684 people. Agbogbloshie, like most (sub)-urban areas in Ghana has no structured ewaste disposal. Scrap dealers have traditionally relied on open burning as means of recycling or disposal of e-waste. Open burning of e-waste emits particulate matter into the air. Air pollution occurs when a chemical or substance enters the atmosphere; it could be harmful to the health of humans and animals or cause damage to plants and materials. Since Agbogbloshie is closed to the urban cities, there is the need to assess the health impact from the e-waste site on the inhabitants in the city. For that matter, there is need to do detailed work to determine the percentage contribution of e-waste burning in Agbogbloshie.

For the characterization or measurement of aerosols elemental and trace

Figure 1.1: Location Map of Agbogbloshie

composition, etc. numerous analytical techniques can be employed for the analysis, however, the chosen technique must have the following qualities: for its sensitivity, multi-elemental capability, non-destructiveness, and the accuracy of the information it provides over the rest. Ion Beam Analysis (IBA) can best be described to have all the stated qualities above. IBA is capable of providing a wide range of information on aerosol samples collected at Agbogbloshie; however, it requires statistical tools to link them to, and disentangle the pollution sources from which they emanate. Key among such tools is positive matrix factorization (PMF) method for pollution sources identification (speciation) and the apportionment of their contributions as one of the key subjects of this thesis.

1.4 Objectives

The main objective of this work is to assess the effect of e-waste burning at the landfill sites at Agbogbloshie on the ambient air quality. Specifically this work seeks to:

1. Identify particle composition of APM and assess their compliance to air quality criteria.
2. Derive the source profile or finger print of pollutants associated with e-waste burning.

3. Carry out source apportionment in order to determine relative contribution of identified pollutants.

The outcome of this work will be contribution to the already existing public debate on the air pollution issues,and it will go a long way in helping the agencies responsible for drafting pollution levels policies, protecting the public health, and managing environmental pollution.

1.5 Scope of the project

In this work, the Gent Stack Filter Unit (SFU) sampler and nuclepore filters were used for almost two years, that is from May 2010 to August 2011 continuously to sample for both fine $PM_{2.5}$ and coarse $PM_{10-2.5}$ fractions of particulate matter (PM) at Agbogbloshie. Daily PM concentration was done using micro-sensitive balance as mean of the determining gravimetric analysis. The techniques employed in the determination of the elemental concentration : Particle Induced X-ray Emission (PIXE), Particle Induced Gamma-ray Emission (PIGE), and Energy Dispersive Polarised X-ray Fluorescence (EDPXRF). These techniques were used to help in the characterization of aerosol in the Agbogbloshie e-waste burning sites. To determine factors and sources that contribute to the deterioration of the air quality in Agblogloshie, Positive Matrices Factorization(PMF) and Enrichment

Factor (EF) are employed on both the mass and elemental concentration data.

1.6 Challenges of the project

Levels of particles in the atmosphere are not solely dependent on the emission rates of particles, no matter how well characterised, but meteorological factors played a very important role. Any change in parameters like wind speed, temperature, relative humidity, and precipitation, along with terrain and geographical factors, demands many measurements in space and time before levels can be adequately characterized for health and welfare. Knowledge on any changes occurring in the meteorology will enable us derive a better explanation of the source-to-concentration relationship. In this work, due to lack of needed instrument, meteorology data could not be obtained at the site. The data were then supplied by the meteorological station (the Ghana Meteorological Service (Gmet)) is in Accra. Erratic power supply and and equipment breakdowns did not allow continuous sampling over the entire duration.

1.7 Overview of the thesis

The thesis comprises five chapters. Chapter 1 provides an overall introduction and briefly describes particulate matter PM, its health problems, status of the air pollution in the country, the objectives of the study, scope of the project and the challenges face throughout the project.The second chapter provides background information on the urban nature of PM, sources, health and environmental effects, air quality monitoring and the various techniques available, meteorological parameters and relevant air-quality guidelines and standards. Chapter 3 describes the monitoring site, the criteria applied, the approach used and the sampling plan and presents in detail the sampling methodology adopted as well as the chosen monitoring methods. In Chapter 4, the results of PM_{10} and $PM_{2.5}$ and their implications are explored and discussed in comparison with national and international annual guideline values. Chapter 5 presents the final conclusions from the thesis together with recommendations for monitoring PM in urban areas and possible issues for further research.

Chapter 2

Chapter 2: Literature Review

Particulate matter PM is one of the most dangerous forms of air pollution. United States Environmental Protection Agency USEPA, described PM as combination of solid particles and liquid droplets formed in the atmosphere (Hinds, 2012), variable in size and chemical constituents (Murray et al., 2010). These are particles that are small enough to remain air-borne for an extended time, for example hours or days and that can travel considerable distances from their sources. For sake of Research PM have been grouped into two main particulate matter size fractions: PM_{10} and fine $PM2.5$ (PM <10 and 2.5µm in aerodynamic diameter, respectively) (Balakrishnaiah et al., 2011) (Ostro et al., 2011). The size of particles play a major role in both transportation and health effect in humans. Mostly fine particle (<2.5 µm) and especially ultra fine (<0.1 µm). They are able to travel to deeper areas of the lung. Both fine and ultra fine come as result of combustion sources,they have a stronger association with adverse health effects than coarse particles. (Hinds, 2012) (Smolders et al., 2008) ((Bezemer, 2009), (Nel, 2005), (Oberdörster et al., 1995), (Oberdörster and Utell, 2002), (Utell and Frampton, 2000), (Peters et al., 1997), (Samet et al., 2000). Coarse particles can not go further than the area of the nose and throat.

According to this research work (Smolders et al., 2008) Fine particles are present in greater numbers and have greater surface area than larger particles of the same mass, and they are generally considered to be more toxic.

2.1 Work done on APM in Africa

The causes of air pollution in many urban cities in developing countries can be attributed to multiple sources. Air pollution can be transported over long distances and have impacts far from their point of emission. Most of the cities in the developing countries are now experiencing similar air pollution problems, especially anthropogenic particulate matter arising from the rapid growth of vehicle traffic, open waste burning, and the presence of major industries close to residential areas. In the areas of air pollution studies in Africa, some works have been done, however level of studies so far is still in its infancy. Only a few source apportionment studies of particulate matter have been carried out in Africa countries. Chemical characteristics and source apportionment of particulate matter using receptor modelling have been studied in South Africa (Engelbrecht et al., 2001), (Kgabi, 2010), Ghana and Gambia (Zhou et al., 2013), (Zhou et al., 2014), Nigeria (Oluyemi and Asubiojo, 2001) , Tanzania (Bennet et al., 2005), (Mkoma et al., 2010), Ethiopia (Etyemezian et al., 2005) and Benin(Fourn and Fayomi, 2006). Some studies were carried out in the characterization of APM and their sources in some parts (cities) of the country in the past years, their findings have shown the presence of different sources. These sources were emissions from exhaust vehicles, burning of waste and other material openly, industrial emissions sources, domestic cooking, commercial activities and wind-blown dust are the major contributors to the air quality measured at the monitoring sites.(Aboh, 2000), (Ofosu et al., 2012). The outcome of their findings revealed that there were high particulate matter concentrations in the most of the areas. In the wet season, APM concentration recorded were very low as compared to the concentration of APM recorded in the harmattan period.

2.2 Characteristics of particulate matter

2.2.1 Size distribution

Size is the single most important determinant of the properties of particles and it has implications on formation, physical and chemical properties, transformation, transport, and removal of particles from the atmosphere (Vallius, 2005).The size of particle also plays the most important role in the understanding of the deposition in the human respiratory system. Work done by both Finlayson Pitts and Pitts in 1986 and Seinfeld and Pandis in 1998 described the various changes that occurred when a particle is emitted into the atmosphere (Seinfeld and Pandis, 2016), (Finlayson-Pitts and Pitts Jr, 1986). They have also shown that there were a change in the size and the chemical composition by processes like condensation of vapour species, evaporation, deposition (both wet and dry) and coagulation. The chemical compositions of these particles are determinants for the types of effects caused by particulate matter on humans, vegetation, and materials. Characterization of the physical behaviour of particulate matter depends greatly on the size of the Particle. Properties such as as volume, mass, settling velocity,transport, deposition and migration through the environment are affected by the size of a particle (Aboh, 2000), (Angle, 2014). Particles can be classified by their physical size; the size is from a few nanometres (nm) to tens of micrometres µm in diameter (Mkoma, 2008). Particle size is a very important factor when related to health and environmental effects (Grover, 2006). According to Finlayson-Pitts and Pitts particulate matter of the size range from 0.1 to 10 µm is noted to have serious health, climatic and environmental effects (Finlayson-Pitts and Pitts Jr, 1999). The most commonly used definition of particle diameter is the aerodynamic diameter. Aerodynamic diameter (D_p) compares the terminal falling speed of the particle under consideration with a spherical particle that has a density of 1gcm3 (Finlayson-Pitts and Pitts Jr, 1999), (Hinds, 2012).

$$D_p = D_g k \sqrt{\frac{\rho_p}{\rho_o}} \tag{2.1}$$

where D_g is the particle geometric diameter,ρ_p is the density of the particle,ρ_o is the reference density (1gcm3),and k is a shape factor,which is 1.0 in the case of a sphere (Finlayson-Pitts and Pitts Jr, 1999).In this work,particle diameter unless otherwise indicated,refers to the aerodynamic diameter.

2.2.2 Different modes of formation

For instance, the life time of particulate matter is defined by the size of the aerosol particles. Particle size formations are mostly classified in three major groups, they are nuclei- (6 0.1µm), accumulation (0.1-2.5 µm), and coarse particle-mode (2.5-100 µm). When primary and secondary particles are found close to their emission sources that process can be described as the nuclei mode (also known as Atiken mode), examples of these primary pollutants are carbonaceous dusts and sulphur dioxide (SO_2) (Foltescu, 1995), (Hinds, 2012). They can be easily clear out of the atmosphere by rain. Another characteristic of the nuclei particles is that they can move very fast into the accumulation mode due to gas to particle conversion and by coagulation with other aerosols. Due to the diversity of primary particles and the different chemical processes the secondary particles have an enormous mixture in characteristics and reactivity. Ozone (O_3) and (H_2SO_4) are examples of secondary formed pollutants. Second stage of aerosol formations is known as the accumulation mode, in this stage particles remained there for very long time, for about one to two weeks. Particle coagulation still occurs in the accumulation mode; however particles do not become big enough to end up in the coarse mode.The main removal mechanisms in the accumulation mode are rain-, and washout (Sillanpää et al., 2006). The particles in the coarse mode have different origin than the nuclei-, and accumulation-particles. Examples of coarse particles are coal-, cement-, and agriculture-dust and sea salt particles. These relatively large particles usually settle out within a few hours or days in the atmosphere depending on their size, prevailing meteorological conditions, and altitude (Aboh, 2000). In literature particle size ranges are often classified as coarse (<2.5 µm in diameter), fine (<2.5 µm) and ultra fines (0.001-0.1 µm). Summary of aerosol origins and size distributions are shown in figure 2.1

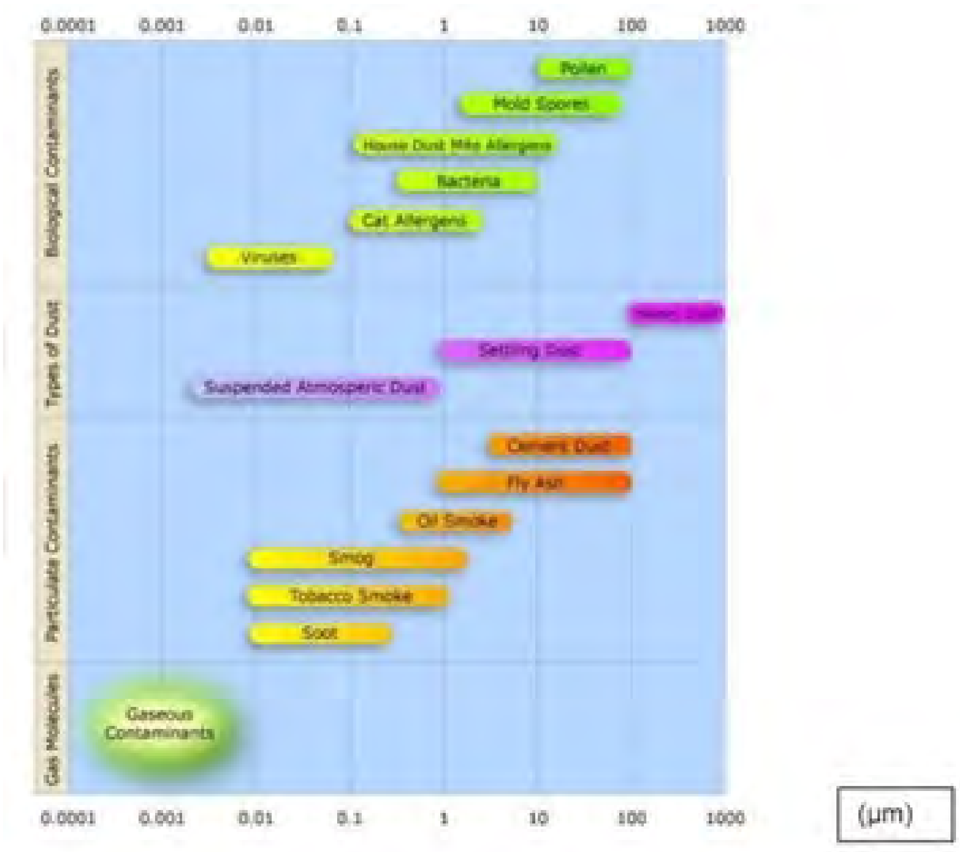

Figure 2.1: Types, and size distribution of APM

2.2.3 Chemical composition of APM

According to report from Air Quality Expert Group (Grover, 2006), (Harrison and Yin, 2000), (Kaur et al., 2005), each of the aerodynamic diameters have many different chemical substances, indicating that these particles originate from different sources.The location of the polluting source, chemical reactions in the atmosphere, time of the day, and meteorological conditions results in significant variations in the chemical composition of these particles (Finlayson-Pitts and Pitts Jr, 1999).

2.2.4 Transport of atmospheric particulate matter

According to Zufall and Davidson, they described the process where aerosol particles are transported in the atmosphere between emission and removal process as the particle transport. the source -transport -sink sequence determines the residence (life)time of the particle in the atmosphere (Caffrey et al., 1998).

2.2.5 Residence time

Nucleation mode particles in the atmosphere have very short life of the order of a few minutes to several hours; this is due to their rapid coagulation with larger particles or growth into larger sizes by condensation. They are removed through diffusion of falling rain drops. Ultrafine particles include the nucleation mode and much of the Aitken mode. Accumulation mode particles the largest surface area and therefore account for a significant fraction of the total particle mass. As the mode name suggests, the particle removal mechanisms are least efficient in this size range. Hence, they can be transported over thousands of kilometer and remain airborne for days to weeks. They also account for most of the visibility impairment in the dry atmosphere. Accumulation mode particles can be removed from the atmosphere by rainout or washout (Sillanpää et al., 2006). Coarse or sedimentation mode particles originate mainly from mechanical processes such as grinding, wind or erosion. Particles in the coarse range are relatively large and usually consist of mostly anthropogenic and natural dust particles that normally settle out of the atmosphere relatively quickly by sedimentation and impaction on surfaces(Seinfeld and Pandis, 2016). Coarse or sedimentation mode particles residence time in the atmosphere is only a few hours or days depending on their size, prevailing meteorological conditions, and altitude (Aboh, 2000)

2.2.6 Particle removal

Many factors, such as inflow conditions (wind speed, wind direction and turbulence), building geometry (height, width, roof type), surrounding building layouts (street width and configuration), thermal stratification (solar insulation and orientation, building and street thermal capacitance) and traffic conditions (traffic intensity, vehicle emissions, vehicle movement), have influenced the transport behaviours and mechanisms of PM_{10} and $PM_{2.5}$ (Chang et al., 2009). However the motion of APM is governed by two forces, they are gravity and resistance of the gas due to particle motion. The gravitation settling is very important for large or coarse particles. Dues to this rapid depletion by gravitational sedimentation, coarse particles are mainly present in the atmosphere close to their sources. One of the most important parameters in the analysis of complex particle motion is known as The particle relaxation time (τ). It is proportional to the square of the diameter and inversely proportional to the viscosity of the gaseous medium. It also characterizes the time required for particle to adjust or relax its velocity to new conditions in the atmosphere. It depends on the mass and mobility of the particle and is not affected by the nature and magnitude of the external forces acting on it. Hence the particles have long (large) relaxation time. The particle stopping distance S_x or inertial range is defined as the the distance traveled by particle relative to the gas medium before catches up with the flow. The particle stopping distance S_x is related to the relaxation time (τ), and the particle initial velocity relative to the gas.

$$S_x = V_{xo}\tau \tag{2.2}$$

where The particle stopping distance S_x, particle initial velocity relative to gas V_{xo}, the relaxation time (τ) On the displacement scale, the stopping distance represents a measure of a particles effective initial momentum, which is diminished to zero by air friction over a distance equal to the stopping distance.

The relaxation time (τ) = mB, where m is the particle mass and B is the particle mobility and its initial momentum is given by

$$S_x = BmV_{xo} \tag{2.3}$$

Stopping distance represents the distance a particle will travel in still air if an external force acting on the particle were turned off.

2.3 Particle size distributions

Modeling respiratory deposition The fraction of particles that enters the nose or mouth is called the inhalable fraction (IF). Factors influencing inhalability are the size and density of the particle and the wind velocity and direction. Wind tunnels with mannequins that are connected to a breathing machine are used to experimentally determine the IF. Upon inhalation, particles can either deposit somewhere along the respiratory tract or they can be exhaled. The fraction of inhaled particulates that deposit in the respiratory tract is called respiratory tract deposited fraction (DF). Human in vivo experiments are used to calculate the DF under different conditions; however regional deposition doses cannot be obtained using this technique. Moreover there are restrictions in the particles that can be used for human exposure. The site of deposition within the respiratory tract influences the effects of particles within the organism. Regional dosimetry is important for assessing the potential hazard of inhaled particles. Mathematical

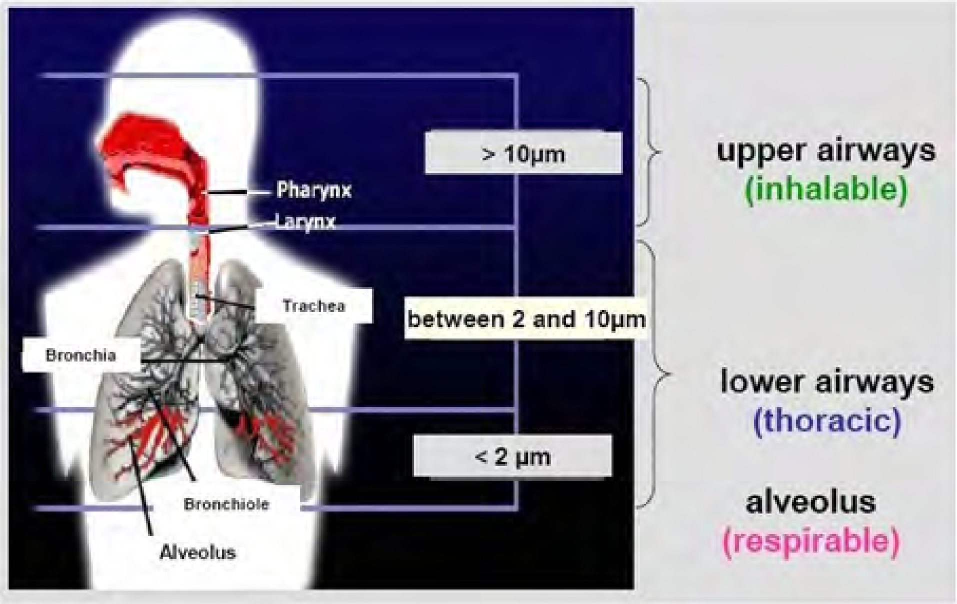

Figure 2.2: : Respiratory System and particle deposition

models have been developed to predict regional particle deposition. These models are based on (1) lung morphometry, (2) physical and chemical particle properties, (3) gas and vapor properties of the air and (3) breathing patterns(Rostami, 2009).

2.4 Mechanisms of Particle Deposition in Lung

Deposition mechanisms of particles in the lung are usual based on five processes, they are inertial impaction, gravitational settling, diffusion, interception and electrostatic attraction, its modeling is made simply by using these five processes(Rostami, 2009), (Stuart, 1984).

2.4.1 Inertial impaction

Inertial impaction occurs when airflow changes direction and the particle, which happens to be closed to the airway wall, follows its original direction instead of adjusting to the airflow. The probability of deposition by impaction depends on the ratio of particle stopping distance to airway dimensions at an airstreams velocity. The stopping distance is equal to the velocity before the change in current, times the relaxation time, which is the time required for a particle to adjust its velocity to a new condition. The higher the particle mass and its mobility, the more difficult it is for the particle to adjust for a curving air stream. Large particles have a higher relaxation time compared to small particles . The Stokes number (Stk) is used to predict impaction driven impaction. It combines all parameters that are important for inertia . When the size of a particle approaches the mean free path of air its properties change because of slip at its surface. This error becomes significant for particles less than 1 µm. The slip correction factor (C_c) is inserted in the deposition equations to correct for this error.

$$Stk = \frac{U\rho_p d_p^2 C_c}{9D_j\eta} \tag{2.4}$$

where U: Flow velocity, ρ_p : particle density, C_c : slip correctionfactor, η : air viscosity, D_j: airway diameter.

The Stk number shows that the probability of a particle to deposit due to impaction is directly proportional to particle density, diameter 2 and flow velocity whereas it is inversely proportional to the distance to the surface (the airway diameter). Thus: deposition by inertial impaction is most important for larger particles at high velocity close to the surface. Particles come close to the surfaces at high bend angles, which can be found in the head airways and the conducting airways (nasal passages, the larynx, the carnia and further bifurcations).

2.4.2 Gravitational settling

Settling or sedimentation is driven by the influence of gravity, which makes particles to depart their original air stream. The probability of a particle to deposit due to gravitational settling depends on the ratio of particle settling distance to airway dimensions at an airstreams velocity. The particle settling distance is equal to its terminal settling velocity V_{ts} times the residence time in each airway compartment. V_{ts} is given by the gravitational acceleration times the relaxation time.

$$V_{ts} = \frac{g\rho_p d^2 C_c}{18\eta} \tag{2.5}$$

where g: acceleration of gravity; ρ_p : particle density; C_c: slip correction factor; η air viscosity. Equation above shows that the probability of a particle to deposit due to gravitational settling is directly proportional to its particle size 2 and density. In contrast to inertia it is inversely proportional to the air stream velocity because the residence time decreases at increasing velocity. This mechanism is therefore most important in the smaller airways and in the gas exchange region where the air velocities are low. Sedimentation has its maximum removal effect when airway surfaces approaches horizontal configurations, which is the case in the alveolar region.

2.4.3 Diffusion

Diffusion is a disperse mass transfer that is caused by random molecular motions also called Brownian motion. Small particles displace when they collide with air molecules. This mechanism can be explained by the diffusion coefficient (D) of an aerosol particle which is given in the Stokes-Einstein equation.

$$D = \frac{K_B T C_c}{3 d_p \pi \eta} \tag{2.6}$$

Where K_B: Boltzmanns constant; T: Temperature; C_c :slip correction factor; d_p :particle density; η :viscosity. The probability of a particle to deposit due to diffusion depends on the ratio of the root-mean-square of the displacement during residence (2 Dt) to airway dimensions. Similar to gravitational settling, deposition due to diffusion is also increased where airway diameters are small and where residence time is long.

2.4.4 Interception

Interception is the result of physical contact of a particle with the airway surface because of geometrical features. An assumption made for pure interception suggested that the particles follow the airstream and thus its inertia, settling and Brownian motion are negligible,. The particle does not depart its original air streamline but makes contact due to its physical size. Interception depends on the ratio of particle size to airway diameter which means that interception is most important for elongated particles, like fibers, which are long in one dimension but have small enough diameters to reach the small airways.

2.4.5 Electrostatic attraction

Electrostatic attraction is important for electrically charged particles. These particles can deposit when large numbers of mutual charged particles drive them towards the airway wall. In absence of mutual repulsion, a neutral surface by image forces is attracted by a charged particle. An image force is created by the particle itself and is equal but opposite of its own charge. Image forces are weaker than Coulomb forces and are only created when the particle is at close range to the surface. Freshly generated particles have higher surface reactivity than aged aerosols. These freshly generated particles may be more charged which results in higher deposition when compared to aged particles.

2.5 APM Sampling

The choice of the APM sampling instrument depends on the substance to be measured, the properties it has, and the information to be gained from the measured values. The first aim of the measurements is to determine the levels of air pollutants but the mass flow rates are also very important to determine effect on the emission. However all APM samples collected are the representative samples for analysis. Both concentration and size distribution should be true representative of the airborne particles.

2.5.1 Types of samplers

There are different types of samplers in APM sampling methods. However in this work, the GENT sampler, which is a low volume, filter-based sampler having a stacked filter unit for simultaneous, sequential collection of coarse and fine airborne particulates was employed. Gent sampler was used because it allowed for collection of particles on a filter that is weighed and subsequently subjected to analytical analysis such as PIXE and XRF easily (Wilson et al., 2002).

2.5.2 The GENT sampler

The Gent Stacked Filter Unit (SFU) PM_{10} sampler owed its name to the designer and manufacturer, which is the the University of Ghent. The international Atomic Energy Agency (IAEA) has several coordinated research programmes in which the participants are to collect and analyze samples of the ambient aerosol. In order to have comparable samples taken in the variety of locations around the world, the IAEA contracted with the University of Gent to design and construct a sampler that would generally follow the requirements of a PM_{10} sampler. The air enters the unit through an impactor stage designed to have a 50% collection efficiency at 10 µm

equivalent aerodynamic diameter. It then is drawn through a stacked-filter unit (SFU). The SFU consists of a holder for two sequential filters

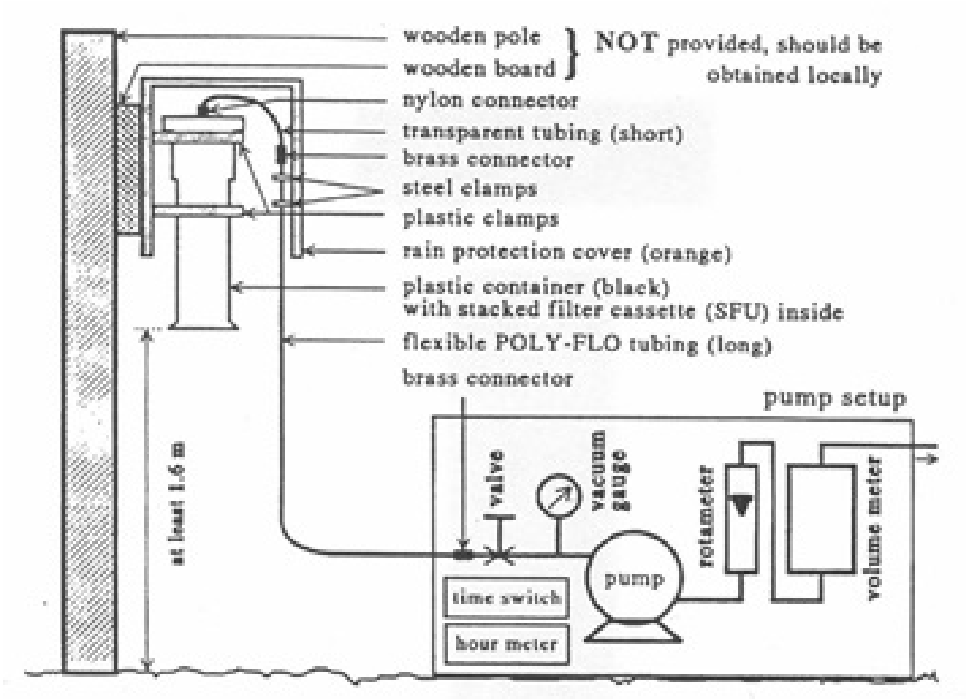

Figure 2.3: : Gent Sampler Unit

constructed by the Norwegian Institute for Air Research (NILU). The initial filter is an 8 µm pore 47 mm Nuclepore filter and the second filter is an 0.4 µm pore Nuclepore filter. At a flow rate of 16 l/min, the unit act as a dichotomous sampler. The flow through the 8 µm pores will result in collection of 2.2 µm particles with 50% efficiency (Cahill et al., 1979). The <2.2 µm particulates are then collected on the 0.4 µm filter (Cahill et al., 1979)

2.5.3 Filters

The material on which the aerosol sample is collected is very important if any meaningful results are to be obtained from analysis. The material

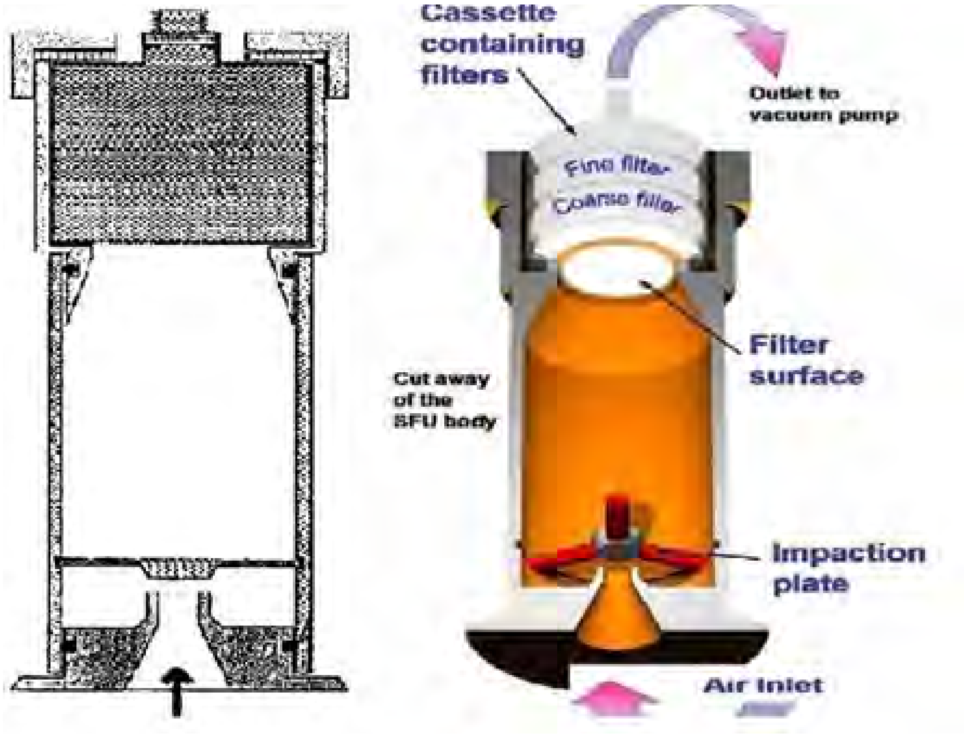

Figure 2.4: : Stack filter Unit

should have a very good properties like the ability of retaining the particle, without it coming off easily, but must permit air flow readily through it. the sample collected should be provided in manner that would make it easy to analyze both for mass concentration and chemical composition. Fibrous and porous membrane filters are most commonly and important filter types used in aerosol sampling.

2.5.4 Fibrous membrane filters

Glass fiber, quartz and cellulose (paper) are the most common types of fibrous membrane filters. They have high porosity from 70 to greater than 99% and range in size from sub-micrometer to 100 µm . They have lower pressure drops across them and are well suited for high volume sampling. High -efficiency filters have a low air velocity through them. Thus to obtain a large filter area in an element of convenient size the filter element are pleated. The glass and quartz fiber filters have retention of particles with sizes above 0.3µm . Glass fiber filter has very high capacity but the only problem is its ability to convert sulphur dioxide to suplhate hence increasing the load. It also has very high blank values for a lot of elements and therefore it is unsuitable for trace elements analysis especially with nuclear analytical techniques. Quartz filter also has very high blank values for a lot of elements. Cellulose (paper) filter has only one problem, its inability to maintain the same humidity for the exposed and unexposed filters. In general the penetration of particles into the filter mat of fibrous filter is not uniform thus they are not useful for EDXRF, PIXE and PIGE.

2.5.5 Porous membrane filters

Most common filters used in nuclear analytical techniques are Nuclepore and Teflon filters. Researches conducted have really shown the efficiency of porous membrane filters and it has been found that the collection efficiency depends on pore size, especially with the nuclepore filters(Dzubay and Barbour, 1983) (John and Reischl, 1978), (Liu and Lee, 1976). One problem that is associated with these filters is the loss of coarse particles from the filters in handling and transport from sampling site to the laboratory which has been noticed by a number of researchers around the world. Dzubay and Barbour have suggested the use of oil coating on the filters to prevent such shake off effects(Dzubay and Barbour, 1983)

2.6 Particulate matter measurement tools

There are several instruments for measuring different characteristics of particulate matter. The most important measurements of particles are particle concentration and particle size. IBA (PIXE and PIGE) and EDXRF these methods are the most widely used because they are relatively more accessible to many users, are non-destructive techniques, and require no sample preparation. After the analysis, the filters can be reused in the other methods. PIXE, PIGE and EDXRF techniques can be used in the determination of the concentration of elements with atomic numbers ranging from 11 (sodium) to 92 (uranium). In this work the analytical methods used for the determination of elemental concentration in the aerosol samples are:

- Proton Induced X-ray Emission (PIXE) analysis
- Energy Dispersive X-ray Fluorescence (ED XRF) analysis
- Proton Induced Gamma-ray Emission (PIGE) analysis

(Sandström et al., 2005), (Schwarze et al., 2006). A multi-national team of researchers have really shown that these techniques provide an excellent elemental concentrations with hourly resolution and the Lower Detection Limits (PIXE) of the order of ngm3 for most elements (Annegarn et al., 1988). These techniques are the best option in the area of determination of elemental concentrations in airborne particulate matter . Moreover, elements with atomic number below 11 (Na) cannot be detected by PIXE, because of the X-rays self-absorption in the sample and in the detectors dead-layers. However, the elements detected by PIXE contribute to a fraction of particulate matter ranging from 10 30% but comprises the tracers used to identify the particulate matter sources and potentially harmful elements (like As, Se, Ni, Cr, Zn, Cu). A lot of researches have shown and proven the qualities of PIXE in the field of aerosol studies in the world (Johnson et al., 2006), (Maenhaut et al., 1996) (Marcazzan et al., 1987), (Prati et al., 2000).

2.6.1 Proton induced x-ray emission, PIXE

This is technique where x-rays from inelastic collision of the projectile with inner core electrons are detected. PIXE is especially sensitive to trace elements and allows the determination of concentrations at a ppm level (Garman and Grime, 2005). However, PIXE generally does not yield depth information. When lower Z elements are detected , the preferred technique is PIGE. PIXE is one of the variants of X-ray emission techniques. This technique has also been using in the field APM analysis(Lannefors et al., 1983) of PIXE, the ion knocks an inner-shell electron out of the atom and an X-ray is emitted as the vacancy is filled by an outer-shell electron. The energies of the X-rays are characteristic of the elements in the sample and the intensities of the X-ray lines can be used to calculate the concentration of the elements. This technique provides information on selected elements from Si to U with good sensitivity. Minimum detectable limits for PIXE analysis of aerosol samples are typically on the order of a few ngm3 (Johansson et al., 1995). A beam of energetic protons are accelerated onto a target (sample) of interest. This causes ionization and atomic excitation, leading to the ejection of inner-shell electrons from atoms in the target. The inner vacancies created are filled by outer shell electrons resulting in the emission of X-rays which are characteristic of the targets elemental composition and concentration. The X-ray spectrum is usually recorded in an energy dispersive mode using a Si(li) detector. The energies of the emitted X-rays are used to identify the atoms or elements in the target, and the X-ray intensities used to determine the element concentration. The PIXE facility, like any accelerator-based facility, consists essentially of ion sources, an accelerator system, a beam transport system, end stations (scattering chambers), and computer control system.

2.6.2 Quantification analysis using PIXE

The main parameters needed to quantify the elements of interest in a sample is the number of x-rays from a transition j of the element z detected during PIXE measurement. It is known as yield and written as as follows:

$$Y_{0Xj}(Z) = \sigma X_j(Z, E_0).\alpha Z \frac{\Omega}{4\pi}\epsilon._{det}\frac{Q}{e}.\frac{N_{Av}.(\rho t_z)}{A} \tag{2.7}$$

Where: $\sigma X_j(Z, E_0)$ is the x-rays production cross section; αZ is the fraction of transmitted x-rays from the target to the detector sensitive area; Ω are the solid angle covered by the detector and its intrinsic efficiency; ρt_z is the mean a real density of the element Z in the surface impinged by the beam, N_{Av} the Avogadro number and A the atomic mass of the element Z; Q is the integrated beam charge, e the unit charge of the particles. For a given x-ray, beam energy, detector, and measurement geometry, an efficiency factor η can be defined as follows:

$$Y_{0X_j}(Z) = \eta.Q.(\rho t)z \tag{2.8}$$

Equation **??** hence becomes:

Provided η is known, the areal density $(\rho t)z$ of a given element can be obtained by measuring the corresponding x-ray yield on the detector and the integrated beam charge on the target. However the efficiency factors $\eta(Z)$ are usually obtained experimentally using equation **??**. This is performed by irradiating elemental standards with known quantities $(\rho t)z$ of various elements and measuring the corresponding x-ray yields. The same conditions (same geometry and same beam energy) must be used for the standard and the samples to be analysed. When target cannot be assumed to be thin, corrections to the x-ray yield are required due to energy loss of the proton beam in the target matrix and attenuation of the emitted x-rays passing through the target. A matrix correction factor F_{Xj} can hence be introduced. The factor is defined as the ratio between the ideal yield Y_0 that would be obtained from the same target, in the absence of matrix effects, and the actual yield Y:

$$F_{Xj}(Z) = \frac{Y_{0Xj}(Z)}{Y_{Xj}(Z)} \tag{2.9}$$

Putting equation **??** and equation 2.9 the corrected elemental areal density $(\rho t)z$ can be rewritten as :

$$(\rho t)_Z = \frac{Y_{Xj}(Z)}{Q.\eta z, E_0}.F_{Xj}(Z) \tag{2.10}$$

According to Boni and Jex, apart from these low Z elements (Na, Mg, Al, and Si) which cannot be detected due to their self-absorption effects within the sample. The equation 2.10 can be used to approximate an aerosol sample to a thin target with the aim of simplifying the quantitative analysis, and apply the needed correction afterward (Boni et al., 1990), (Jex et al., 1990) .

2.7 APM analysis using PIGE technique

PIGE technique, (PIGE is an acronym (Proton Induced Gamma Emission)), is used for detection of gamma rays. Proton induced γ-ray emission PIGE is a nondestructive technique for material analysis with ion accelerators. When charged particles, such as MeV protons, hit matter nuclear reactions can be induced and characteristic γ-radiation is emitted. These γ-rays allow to identify the elemental composition of the sample.

2.7.1 Concentration calculation using PIGE

The level of concentrations N_t in PIGE are obtained from measured quantities(i.e γ-ray peak areas) and the microscopic data such a stopping powers and differential cross sections of the interaction as well as the detector absolute efficiency. The gamma-yield η_γ for a detected element is given as:

$$\eta_\gamma = \eta_p.N_t.\triangle\Omega.\epsilon \int_{E_{0-\triangle E}}^{E_0} \frac{d\sigma}{d\Omega}(E,\theta)\frac{dE}{S(E)} \tag{2.11}$$

Where η_γ is the beam intensity; 4Ω is the detector solid angle; ϵ is detection efficiency;$\frac{d\sigma}{d\Omega}(E,\theta)$ is energy dependent differential cross section; $\frac{dE}{S(E)}$ is the stopping power of the target.

2.7.2 Quantification of APM samples using PIGE

Light elements like Na, Mg, Al and Si with no self-absorption of emitted gamma radiation inside the sample can be determined quantitatively using PIGE, the unknown elemental concentration are deduced by comparing the γ-ray yields with those of thin elemental standard. Choosing the beam energy is crucial since the gamma emission cross sections have to be constant over the energy loss in the sample. If the PIGE cross section is constant over energy range $\triangle E$ the equation **??**can be rewritten as

$$\eta_\gamma = \eta_p.\sigma.\epsilon.\triangle\Omega.N_t \tag{2.12}$$

The unknown concentrations can be deduced by comparing the γ-ray yield to those of thin elemental standards as follows:

In this work, approximation of thin target were done for Na and Al. This was to enable us correct for underestimation of Na and Al that occurs in PIXE analysis due to low energy x-ray absorption in the aerosol particles.

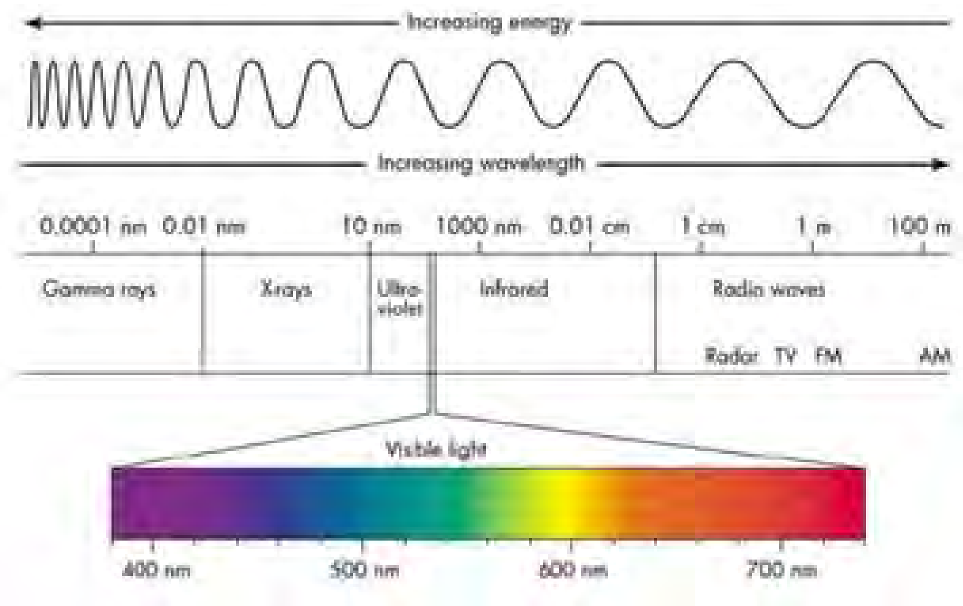

Figure 2.5: : Electromagnetic Spectrum

2.8 X-Ray Fluorescence Analysis

X rays are electromagnetic radiation. All X-rays represent a very energetic portion of the electromagnetic spectrum and have short wavelengths of about 0.1 to 100 Å. They are bounded by ultraviolet light at long wavelengths and gamma rays at short wavelengths X-rays in the range from 50 to 100 Å are termed soft X-rays because they have lower energies and are easily absorbed.

X-Rays have the following general properties:

- Invisible;
- traveled at the speed of light (3 108m/s)
- not affected by both electrical and magnetic fields

- Differentially absorbed in passing through matter of varying composition, density and thickness;
- Reflected, diffracted, refracted and polarized;
- ionizing of gases is possible ;
- affect electrical properties of liquids and solids ;
- blacken a photographic plate;
- capable of liberating photoelectron and recoils electrons
- Emitted in both a continuous spectrum and with a line spectrum characteristic of the chemical element;
- have absorption spectra characteristic of the chemical element

2.8.1 X-Ray Emission

X-rays are produced from the disturbance of the electron orbitals of atoms. This may be achieved in so many ways, the bombardment of a target element with high energy electrons is regarded as the most common, X-rays or accelerated charged particles. The first two are frequently used in X-ray spectrometry, either directly or indirectly. Electron bombardment results.

in both a continuum of X-ray energies and radiation that is characteristic of the target elements.

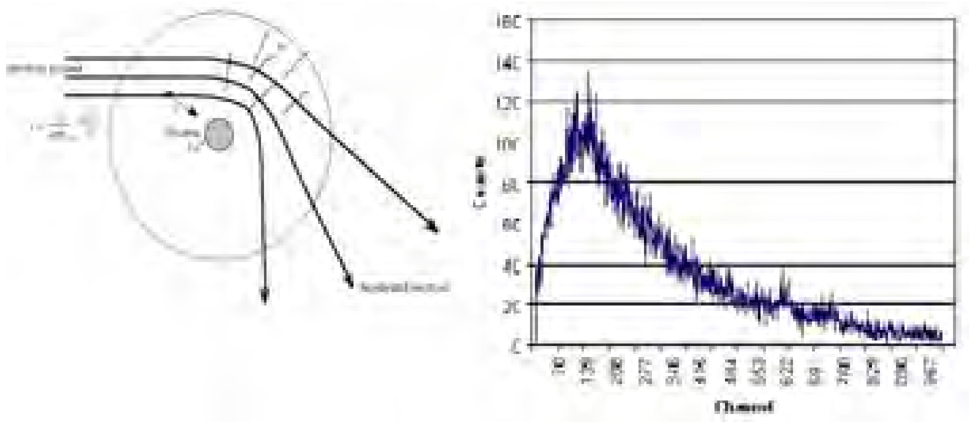

Figure 2.6: : Bremsstrahlung

2.8.2 Continuum X-rays

They are produced when electrons or high energy charged particles lose energy in passing through the Coulomb field of a nucleus. In this interaction, the radiant energy (photon) lost by the electron is called Bremsstrahlung as shown in the figure 2.6. The emission of continuous X-rays finds a simple explanation in terms of classic electromagnetic theory, since according to this; the acceleration of charged particles should be accompanied by emission of radiation. In the case of high energy electrons striking a target, they must be rapidly decelerated as they penetrate the material of target, and such a high negative acceleration should produce a pulse of radiation.

2.8.3 Characteristic Emission

The purpose of X-ray fluorescence is to determine chemical elements both qualitatively and quantitatively by measuring their characteristic radiation.

To do this, the chemical elements in a sample must be caused emit X-rays. As characteristic X-rays only rise in the transition of atomic shell electron to lower, vacant energy levels of the atom, a method must be applied that is suitable for releasing electrons from the innermost shell of an atom. This involves adding to the inner electrons amounts of energy that are higher than the energy bonding them to the atom. This can be done in a number ways:

- Irradiation using elementary particles of sufficient energy (electrons, protons, a-particles) that transfer the energy necessary for release to the atomic shell electrons during collision processes.
- Irradiation using X- or γ-rays from radionuclides.
- Irradiation using X-rays from an X-ray tube

2.8.4 X-Ray Interactions with Matter

When X-rays of intensity, I_0 are directed into an object of finite thickness, d, and density, , the transmitted intensity of photons which have not suffered interactions, I, in the object is given by the Beer-Lambert law.

$$I = I_0 e^{\mu\rho d} \tag{2.13}$$

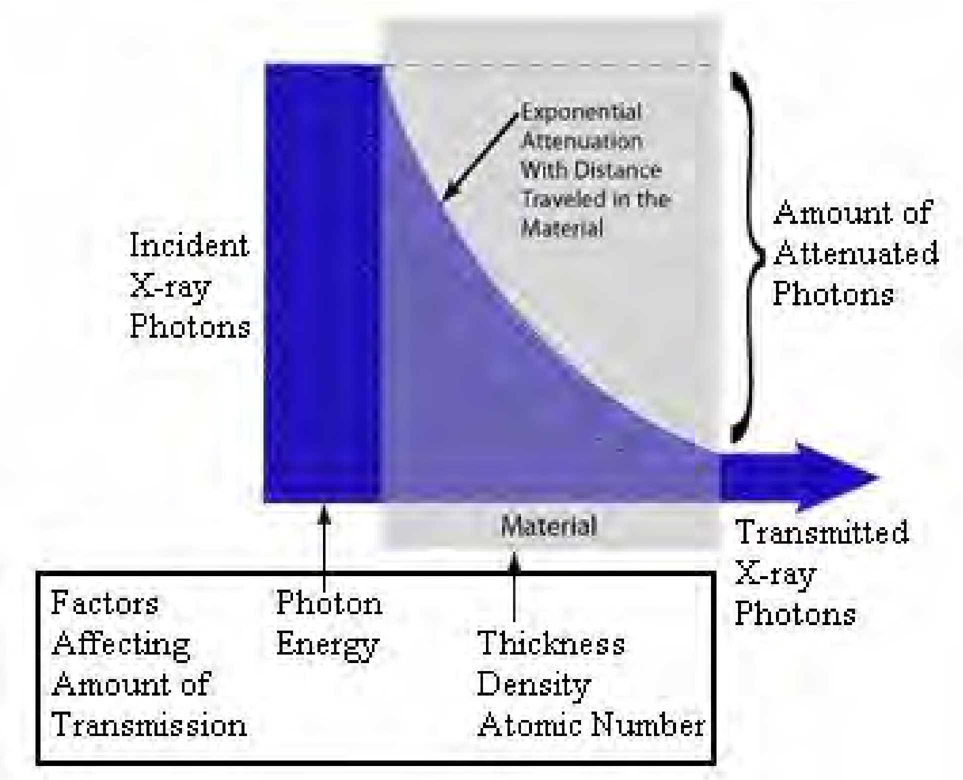

Figure 2.7: : the transmitted intensity of the photon

The linear absorption coefficient has the dimension [1/cm] and is depend on the energy or the wavelength of the X-ray quantity and the special density (in gcm3 of the material that was passed through. It is not the linear absorption coefficient that is specific to the absorptive properties of the element, but the coefficient applicable to the density ρ of the material that was passed through:

The mass attenuation coefficient accounts for the various interactions and is therefore composed of here major components:

$$\mu(E) = \tau(E) + \sigma_{coh}(E) + \sigma_{inc}(E) \tag{2.14}$$

$\tau(E)$ is the photoelectric mass absorption coefficient; $\sigma_{coh}(E)$ is the coherent mass absorption coefficient; $\sigma_{inc}(E)$ is the incoherent mass absorption coefficient. some of the photons interact with the particles of the matter and their energy can be absorbed or scattered. This absorption and scattering is called attenuation. Other photons travel completely through the object without interacting with any of the materials particles. The number of photons transmitted through a material depends on the thickness, density and atomic number of the material, and the energy of the individual photons. Even when they have the same energy, photons travel different distances within a material simply based on the probability of their encounter with one or more of the particles of the matter and the type of encounter that occur. Since the probability of an encounter increases with the distances traveled, the number of photons reaching a specific point within the matter decreases exponentially with distance traveled.

2.8.5 Energy dispersive x-ray fluorescence (EDXRF) spectrometry

Energy dispersive X-ray fluorescence (EDXRF) spectrometry is one of the most commonly used analytical technique to determine the elemental composition of airborne particulate matter collected onto filter (Bandhu et al., 2000). It is capable of providing the composition of a variety of materials in a non-destructive manner. This technique is able to provide qualitative and quantitative information on multi-elemental concentration data of particulate matter. This data is essential for source identification work and for application of receptor models for source apportionment. A large number of studies on the elemental concentration of particulate matter using EDXRF spectrometry technique have been reported (Aboh, 2000), (Hung et al., 2002), (Watson et al., 1999). In EDXRF method, the sample on the filter is irradiated with a high intensity beam of X-rays. This causes electrons to be ejected from the inner shell orbital of atoms in the sample and the vacancies created are filled by electrons in the outer atomic shells. The excess energy is released in the form of (fluorescence) X-rays which is seen as a line in a spectrum whose energy is characteristic of the elements present. The intensity of the characteristic (fluorescent) X-rays is proportional to the concentration of the element in the sample. The X-ray fluorescence emitted from the irradiated sample is captured by the semiconductor detector and processed by the signal processing unit. Some advantages of EDXRF over other analytical techniques are:

- It is non-destructive; therefore samples are left intact after analysis so they can be submitted for additional analyses by other methods as needed.

- It requires little or no sample preparation or operator time after the samples are loaded into the analyser.
- It is fast and can be used to simultaneously quantify the concentrations of elements with atomic numbers ranging from 11 (Na) to 92(U).

2.8.6 Basic configuration of XRF

A basic X-ray spectrometer system consists of a source that generates Xrays, a solid state detector that measures the different energies of the characteristic radiation from the sample, a sample holder and a signal processing unit that records the emission or fluorescence energy signals and calculates the elemental concentrations in the sample.

2.8.7 XRF quantitative analysis

Quantification of the element of interest in XRF is given by the equation below

$$I_a(E_i) = I_0.G.\sigma_i(E_0).f_{ab}(E_i).\epsilon_d.C_a\frac{1 - exp[-\mu_s(E_0, E_i)\xi]}{\mu_s(E_i)} \tag{2.15}$$

where I_0: incident beam intensity; $I_a(E_i)$:characteristic x-ray intensity; G:geometrical factor; $\sigma_i(E_0$:cross section of element i; $f_{ab}(E_i$: air absorption; d: detector efficiency; C_a: Analyte concentration;$\mu_s(E_0, E_i$:Selfattenuation coefficient; ξ: target thickness There are three ways by which this equation can be applied, they are fundamental parameters approach,elemental sensitivities approach and the direct comparison of count rates.

2.8.8 Fundamental parameters approach

In this approach,the concentration can be calculated from the intensities of characteristics lines of the elements and a lot of theoretical values are always taken into account. Theoretical values like: the spectral distribution of the excitation source,the fundamental parameters, various absorption corrections, the inter-elements(enhancement) effect, and the detector efficiency are needed in the concentration calculation. The scatter peaks are used to correct the sample self-absorption by the dark matrix.

2.8.9 Elemental sensitivity approach

In this method, the sensitivity of characteristics lines from standards, taking into account the self absorption standard. The sensitivity calculated can now be used to determine the concentration of elements in unknown sample. But in this case the composition of the dark matrix is known.

2.8.10 Direct comparison of count rates

The simplest techniques for quantitative analysis is direct comparison of count rates. By using the sensitivities determined from standards,concentrations of elements in unknown can be determined. No absorption correction are calculated. Therefore it is advised to work with this technique only as long as these corrections are equal for standards and unknown samples.

2.9 Source apportionment of APM

A better policy strategies can be drawn for the reduction of APM concentration in ambient air, if the original sources of the particulate matter is known, and we can easily quantitatively apportion the observed aerosol particle concentrations among the various source types. Source apportionment methods provide the tools to formulate efficient and effective particulate matter control strategies and to develop policy to prevent human exposure. Pant and Harrison defined SA as the methods used to quantify the contributions of different source categories to the particulate matter concentrations measured in the atmosphere (Pant and Harrison, 2012). Emissions of APM are the combination of the different chemical species from various sources. Source apportionment models use the mass and chemical compositions of the particulate matter measured at a sampling site to resolve the main source types and estimate their contributions to the measured ambient particulate matter at that site (Belis et al., 2013). Particulate matter emissions from specific sources often have unique fingerprint by which the contribution of these sources to the total aerosol particles at the receptor can be recognized(Watson, 1984).

2.9.1 Receptor modelling methods

Receptor models are mathematical or statistical techniques used to identify and quantify the sources of airborne pollutants at a receptor or sampling site. The fundamental principle of receptor modelling is that mass conservation is assumed and on this basis a mass balance analysis can be used to determine and apportion ambient particulate matter concentrations to individual emitting sources (Dominici et al., 2010). Most receptor models used for source apportionment are in principle based on the assumption that the concentration of the pollutants measured at the receptor site is equal to the sum of the concentrations induced by the surrounding emission sources emitting the pollutants(Belis et al., 2013), (Fabretti et al., 2009). The main objective of receptor models is, therefore, to identify the possible sources of particulate contaminant and to obtain data on their contributions to the bulk particle mass. Receptor models are commonly divided into two primary categories: chemical mass balance and multivariate methods(Pollice, 2011). The selection of the appropriate method depends on prior knowledge on the sources and source profiles. If the sources are known and detailed information on source profiles is available, Chemical Mass Balance (CMB) models can be applied. Alternatively, in cases where the sources are unknown and only the concentration of ambient pollution is known, multivariate methods such as Positive Matrix Factorization (PMF) methods are preferred. Examples of the commonly used receptor model software in physical and chemical sciences applications include the USEPAs Positive Matrix Factorisation ((PMF 5.0) (Norris, 2008), Unmix 6.0 and Chemical Mass Balance (Chan et al., 2011). Enrichment factor analysis and multivariate techniques such as correlations and Positive Matrix Factorization (PMF) were used to define a relationship between the sources and the receptor. These analytical methods were combined to assist in the identification of sources and the apportionment of the observed pollutant concentrations to those sources in Agbogbloshie ,Accra, Ghana. Receptor models of positive matrix factorization (PMF) and enrichment factor (EF) were used in this study.

2.9.2 Positive matrix factorization

USEPA Positive matrix factorization (PMF) is a powerful and widely used multivariate method used extensively for source apportionment of ambient particulate matter (Paatero, 1997), (Paatero and Tapper, 1994). USEPA

PMF model resolves the dominant positive factors that contribute to PM samples without prior knowledge of the sources. This is achieved by using measured concentrations of particulate matter to estimate the number of sources, the source composition, and the source contribution to each sample. The goal of PMF modelling is to

- determine the number of factors (sources or chemical/physical processes) that adequately explain the input data set variability and
- find correlation among the measured variables.

The advantages of the PMF relative to the traditional factor analysis methods such as Cluster Analysis (CA) and Principal Component Analysis (PCA) are:

- Unreliable data, such as observations below detection limit or missing values,can be included in the PMF analysis by giving them low weights to decrease their influence in the modelling (Paatero and Tapper, 1994).
- Data characterized by heavy positive skewed distribution can also be handled by down-weighting those extreme points to reduce undue influence in the model (Huang and Conte, 2009).
- PMF model assumes the non-negativity of factors and does not rely on information from the correlation matrix but utilizes a point-bypoint

least- squares minimization scheme by taking into account the uncertainty of each data point(Pongkiatkul and Oanh, 2012).

In PMF, a matrix $X(m \times n)$, where n is the number of samples and m is the number of chemical species is factored into two matrices, $G(n \times p)$ and $F(p \times m)$, where p is the number of independent source types or factors extracted, and a residual matrix E is used to account for the unexplained part of X. The factor analysis model can be written in matrix form as shown in equation 2.16. in component form as

$$X = G.F + E \tag{2.16}$$

in component form as

$$x_{ij} = \sum_{k=1}^{p} g_{ij} f_{kj} + e_{ij} \tag{2.17}$$

where x_{ij} is the measured concentration at a receptor for the j_{th} species in the i_{th} air sample, g_{ik} is the particulate mass concentration from the k_{th} source type contributing to the ith air sample,f_{ik} is the j_{th} species mass fraction from the k_{th} source, and e_{ij} is the residual between measured and modelled concentrations for the j_{th} species in the ith sample. The objective of the multivariate receptor modelling is to determine the number of sources(p), the source contributions g_{ik} , and the chemical profiles f_{ik} of the identified sources that best reproduce x_{ij}. To obtain the best fit of the model, PMF minimizes the object function, Q or chi-squared based upon the uncertainties of σ_{ij} of each observation.

The object function is given by the equation:

$$Q = \sum_{i=1}^{m} \sum_{j=1}^{m} \left(\frac{e_{ij}}{s_{ij}} \right)^2 \tag{2.18}$$

$$Q = \sum_{i=1}^{m} \sum_{j=1}^{m} \left(x_{ij - \sum_{k=1}^{p} g_{ik} f_{kj}} \right)^2 \div s_{ij}^2 \tag{2.19}$$

where s_{ij} is the uncertainty in the j_{th} species in the i_{th} sample; $g_{ik} \geq 0$; and $f_{ik} \geq 0$; k = 1,...,p. PMF simultaneously adjust the elements of G and F in each iterative step until a minimum value of Q is obtained (Paatero, 1997), (Polissar et al., 1998). The Q value can be used to determine the optimum number of the factors. The theoretical Q value should be approximately equal to a value of$X(n \times m)$, the number of entries of data array or the number of degree of freedom of the datum in the data set.

2.9.3 Enrichment Factor (EF)

Enrichment factor model is an indicator used to assess the presence and intensity of anthropogenic contamination and those from natural sources. It also helps in the estimation of the degree of anthropogenic contamination. A lot of research works have been done using Enrichment factor (EF) in the field of APM. It is used in particle source apportionment studies to identify the major sources of air pollution and to quantify contributions of all sources of all measured pollutants(Cao et al., 2003), (Chao and Wong, 2002),(Davidson et al., 1986),(Winchester et al., 1981),(Zhang et al., 2008).

$$EF = \frac{\left(\frac{C_X}{C_{Ref}}\right)_{Sample}}{\left(\frac{C_X}{C_{Ref}}\right)_{Background}} \tag{2.20}$$

where C_X is the concentration of the element of interest and C_{Ref} is the concentration of reference element for normalization.

Chapter 3

Chapter 3: Methodology

3.1 Aerosol characterisation at Agbogbloshie

Agbogbloshie is situated between the latitude $05°35'45''N$ and the longitudes $00°06'45''W$. Approximately, it covers an area of $16km^2$, and has an estimated population of 80000 people (Amankwaa, 2013). Agbogbloshie is connected to the capital city of Ghana by road with less than a kilometre. Agbogbloshie is a suburb of Accra. Accra is located along the coast of Gulf of Guinea.

The location and the major activities of the area give reason for one to expect air pollutant contributions from various sources. However the major potential source of air pollutants in that area is expected to be e-waste burning from the scrap markets; other potential sources of air pollutants include vehicular emission, open burning of refuse, and windblown dust

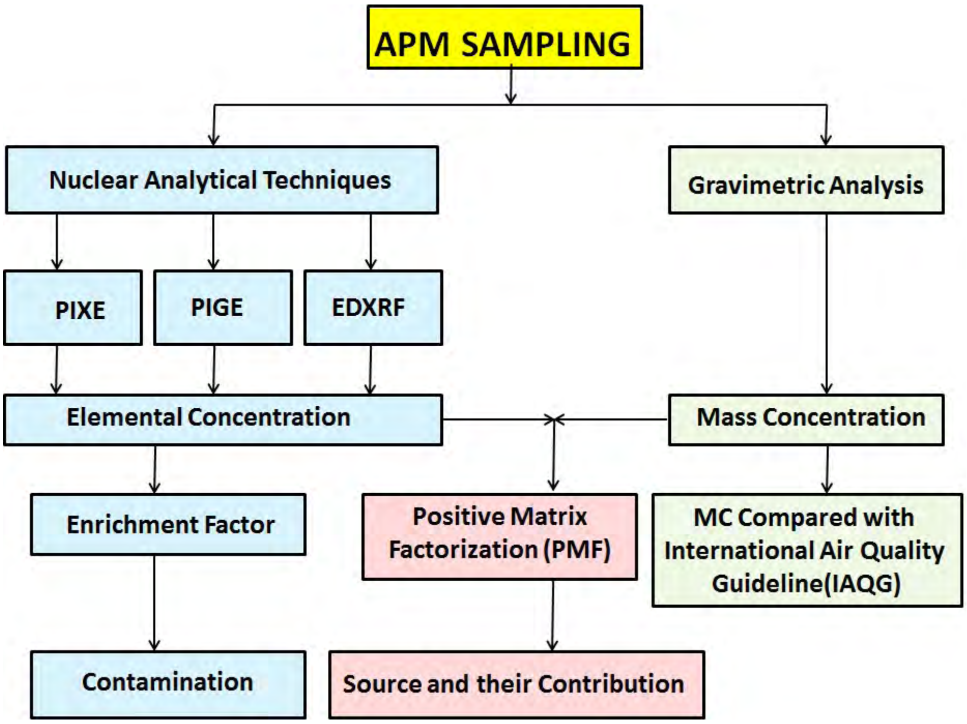

Figure 3.1: Designed protocol for the investigation

from the market as a result of the activities of buyers and sellers. At Agbogbloshie, measurements were made for the particulate matter (PM) mass and several elements in $PM_{2.5}$ and in $PM_{10-2.5}$. The aim was to characterize the aerosol composition in the Agbogbloshie scrap market. Data were collected for a period spanning from May 2010 to April 2011 in order to cover both dry and wet seasons. These data were used to examine to what extent the gravimetric PM mass could be explained by the measured components, and thus aerosol source apportionment could be achieved. A designed strategy used for the entire project is shown in figure 3.1.

3.1.1 Selection of sampling area

Agbogbloshie is small area and densely populated area, moreover on that small area there are lots of mixed activities like industries, markets , banks and the e-waste (dismantling and burning).

APM samples were collected at the scrap market in Agbogbloshie, where they usually openly burned the e-waste between this period of time that is from May 2010 to April 2011. The field measurements of fine and coarse PM was carried out at a monitoring site located at the Agbogbloshie Unilever depot premises, which is 0.5 km away from the burning yard.

3.1.2 Sampling and gravimetric procedures

The operation procedure of the Gent sampler used in this work was adopted from Andreas Markowitz instructions and installation manual(Maenhaut et al., 1994). The Gent sampler was placed at about 2.0 m above the ground level. The Gent sampler was set up in an open area, so that the circulation of air around it is not hindered by anything. The Gent sampler is made up of compact vacuum pump system that is controlled by a timer and connected to the stacked filter head unit, into which the different size faction filters are loaded. Its flow rate is regulated between 16-17 l per min. Particles with aerodynamic diameters greater than 10 micrometers are removed from the air sample by inertia separation on a pre-impaction plate with a greased surface. Particles smaller than 10 m are drawn through the tube onto the stacked filter cassette unit containing two filters but the bigger particles are caught up in the grease. The nuclepore polycarbonate filters used for the coarse and fine participate collection are arranged in series. The particles are first directed onto the coarse filter where the coarse particles > 2.5µm settles but the fine particles <2.5 µm pass through and continue onto the fine filter. The samples were collected during the period May 2010 to April 2011. The sampling time were approximately Twenty-four (24) hours of continuous sampling. However, the actual time of collection of PM on the filter varied between 8 and 16 hours depending on weather conditions so as to avoid overloading of the filters, also to make sure the flow rate remained within the recommended range of the sampler. The filters were conditioned for 48 hours, before and after sampling in the laboratory. The weighed filters were put in Petri dishes, and put in the desiccator. The net mass of each samples collected can be calculated by subtracting that of the empty filters from the loaded filters. The total volume of air sampled is determined from the total volumetric flow rate (l per min) and sampling time in seconds. The mass concentrations of coarse and fine particulates in the APM are calculated as total mass concentration of collected particulates divided by the volume of air sampled in actual conditions (Ayers et al., 1999). It is usually measured in $\mu g/m^3$

$$C_m = \frac{M_{LF} - M_{BF}}{V_{FR} \times S_T} \tag{3.1}$$

Where

C_m = concentration in $\mu g/m^3$; M_{LF} = loaded filter mass in g; M_{BF} = blank filter mass in g; V_FR = volume flow rate in m3h1, St = sampling time in hours. Fisher brand PS-60 micro-balance with readability of 0.1 mg was used for the mass measurement. The mass of the APM of the two fractions is tabulated in table 4.1. Consequently, calculated daily mass concentrations of all the particle size fractions (fine, coarse and PM_{10} are shown in table

3.1.3 Analysis of APM sample

PIXE techniques is used for multi-elemental determination, is non-destructive, no sample preparation is needed and sensitive to trace elements. Measurement time of the sample ranges between (2-10 min), and detection element as low as (0.10 ppm). Since the APM samples are thin samples, it is an appropriate technique for this work (JOHANSSON, 1992).

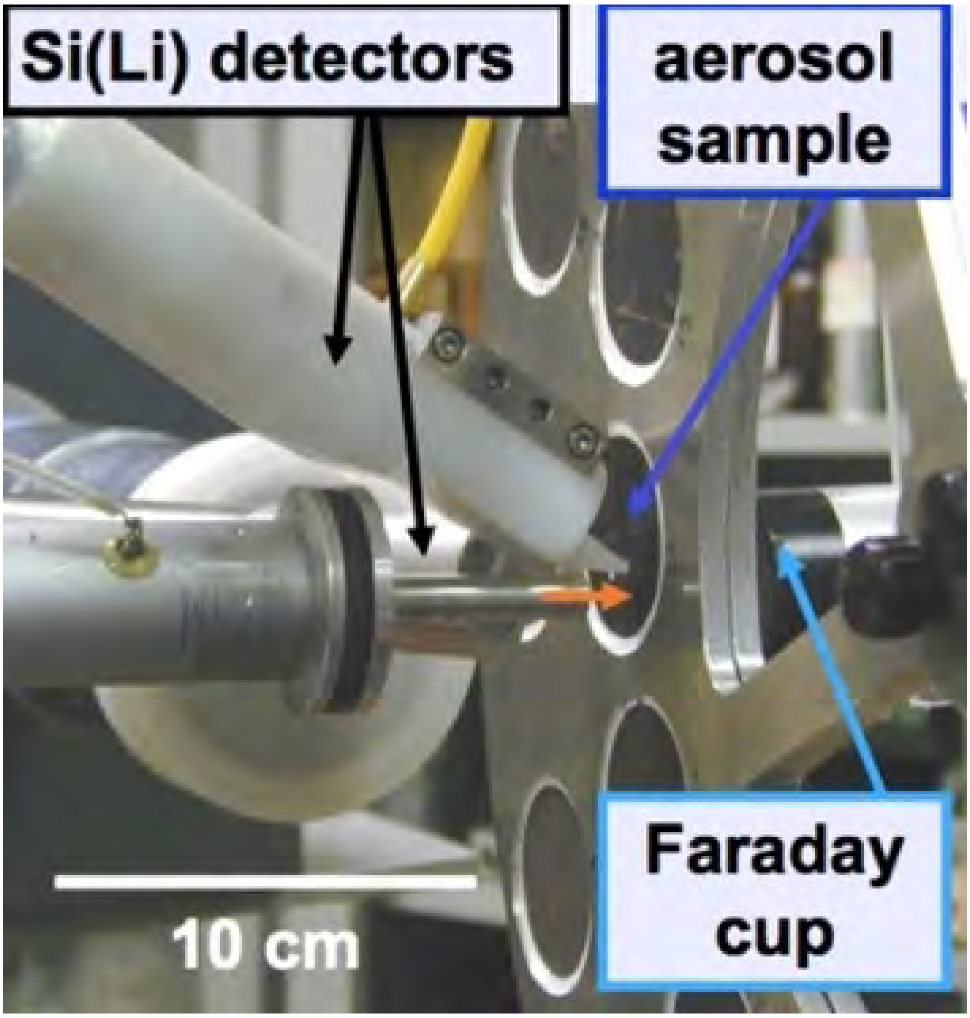

Figure 3.2: LABEC laboratory of INFN in Florence, Italy

3.1.4 Experimental setup for ion beam analysis

Analysis of the APM samples were done at the National Institute of Nuclear Physics (INFN) Accelerator Laboratory in Florence, Italy as shown in the figure 3.2. The laboratory has an external beam for the measurements of elemental composition of APM. The PIXE and PIGE techniques were employed in the analysis of all APM sample collected.

Ion source was used to generate proton beam energy of about 3 Mev and a charge of 11 μC. The beam is then extracted in air through a 500 nm thick Silicon Nitride window. The APM samples were placed at distance of about 1 cm,from the detector perpendicular to the beam. The size of the beam was determined by the bare collimation in vacuum in the last section of the beam line. Efficiency of all the elements can be obtained by balancing the counting rates of the different X-rays. This can be achieved by using high beam current (5-15 nA) and the optimisation of the two silicon drift detectors (SDD-1 and SDD-2) were done for low and medium to high X-ray energies respectively. SDD-1 has a resolution of 170 eV, thickness of 8 mm and an active area of 13 mm^2, it was placed at about 45° relative to the beam direction, at a distance of about 6 cm from the target. SDD-1 has an ultrathin entrance window (8m of Be) and with the use of a helium (He) gas flow into the volume in front of the detector, it can detect with good efficiency X-rays of very low energies, up to about 1 keV (K line of Sodium). The SDD-2 has a resolution of 190 eV, thickness of 25 mm and an active area of 80 mm^2, it is positioned at an angle of 55, at a distance of about 2-3 cm. A Mylar foil of about 400 mm is used to attenuate the low energy X-rays; SDD-2 was used to measure high-Z elements (Ca and above). High purity germanium (HPGe) detector has a resolution of 1 keV with thickness of 23 mm and an active area of 2800 mm^2, it was placed at an angle of 125° and at a distance of about 10 cm from the target was used for the PIGE analysis. Since this detector was to measure characteristic γ rays form the target, lead blocks was used to shield the background γ rays produced by interaction of beam protons with elements of the beam-line. The X-rays and γ-rays measured by each detector were processed by an acquisition system that consists of conventional preamplifier-shaper-ADC electronic components for nuclear spectroscopy (one for each detector). Each preamplifier produces a signal (whose rise time is about 100 ns), sends it to a shaper-amplifier to obtain a quasi-gaussian output; a shaping time 61 s) is carefully chosen to obtain a good energy resolution without producing high pile-up effects (at a rate of about 1-2 kHz). The shaped pulses are fed to an Analogue-to-Digital Converter (ADC) which is coupled to a computer for the visualization and storage of the spectrum through a multichannel analyser (MCA). Likewise, the charge integrated by the Faraday cup is converted into logic pulses by a Charge-Frequency-Converter (CFC); these pulses are also shaped and sent to one of the shaping amplifiers together with the real preamplifier signals.

3.1.5 Sample preparation in PIXE and PIGE analytical techniques

No sample preparation is required, the APM samples do not need any chemical preparations or treatment before analyses. However care need to to be taken when mounting them on the sampler holder. Naturally aerosol filters are fragile, they must be handle well, to avoid destroying them. Total number of filters analysed are summarised in AppendixA and AppendixB.

3.1.6 Sample analysis using PIGE and PIXE techniques

Both PIGE and PIXE techniques were used in the analysis of APM samples. For easy correction of matrix absorption of low-Z elements (Na, Mg, Al and Si) PIGE measurements of Na and Al were carried out. This required a careful choice of the proton beam energy so as to produce proton-gamma reactions 23Na(p,p0)23 Na and 27Al(p, p0)27 Al for Na and Al respectively. To achieve this half of the samples were analysed at a beam energy of 2870 keV and the other half at the energy of 2930 keV. Gamma-ray cross sections at energy regions around 2870 keV and 2930 keV vary very slowly for Na and Al respectively; hence, PIGE analyses for both elements were performed successfully. In both cases PIXE analyses were also carried out successfully as x-ray cross section does not vary much with changing energy. A beam spot size of 3 mm diameter was used to scan filter area of about 1 cm^2 for an irradiation time of 3 minutes per sample. Spectra for PIXE and PIGE were collected for onward analyses. The spectrum acquisition time was 180 seconds per sample, and the Procemxr software was used for this purpose.

3.2 PIXE elemental quantification

3.2.1 Spectrum integration

The PIXE x-ray spectra (collected with the two silicon detectors) deconvolution was done using the Iterative Least Squares fitting of GUPIXWINr software package (Maxwell et al., 1989) which uses an X-ray spectrometry library and some information about the experimental set-up. Before a spectrum is fitted to obtain the net x-ray counts the continuous background, made up of the bremsstrahlung (break radiation) emitted by secondary electrons ejected in the sample and the Compton background, is subtracted applying a digital filter operator. The net peak area for each (in both samples and standards) are recorded for use in elemental concentration calculation. The choice of GUPIXWINr is based on several considerations, the main ones being the better status of the databases (cross sections, stopping powers and attenuation coefficients). Another advantage is its availability as well useful options such as matrix iterations, layer thickness iteration and analyzing spectra in batches. In this study, GUPIXWINr was used only to calculate the peak areas because of data imperfection it exhibits when it is used to calculate concentration values for thin target samples. In addition, the INFN Accelerators end station has good shaping time analyzers which automatically measure experimental parameters (live-time, pile-ups, charge, etc.) required for absolute calculation of elemental concentrations

3.2.2 Sensitivity calculation of elements

According to Maenhaut and Raemdonck, the detection efficiency for each element was computed from data collected on all the three detectors (SDD-1, SDD-2, and SDD-3) for PIXE using equation **??** (Maenhaut and Raemdonck, 1984).

$$\epsilon_z\left(E\right) = \frac{P_A}{C_{std}Q_{me}}.\frac{It_Q}{It_{std}}.\left(\frac{rt_{std} + p\mu_{std}}{rt_{std}}\right) \tag{3.2}$$

Where,C_{std} : thin standard areal density; P_A : net peak area; Q_{me} : measured charge; It_Q : live time recorded on the charge detector; It_{std} : live-time recorded on the PIXE detectors, rt_{std} : real-time of measurement; and $p\mu_{std}$: detector pile-up time.

3.2.3 Calculation of concentration of elements

Data from GUPIXWINr peak fitting were used for the concentration of element and uncertainty calculations in a thin target approximation. Blank nuclepore filter concentrations of element were deducted from sample compositions to obtain the net aerosol concentrations of element.

3.3 Determination of Na and Al using PIGE technique

Majority of high -Z elements were determined by PIXE technique but low -Z elements are always underestimated due to their x-ray absorption in the sample. This happened only in the coarse fractions. For that matter, the concentration of low -Z elements (Na and Al) in the coarse fraction were measured by PIGE technique. However the concentration of Mg and Si were determined by an interpolation. PIGE spectrum fitting was done using jRadView software. Elemental concentrations were calculated using the absolute reference method expressed in equation **??** (Calzolai et al., 2010). This has been rewritten to take into account the blank filter values and the background counts recorded on the Faraday cup:

$$(\rho_z t)_{samp} = (\rho_z t)_{std} \left(\frac{Y_{samp} - Y_{blank}}{Y_{std} - Y_{FC}} \right) \cdot \left(\frac{Q_{std}}{Q_{samp}} \right) \tag{3.3}$$

The measurement uncertainty was given as follows:

$$\delta = \sqrt{(\frac{\delta Y_{samp}}{Y_{samp}})^2 . (\frac{\delta Y_{std}}{Y_{std}})^2 . (\frac{5}{100})} \tag{3.4}$$

where δY_{samp} and δY_{std} are errors in peak fitting for sample and standard respectively; Y_{samp} and Y_{std} are net peak areas for sample and standard

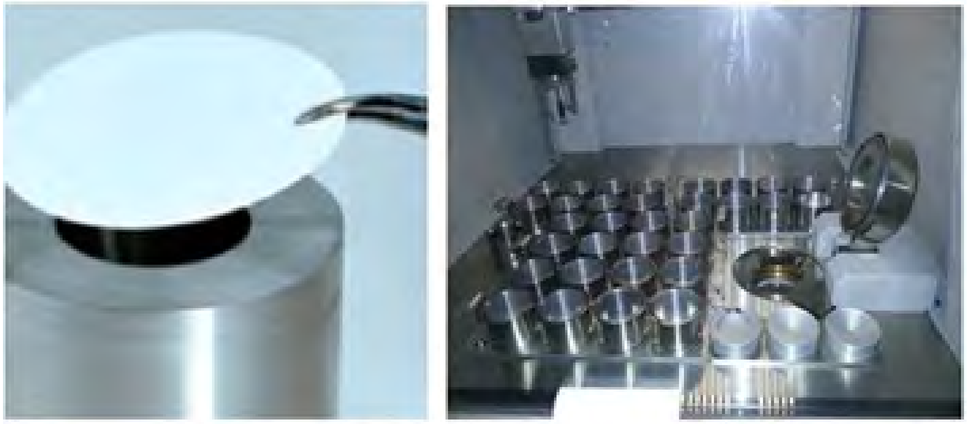

Figure 3.3: A filter being mounted on a holder-cup (left); and samples loaded in the spectrometer (right)

respectively; 5/100 (5%) is the error associated with the measurement instruments. PIGE results were plotted against those obtained with PIXE to determine the correction factor for the underestimation of Na and Al, whiles interpolated factors were used Mg and Si.

3.4 Analysis of Pb using EDPXRF

Some of the samples (fine and coarse) were analysed for elemental composition using energy dispersive X-ray fluorescence spectrometry (ED-PXRF) at the National Institute of Nuclear Physics (INFN) Accelerator Laboratory in Florence, Italy. Here again the sample did not need any special preparation and were mounted at the bottom of stainless steel holder-cups and place directly in the spectrometer for irradiation figure 3.3.

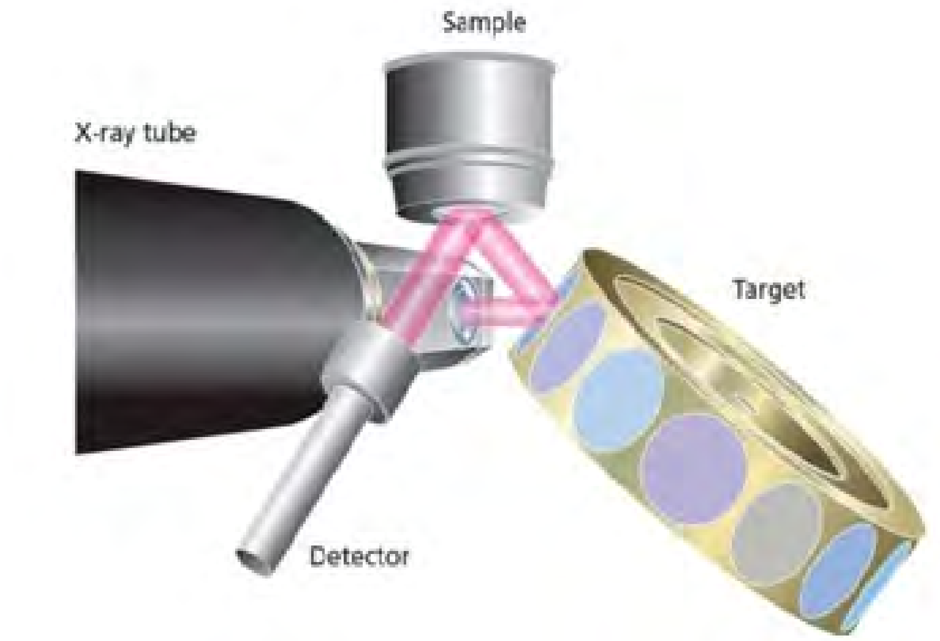

Figure 3.4: Schematic diagram of Epsilon 5 Spectrometer in 3 D

The spectrometer used in this study was an Epsilon 5r (PANalytical, Almelo, The Netherlands) equipped with a Gd anode x-ray tube operated at maximum values of 100 kV, 600 W, and a current of 7.5 mA. The Samples were irradiated by X-rays from Gd tube under vacuum equipped with a liquid nitrogen (N_2) cooled PAN-32 Ge X-ray detector having a beryllium window thickness of 8 μm. The primary x-ray from the Gd tube irradiated a secondary target to produce a near monochromatic x-ray which in turn impinge on the sample. The resultant characteristic x-rays are then collected on the detector figure 3.4.

The systems in-built software (Epsilon 5 software) automatically analysed the sample spectrum and determined the net peak intensities corresponding to detected elements. Concentration in ($\mu g/cm^2$) of element of interest were calculated using the direct comparison of counts approach with the equation 3.5:

$$(\rho t)_z = (\rho t)_{std} \cdot \left(\frac{Y_{samp} - Y_{blank}}{Y_{std} - Y_{blankMylar}} \right) \tag{3.5}$$

where, nuclepore blank (used in sampling) and Mylar blank (used in preparing the thin standards) filters were used to account for filter components. Minimum detection limits (MDLs) were calculated using three times the square root of the background as recommended by L. Currie (Currie, 1999).

$$LLD = \left(\frac{M}{A} \right)^i_{min} \tag{3.6}$$

$$LLD = 3.\frac{\sqrt{BG_i}}{S_i t} \tag{3.7}$$

$$LLD = 3.\frac{\sqrt{BG_i}}{N_i t}.\left(\frac{M}{A} \right)^i_{standard} \tag{3.8}$$

where LLD is lower limit of detection, BG: background,

3.5 Data Analysis

3.5.1 Enrichment Factor (EF)

A very good description of APM elemental concentration was obtained by calculating the EF. It was computed by using Wedepohls values for the elemental composition of crustal rock (Wedepohl, 1995). However silicon (Si) was chosen as the normalizing element, because of its abundance in the earth crust and less affected by anthropogenic pollution.

$$EF = \frac{\left(\frac{C_X}{Si}\right)_{Sample}}{\left(\frac{C_X}{Si}\right)_{Background}} \tag{3.9}$$

where C_x is the concentration of the element of interest and Si is the concentration of reference element for normalization.

3.5.2 Source identification and apportionment of APM samples

The results obtained for the gravimetric and elemental analyses of APM samples for one year sampling have given enough data for the comprehensive interpretation of data using statistical tool. Both size fractions $PM_{2.5}$ and PM_{10} were employed in the identification of APM sources and their various percentages portion occupied. The identification of various types of sources were done on both coarse and fine fractions $PM_{2.5}$, it was done by using the gravimetric and elemental composition data analysed in Positive Matrix Factorization (USEPA PMF 5). Both error estimates of the measured concentration and the measured concentration of APM samples collected were input in the USEPA PMF 5 software. The concentrations of all species for all of the samples form a matrix. This matrix was decomposed into two matrices representing source contributions and source profiles. The identification of source categories was undertaken by examination of their profiles. The USEPA PMF 5.0 software was used to run the model for 25 runs with different combinations of number of factors until a meaningful solution was found. The PMF is one of the best tools used in the determination of the number of factors. The results of a PMF analysis of higher dimension solution does not necessarily contain all the factors of the lower dimensions, because orthogonality is not required.

3.6 Quality control measures taken

Very rigorous and rigid quality assurance and quality control (QA/QC) measures were adopted to achieve the following properties, i.e the results are truly representative of the sample that they are traceable and can be trusted by other laboratories or analyst.

3.6.1 Sampling area

A lot of measures were put in place so as to achieve quality sample collection, and a good quality protocols were adopted. Though I was not able to measure Meteorology data could not be measured at site, GMetro provided all the needed information.

3.6.2 QA/QC as applied to APM data

Each measurement contains a degree of uncertainty due to the limits of measurement equipment and the human error using the equipment. The major sources of error concerning the sampling and analyses of particulate matter samples.However it is good to adopt quality control and quality assurance (QA/QC) measures in sampling, sample preparation and, more importantly, sample analysis. Issues such as uncertainty, sensitivity, detection limits, precision, reproducibility, data reporting, etc. that affect the quality of results obtained by techniques used require serious attention. Hence, irradiation facility inherent characteristics such as measurement geometry, energy calibration, beam diagnostics, beam charge integration, and detection efficiencies which have a major influence on the quality of results have all been evaluated. The method performance has also been assessed for the analysis of APM samples by techniques.

Chapter 4

Chapter 4: Results and Discussions

4.1 Mass Concentration of Particulate Matter

A summary of PM_{10}, $PM_{2.5}$ and $PM_{10-2.5}$ mass concentrations measurements for the monitoring site in Agbogbloshie covering the period May 2010 April 2011 is presented in table 3. The parameters recorded in table 3 are total numbers of samples sampled throughout the study period, the minimum , maximum and median mass concentration of PM_{10}, $PM_{2.5}$ and $PM_{10-2.5}$, and the ratios $PM_{2.5}/PM_{10}$ and $PM_{10-2.5}/PM_{10}$ and their percentage ratios respectively. Observations of the variation pattern of the mass concentrations have shown some influence of meteorological conditions on the particulates mass concentrations. In this work, the results obtained have also shown sharp differences in atmospheric particulate matter (APM) concentrations between the two main seasons. The lowest PM mass concentrations were recorded during rainy seasons whilst the sharp increment of PM concentrations were recorded in the harmattan season (December to February). The mass concentrations and the trends observed are in agreement with the results obtained by other researchers in Ghana, Africa and the world (Aboh et al., 2009), (Afeti and Resch, 2000), (Aryal et al., 2013), (Canha et al., 2011), (Gomišček et al., 2004), (Lee and Hieu, 2011), (Ofosu et al.,).

Table 4.1: Summary of daily Mass Concentration gcm^{-3} of APM in Agbogbloshie during the entire sampling period

Date	$PM_{2.5}$	$PM_{10-2.5}$	PM_{10}	$\%(PM_{2.5}/PM_{10})$
05-May-10	51.31	52.37	103.68	49.49
07-May-10	55.57	55.66	111.23	49.96
09-May-10	52.88	54.53	107.41	49.23
11-May-10	49.5	51.1	100.6	49.21
13-May-10	56.13	45.71	101.84	55.11
15-May-10	38.82	60.17	98.99	39.22
17-May-10	51.93	46.33	98.27	52.85
20-May-10	50.89	46	96.88	52.52
23-May-10	43.89	63.27	107.15	40.96

Continued on next page

Table 4.1 – *Continued from previous page*

Date	$PM_{2.5}$	$PM_{10-2.5}$	PM_{10}	$\%(PM_{2.5}/PM_{10})$
26-May-10	56.04	60.08	116.12	48.26
30-May-10	52.03	53.39	105.42	49.36
02-Jun-10	45.02	45.95	90.97	49.48
04-Jun-10	50.43	40.98	91.4	55.17
06-Jun-10	47.5	40.92	88.43	53.72
08-Jun-10	53.11	52.67	105.78	50.21
10-Jun-10	42.23	41.67	83.91	50.33
12-Jun-10	41.24	40.84	82.08	50.24
14-Jun-10	38.24	59.42	97.66	39.15
16-Jun-10	36.09	59.99	96.09	37.56
18-Jun-10	56.33	42.44	98.78	57.03
20-Jun-10	49.48	41.2	90.67	54.56
22-Jun-10	38.75	68.91	107.66	35.99
24-Jun-10	46.93	49.7	96.63	48.57
26-Jun-10	37.81	57.43	95.24	39.7
28-Jun-10	48.61	43.4	92.02	52.83
30-Jun-10	49.72	43.93	93.65	53.09
02-Jul-10	40.31	36.52	76.83	52.47
04-Jul-10	57.57	37.23	94.8	60.73

Continued on next page

Table 4.1 – *Continued from previous page*

Date	$PM_{2.5}$	$PM_{10-2.5}$	PM_{10}	$\%(PM_{2.5}/PM_{10})$
06-Jul-10	53.96	30.9	84.86	63.59
08-Jul-10	51.03	43.85	94.88	53.78
10-Jul-10	51.64	53.93	105.56	48.92
12-Jul-10	51.48	34.3	85.78	60.01
14-Jul-10	39.63	49.57	89.2	44.42
16-Jul-10	52.46	41.28	93.74	55.96
18-Jul-10	56.84	37.03	93.87	60.55
20-Jul-10	53.44	29	82.45	64.82
22-Jul-10	51.38	37.11	88.5	58.06
24-Jul-10	50.58	49.34	99.92	50.62
26-Jul-10	45.45	35.91	81.36	55.86
28-Jul-10	56.27	51.59	107.87	52.17
30-Jul-10	58.33	38.23	96.57	60.41
01-Aug-10	54.35	34.65	89	61.07
03-Aug-10	49.78	36.42	86.19	57.75
05-Aug-10	52.07	36.06	88.13	59.08
07-Aug-10	59.33	38.58	97.91	60.6
09-Aug-10	68.58	29.36	97.94	70.02
11-Aug-10	51.76	25.6	77.36	66.91

Continued on next page

Table 4.1 – *Continued from previous page*

Date	$PM_{2.5}$	$PM_{10-2.5}$	PM_{10}	$\%(PM_{2.5}/PM_{10})$
13-Aug-10	54.77	32.79	87.56	62.56
15-Aug-10	55.27	29.59	84.87	65.13
17-Aug-10	63.04	47.25	110.29	57.16
19-Aug-10	58.88	39.8	98.68	59.66
21-Aug-10	58.09	40.98	99.08	58.63
23-Aug-10	58.57	28.78	87.34	67.05
25-Aug-10	66.5	43.14	109.64	60.65
27-Aug-10	61.22	36.27	97.49	62.8
02-Sep-10	65.1	41.13	106.23	61.28
04-Sep-10	57.59	44.87	102.46	56.2
06-Sep-10	73.07	71.47	144.54	50.55
08-Sep-10	57.89	65.99	123.88	46.73
10-Sep-10	58.47	47.35	105.81	55.26
12-Sep-10	59.91	64.79	124.7	48.05
14-Sep-10	72.66	69.03	141.68	51.28
16-Sep-10	52.42	35.4	87.82	59.69
18-Sep-10	88.43	37.27	125.7	70.35
20-Sep-10	64.74	47.11	111.85	57.88
24-Sep-10	60.64	49.1	109.74	55.26

Continued on next page

Table 4.1 – *Continued from previous page*

Date	$PM_{2.5}$	$PM_{10-2.5}$	PM_{10}	$\%(PM_{2.5}/PM_{10})$
26-Sep-10	71.61	62.77	134.38	53.29
30-Sep-10	87.8	46.08	133.88	65.58
07-Oct-10	55.35	42.38	97.73	56.63
09-Oct-10	57	45.75	102.75	55.47
11-Oct-10	52.96	40.58	93.54	56.62
13-Oct-10	55.27	41.96	97.23	56.85
15-Oct-10	57.23	42.8	100.03	57.21
17-Oct-10	53.68	42.45	96.13	55.84
19-Oct-10	59.77	55.08	114.85	52.04
21-Oct-10	55.92	40.9	96.82	57.75
23-Oct-10	56.92	39.19	96.12	59.22
25-Oct-10	56.28	45.04	101.32	55.55
01-Nov-10	82.5	42.76	125.27	65.86
03-Nov-10	76.58	33.63	110.21	69.49
05-Nov-10	76.04	38.76	114.8	66.24
07-Nov-10	77.41	41.73	119.14	64.98
09-Nov-10	80.17	41.84	122.01	65.71
11-Nov-10	78.65	47.12	125.77	62.53
13-Nov-10	75.62	44.6	120.21	62.9

Continued on next page

Table 4.1 – *Continued from previous page*

Date	$PM_{2.5}$	$PM_{10-2.5}$	PM_{10}	$\%(PM_{2.5}/PM_{10})$
21-Nov-10	67.71	40.13	107.84	62.79
23-Nov-10	80.58	38.75	119.33	67.53
25-Nov-10	75.08	36.36	111.45	67.37
27-Nov-10	81.13	32.99	114.12	71.09
01-Dec-10	147.97	26.39	174.36	84.87
03-Dec-10	158.86	40.25	199.11	79.79
05-Dec-10	151.36	59.68	211.03	71.72
07-Dec-10	136.8	47.5	184.3	74.23
09-Dec-10	152.76	104.09	256.85	59.47
11-Dec-10	153.15	23.03	176.18	86.93
13-Dec-10	206.52	164.66	371.18	55.64
15-Dec-10	153.67	99.05	252.72	60.81
21-Dec-10	159.26	37.35	196.61	81
23-Dec-10	150.84	26.06	176.9	85.27
27-Dec-10	171.94	96.35	268.29	64.09
29-Dec-10	149.01	40.82	189.83	78.5
04-Jan-11	263.38	79.02	342.4	76.92
06-Jan-11	259.52	129.29	388.81	66.75
08-Jan-11	282.26	122.66	404.92	69.71

Continued on next page

Table 4.1 – *Continued from previous page*

Date	$PM_{2.5}$	$PM_{10-2.5}$	PM_{10}	$\%(PM_{2.5}/PM_{10})$
10-Jan-11	257.24	57.47	314.71	81.74
12-Jan-11	287.3	65.04	352.34	81.54
18-Jan-11	344.68	89.33	434.01	79.42
20-Jan-11	257.41	82.47	339.89	75.74
22-Jan-11	349.68	98.99	448.67	77.94
24-Jan-11	258.92	71.93	330.85	78.26
28-Jan-11	282.79	110.54	393.34	71.9
30-Jan-11	265.1	97.53	362.63	73.1
05-Feb-11	147.32	43.67	190.99	77.13
07-Feb-11	141.59	36.4	177.99	79.55
09-Feb-11	139.68	35.27	174.95	79.84
11-Feb-11	150.71	37.95	188.66	79.89
13-Feb-11	138.94	25.01	163.95	84.75
17-Feb-11	145.72	34.28	180.01	80.95
19-Feb-11	132.3	28.53	160.83	82.26
21-Feb-11	137.8	33.8	171.6	80.3
23-Feb-11	132.39	26.85	159.23	83.14
27-Feb-11	129.49	34.41	163.9	79
07-Mar-11	77.66	32.87	110.53	70.26

Continued on next page

Table 4.1 – *Continued from previous page*

Date	$PM_{2.5}$	$PM_{10-2.5}$	PM_{10}	$\%(PM_{2.5}/PM_{10})$
09-Mar-11	80.71	40.09	120.8	66.81
11-Mar-11	68.81	36.89	105.7	65.1
13-Mar-11	67.15	41.14	108.28	62.01
15-Mar-11	82.45	58.28	140.73	58.59
17-Mar-11	65.96	50.72	116.68	56.53
19-Mar-11	74.88	47.33	122.21	61.27
21-Mar-11	67.78	53.88	121.66	55.71
23-Mar-11	62.58	57.4	119.98	52.16
25-Mar-11	62.19	49.39	111.58	55.74
27-Mar-11	62.4	54.13	116.54	53.55
02-Apr-11	37.18	47.95	85.13	43.68
04-Apr-11	49.56	57.16	106.72	46.44
06-Apr-11	46.39	49.26	95.65	48.5
08-Apr-11	40.21	51.1	91.31	44.04
10-Apr-11	48.46	56.5	104.96	46.17
16-Apr-11	54.01	45.72	99.73	54.16
18-Apr-11	35.43	62.31	97.74	36.25
20-Apr-11	46.39	45.37	91.76	50.55
22-Apr-11	55.97	56.17	112.14	49.91

Continued on next page

Table 4.1 – *Continued from previous page*

Date	$PM_{2.5}$	$PM_{10-2.5}$	PM_{10}	$\%(PM_{2.5}/PM_{10})$
24-Apr-11	51.56	34.83	86.39	59.68
28-Apr-11	45.22	40.63	85.85	52.67
30-Apr-11	65.22	50.25	115.48	56.48
Average	88.62		138.31	
N	145	145	145	145
Min	35.43	23.03	76.83	35.99
Max	349.68	164.66	448.67	86.93
Median	58.57	43.93	107.41	58.59

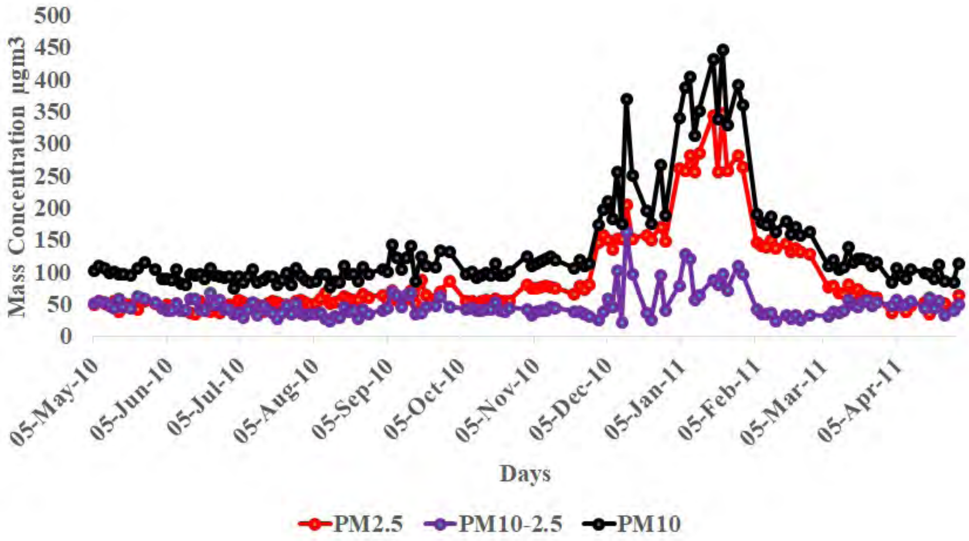

Figure 4.1: Time Series Plot of Particulate Mass Concentrations ($\mu g/cm^3$) for the Entire Sampling Period

Figure 4.1, figure 4.2 and figure 4.3 show the particulate mass concentration variations observed daily, monthly and the percentage ratio of $PM_{2.5}/PM_{10}$

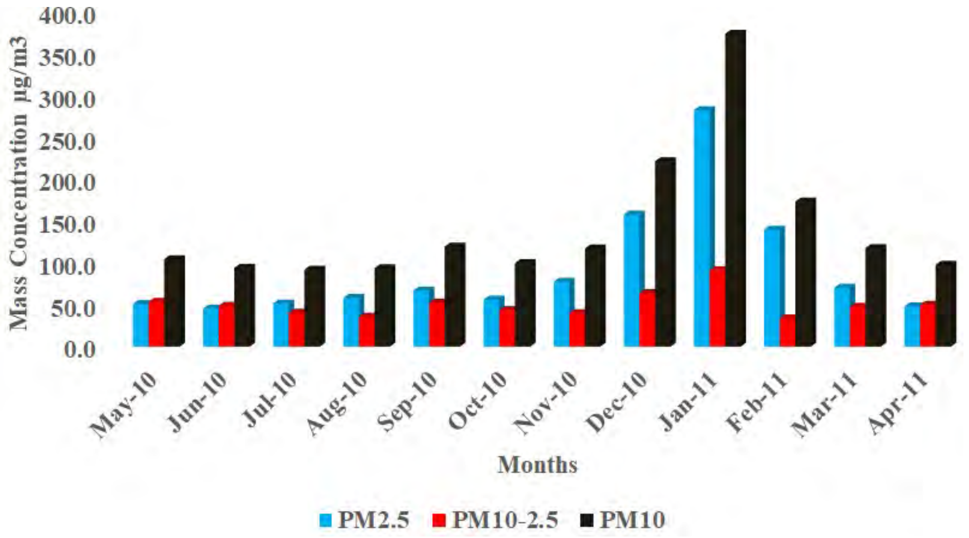

Figure 4.2: Average Monthly Particulate Mass Concentrations ($\mu g/cm^3$) for the Entire Sampling Period

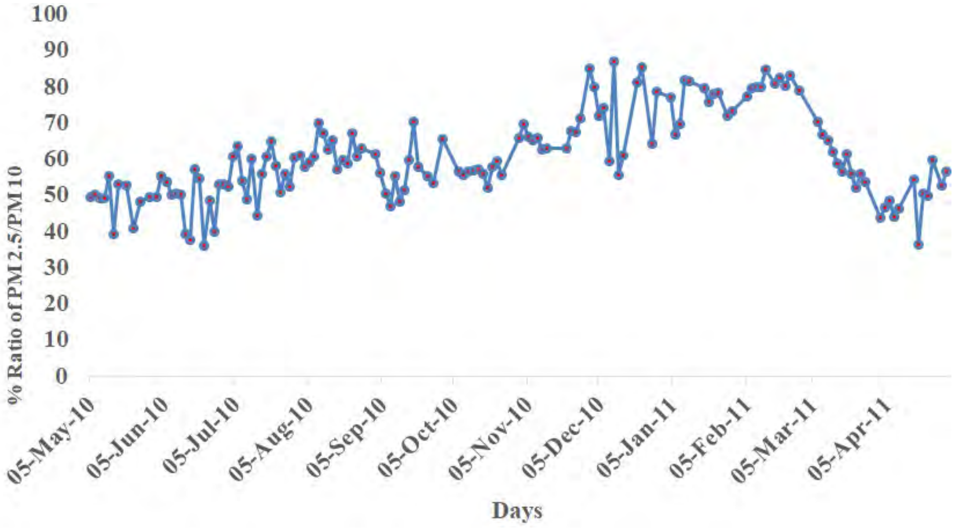

Figure 4.3: Percentage Ratio of $PM_{2.5}/PM_{10}$ for the Entire Sampling Period

respectively. The highest PM mass concentrations were observed in the months of December to February. This period is charactised by northeast trade winds which blow large amounts of dust from the Sahara desert, laden with emissions from dry season bush fires, towards the Gulf of Guinea in a south-westerly direction at an altitude of about 1500 m above sea level (Afeti and Resch, 2000); that is harmattan (Sunnu, 2006). Moreover harmattan is period where there is less or no rainfall (Adefolalu, 1984), (Adetunji et al., 1979). It could be one of the reason for having elevated or very high particulate mass concentrations. The ratio of $PM_{2.5}/PM_{10}$ is crucial and important to identify emission sources of PM. High ratio of $PM_{2.5}/PM_{10}$ shows that the majority contributions are accumulated by fine particle. The results of $PM_{2.5}/PM_{10}$ recorded show that the dominance of fine fractions at the sampling area, Agbogbloshie, could be attributed to smoke from the e-waste burning and other forms of burning (open burning of refuse, domestic waste and commercial waste).

Environmental Protection Agency, Ghana has a standard limit for PM_{10}; but, has currently no standard limit for $PM_{2.5}$. However, the USEPA standard is generally adopted for $PM_{2.5}$. Table **??**shows the Air Quality Guidelines (AQG) for some countries and organizations.

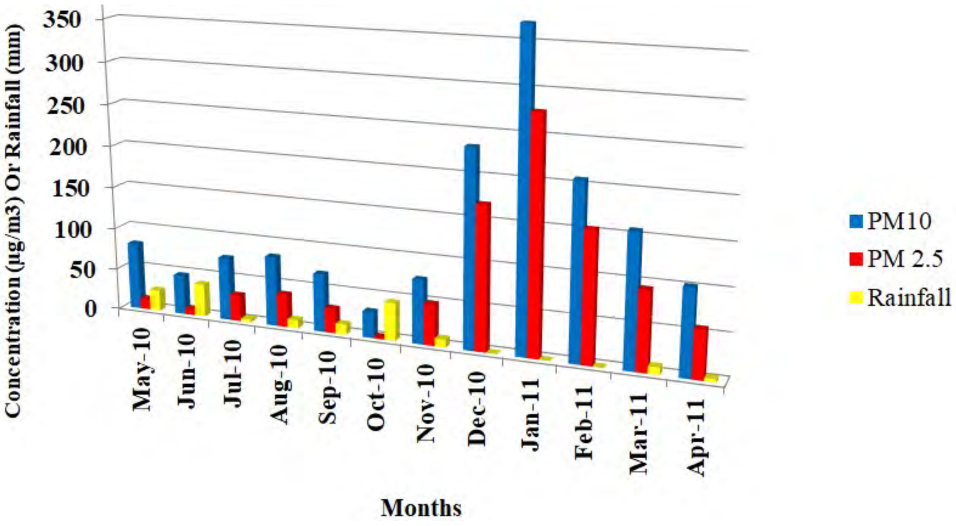

Figure 4.4: Average Monthly Particulate Mass Concentrations

This graph 4.4 shows the seasonal dependence of particulate matter. The blue and red bar graph are showing average monthly mass concentration for both fine and coarse fractions over the entire sampling period however the yellow bar graph represents the monthly average rainfall data for the area over the entire sampling period. We can easily recognize the two rainfall seasons in the southern part of the country. One in June and one in september-October, whenever the rainfall peaks that is where we have the least of particulate matter average mass concentration. In December to February which is the dry season. These are the areas where particulate matter mass concentrations are very high. One will obviously see the influence of the seasonal on the particulate matter level.

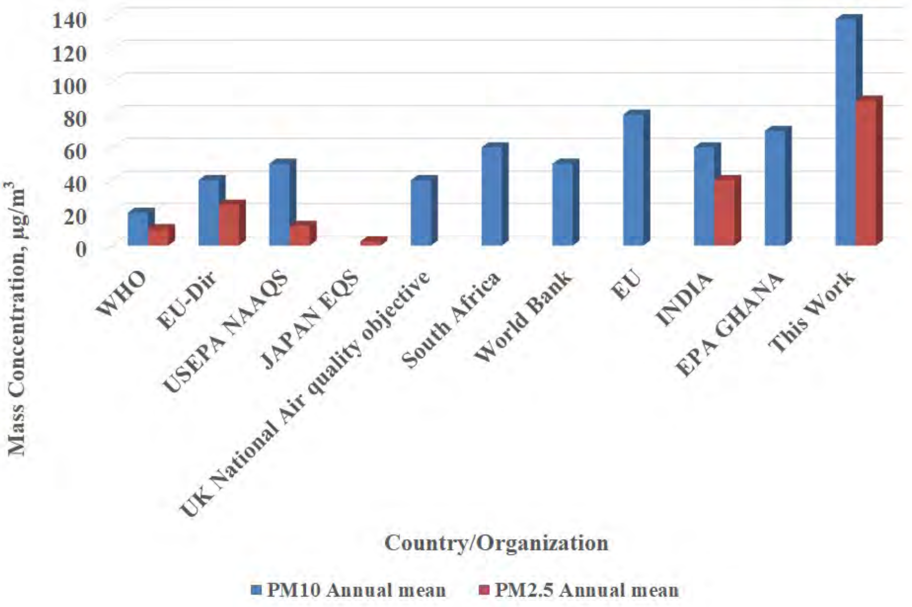

Figure 4.5: Annual Average Air quality standards/guideline for countries and organizations

This graph 4.5 shows the comparison between the annual Average mass concentration measured in this work and that of national and international air quality standards/guideline. In this work, APM annual Average mass concentration obtained at Agbogbloshie are relatively higher than expected treshold values for both national and international (WHO, USEPA, EU etc...) standards and guidelines.

4.2 Influence of Meteorological Parameters on Particulate matter

Meteorological factors such as temperature, relative humidity, rainfall and wind speed play an important role in particulate matter behavior in the atmosphere (El-Sharkawy and Zaki, 2015), (Habeebullah et al., 2015). The relationship between particulate matter mass concentration data and meteorological factors observed in this work are presented in Table 4.3

Table 4.2: Correlation Between Particulate Matter Concentrations and Meteorological Parameters

Particulars	PM_{10}	$PM_{2.5}$	$PM_{10-2.5}$
PM_{10}	1		
$PM_{2.5}$	.977**	1	
$PM_{10-2.5}$	.727**	.562**	1
Minimum Temperature	0.118	0.083	0.189*

Continued on next page

Table 4.2 – *Continued from previous page*

Particulars	PM_{10}	$PM_{2.5}$	$PM_{10-2.5}$
Maximum Temperature	0.352**	.355**	0.221**
Rainfall	-0.086	-0.107	0.011
Relative Humidity	-.175*	-.209*	-0.007
Wind Speed	-.440**	-.437**	-.299**

Table 4.3 shows the Pearsons correlation between meteorological factors and particulate matters. The outcome of the correlation calculation recorded are negative for rainfall, relative humidity and wind speed but only temperatures recorded positive correlation. Negative correlation between these factors (relative humidity and rainfall) and particulate matter is normal because it might be due to washout process as rain exhibits wet deposition effect on particulate matter. Rainfall removes atmospheric particulates and moisture restricts the possibility of resuspended soil particulate by making the soil humid (Leise et al.,),(Misra et al., 2008), so for that reason particulate matter in the atmosphere will have less mass concentration. Wind speed also recorded negative correlation, it plays a major role in the transportation of the particulate matter from one point to another, wind speed affects the turbulence near the ground (Guerra et al., 2006). The greater the wind speed, the greater the dispersion of particulates, the greater the

dilution effects and transport of the particulate hence the lower the mass concentration(Mkoma and Mjemah, 2011),(Oren et al., 2001). Since the temperature recorded positive correlation, this must due to the reason that warm air is good for more atmospheric dispersion.

4.3 APM elemental determination

4.3.1 Validation process

To detect the accuracy and reliability of the quantification method I have used in evaluate the concentrations. Quality control and quality assurance of method validation were applied using Standard Reference Material (SRM 2783) which is an air Particulate sample deposited on nuclepore filter just like the same filter I have in my analysis. I have used my quantification method to calculate the concentrations and and comparing them with the certified values, I realised that the accuracy range fall between 87-97%. This showed that my results are within the acceptable limit.

Table 4.3: Validation of quantification method (SRM 2783) ngm^{-3}

Element	**Measured**	**Error**	**Certified**	**Error**	**Measured/Certified**
Element	Measured	Error	Certified	Error	Measured/Certified
Na	1910	112.69	1860	100	1.03

Continued on next page

Table 4.3 – *Continued from previous page*

Element	**Measured**	**Error**	**Certified**	**Error**	**Measured/Certified**
Mg	8880	523.92	8620	520	1.03
Al	23667	591.68	23210	530	1.02
Si	59389	1722.28	58600	1600	1.01
S	863	215.75	1050	260	0.82
K	5479	487.63	5280	520	1.04
Ca	14794	1287.08	13200	1700	1.12
Ti	1676	284.92	1490	240	1.12
V	52.6	3.63	48.5	6	1.08
Cr	152.5	12.96	135	25	1.13
Mn	329.7	13.52	320	12	1.03
Fe	27498.7	1594.92	26500	1600	1.04
Ni	75.4	6.71	68	12	1.11
Cu	437.8	42.47	404	42	1.08
Zn	1897.8	113.87	1790	130	1.06
As	12.67	1.09	11.8	1.2	1.07
Ba	363.9	40.03	335	50	1.09
Pb	361.2	46.96	317	54	1.14

4.3.2 Acquisition of the Spectrum

Figure 4.6 shows the spectrum of nuclepore filter measured with PIXE, the peak profiles are shown clearly, the position of energy determine the elements in the filter while the areas under the curve determine the concentration of the elements. The spectra were acquired simultaneously with silicon drift detectors (SSD1 and SSD2). Both detectors have different energy resolutions, the detector (SSD1) was only used to detect elements with characteristic X-ray energies up to 7 keV but the second detector (SSD2) was used to detect elements with energies between 7 keV and 30 keV.

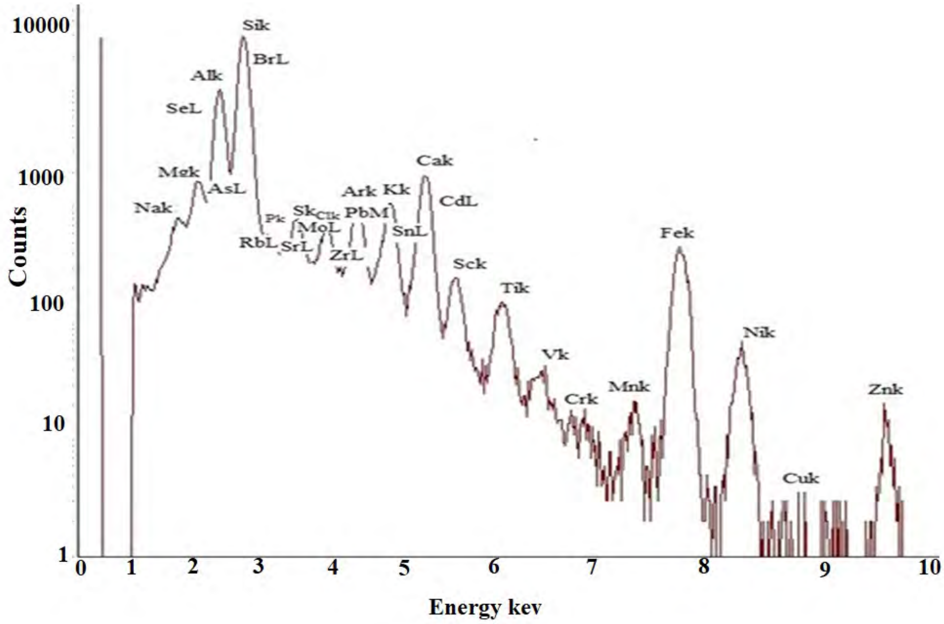

Figure 4.6: Spectrum of a Nuclepore Filter Measured with PIXE

4.3.3 Elemental Concentration (ngm^{-3}) of APM in both Fractions

Elemental concentrations of the following elements: Na, Mg, Al, Si, P, S, Cl, K, Ca, Ti, V, Cr, Mn, Fe, Ni, Cu, Zn, As, Se, Br, Rb, Sr, Zr, Mo, Pd, Cd, Sn, Cs, Ba, Pt, Hg and Pb were determined in 145 samples analysed. The minimum, maximum, median, and the enrichment factors of all the 32 elements were calculated and tabulated as shown in tables 4.5 and 4.8. The five highest elemental concentration in PM102.5 are Si (261.33 to 59950.56 ngm^{-3}) , Al (218.94 to 24719.25 ngm^{-3}), and Fe (182.08 to 18982.45 ngm^{-3}), Cl (587.76 to 15796.13 ngm^{-3}), Na (418.25 to 15010.32 ngm^{-3}); and for the fine fraction they occurred in the following order: Si (1339.93 to 61029.16 ngm^{-3}), Al (888.74 to 25389.05 ngm^{-3}), and Fe (769.28 to 19569.65 ngm^{-3}),Cl (1533.36 to 16741.73 ngm^{-3}), Na (1295.15 to 15887.22 ngm^{-3}). High levels of Na and Cl are recorded in the samples because the sampling site is just about 4 km away from the Atlantic Ocean, hence it received a lot particles from sea spray. Iron, aluminum and silicon are naturally abundant in the soil.

Table 4.4: Summary of Elemental Concentration (ngm^{-3}) in $PM_{10-2.5}$

Element	**Sample**	**Median**	**Min**	**Max**	**EF**
Element	Sample	Median	Min	Max	EF

Continued on next page

Table 4.4 – *Continued from previous page*

Element	**Sample**	**Median**	**Min**	**Max**	**EF**
Na	145	2831.49	1295.15	15887.22	0.77-22.18
Mg	145	771.45	259.92	3857.14	0.26-4.22
Al	145	2498.2	888.74	25389.05	*******
Si	145	3354.95	1339.93	61029.16	0.06-6.00
P	145	95.25	54.35	1125.8	0.69-25.42
S	145	689.3	249.06	3058.79	19.26-363.49
Cl	145	5167.96	1533.36	16741.73	154.82-5138.80
K	145	577.75	226.31	7624.03	0.11-10.10
Ca	145	1040.36	278.07	12892.93	0.11-5.51
Ti	145	67.71	18.03	1135.01	0.02-6.08
V	145	4.86	0.88	60.84	0.12-12.58
Cr	145	10.4	2.49	67.68	0.28-22.51
Mn	145	26.28	3.27	451.84	0.08-6.22
Fe	145	1369.15	769.28	19569.65	0.19-5.13
Ni	145	5.48	3.15	23.93	0.55-10.04
Cu	145	5.66	3.61	32.82	0.85-20.46
Zn	145	44.17	15.65	229.12	5.37-72.16
As	145	46.69	6.97	1113.52	40.51-18574.37
Se	145	0.86	0.27	9.38	78.13-9784.90

Continued on next page

Table 4.4 – *Continued from previous page*

Element	**Sample**	**Median**	**Min**	**Max**	**EF**
Br	145	32.69	9.29	124.85	59.83-2643.35
Rb	145	5.61	4.66	16.67	0.19-6.49
Sr	145	3.86	1.09	29.37	0.05-1.50
Zr	145	3.8	1.72	20.18	0.09-3.51
Mo	145	39.58	28.54	99.48	154.50-2894.68
Pd	145	38.78	17.78	73.2	**********
Cd	145	120.74	14.65	788.35	1494.57-206127.04
Sn	145	1219.54	833.12	4018.75	2416.79-113494.33
Cs	145	163.98	30.75	915.7	188.17-12963.95
Ba	145	247.82	10.81	1455.11	0.95-158.17
Pt	145	185.02	18.09	1040.99	***********
Hg	145	2.59	1.79	13.59	92.75-4297.64
Pb	145	4.91	1.45	117.57	1.83-238.53

Table 4.5: Summary of Elemental Concentration (ngm^{-3}) in $PM_{2.5}$

Element	**Sample**	**Median**	**Min**	**Max**	**EF**
Element	Sample	Median	Min	Max	EF
Na	145	2831.49	1295.15	15887.22	0.77-22.18
Mg	145	771.45	259.92	3857.14	0.26-4.22

Continued on next page

Table 4.5 – *Continued from previous page*

Element	**Sample**	**Median**	**Min**	**Max**	**EF**
Al	145	2498.2	888.74	25389.05	*******
Si	145	3354.95	1339.93	61029.16	0.06-6.00
P	145	95.25	54.35	1125.8	0.69-25.42
S	145	689.3	249.06	3058.79	19.26-363.49
Cl	145	5167.96	1533.36	16741.73	154.82-5138.80
K	145	577.75	226.31	7624.03	0.11-10.10
Ca	145	1040.36	278.07	12892.93	0.11-5.51
Ti	145	67.71	18.03	1135.01	0.02-6.08
V	145	4.86	0.88	60.84	0.12-12.58
Cr	145	10.4	2.49	67.68	0.28-22.51
Mn	145	26.28	3.27	451.84	0.08-6.22
Fe	145	1369.15	769.28	19569.65	0.19-5.13
Ni	145	5.48	3.15	23.93	0.55-10.04
Cu	145	5.66	3.61	32.82	0.85-20.46
Zn	145	44.17	15.65	229.12	5.37-72.16
As	145	46.69	6.97	1113.52	40.51-18574.37
Se	145	0.86	0.27	9.38	78.13-9784.90
Br	145	32.69	9.29	124.85	59.83-2643.35
Rb	145	5.61	4.66	16.67	0.19-6.49

Continued on next page

Table 4.5 – *Continued from previous page*

Element	**Sample**	**Median**	**Min**	**Max**	**EF**
Sr	145	3.86	1.09	29.37	0.05-1.50
Zr	145	3.8	1.72	20.18	0.09-3.51
Mo	145	39.58	28.54	99.48	154.50-2894.68
Pd	145	38.78	17.78	73.2	**********
Cd	145	120.74	14.65	788.35	1494.57-206127.04
Sn	145	1219.54	833.12	4018.75	2416.79-113494.33
Cs	145	163.98	30.75	915.7	188.17-12963.95
Ba	145	247.82	10.81	1455.11	0.95-158.17
Pt	145	185.02	18.09	1040.99	***********
Hg	145	2.59	1.79	13.59	92.75-4297.64
Pb	145	4.91	1.45	117.57	1.83-238.53

4.4 Enrichment Factor (E.F)

To differentiate between the elements originating from human activities and those from natural processes and to assess the degree anthropogenic influence E.F. was used. Elements with E.F approximately to 1 have strong natural component. Elements with high E.F could have anthropogenic origin or other natural sources such as marine aerosol. The contamination levels were calculated by the normalization of metal concentration with respect to the concentration of a reference element. Silicon (Si) was used as a reference element because of its abundance and also being a major constituent of clay minerals and it is less affected by anthropogenic influence (Balls et al., 1997), (Ryan and Windom, 1988), (Sinex and Wright, 1988).

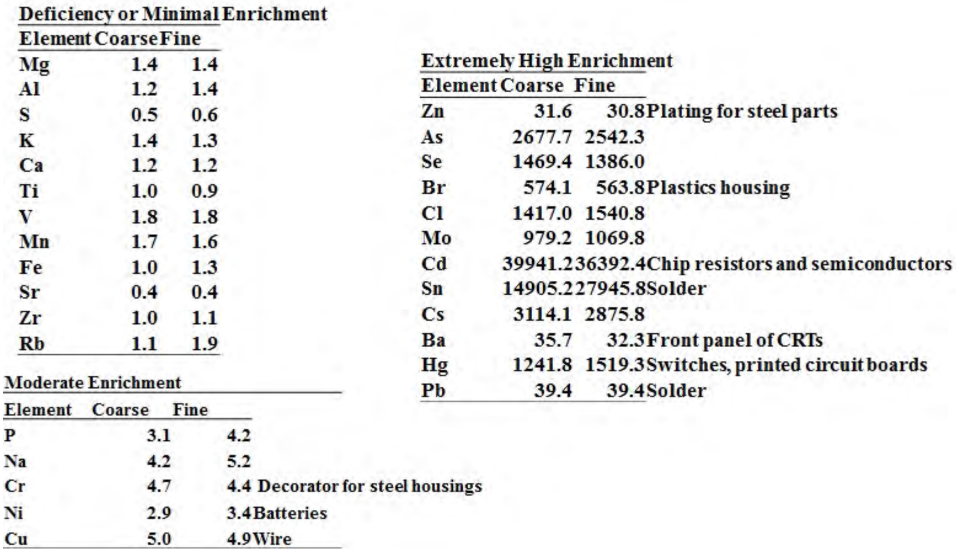

Deficiency or Minimal Enrichment

Element	Coarse	Fine
Mg	1.4	1.4
Al	1.2	1.4
S	0.5	0.6
K	1.4	1.3
Ca	1.2	1.2
Ti	1.0	0.9
V	1.8	1.8
Mn	1.7	1.6
Fe	1.0	1.3
Sr	0.4	0.4
Zr	1.0	1.1
Rb	1.1	1.9

Moderate Enrichment

Element	Coarse	Fine	
P	3.1	4.2	
Na	4.2	5.2	
Cr	4.7	4.4	Decorator for steel housings
Ni	2.9	3.4	Batteries
Cu	5.0	4.9	Wire

Extremely High Enrichment

Element	Coarse	Fine	
Zn	31.6	30.8	Plating for steel parts
As	2677.7	2542.3	
Se	1469.4	1386.0	
Br	574.1	563.8	Plastics housing
Cl	1417.0	1540.8	
Mo	979.2	1069.8	
Cd	39941.2	36392.4	Chip resistors and semiconductors
Sn	14905.2	27945.8	Solder
Cs	3114.1	2875.8	
Ba	35.7	32.3	Front panel of CRTs
Hg	1241.8	1519.3	Switches, printed circuit boards
Pb	39.4	39.4	Solder

Figure 4.7: Enrichment Factors

Enrichment Factor evaluation was carried for both $PM_{2.5}$ and $PM_{10-2.5}$ to ascertain whether the contamination is from natural or anthropogenic sources. By the rule of the enrichment factor evaluation, EF <1 is considered as natural sources whiles EF ≥ 1 is regarded as man-made or anthropogenic sources(Braga et al., 2005) , (Chimidza et al., 2001) , (Kothai et al., 2011). The standard and approved equation 3.9 for the calculation EF was used. The results of EF for both $PM_{2.5}$ and $PM_{10-2.5}$ were tabulated as shown in figure 4.7. The enrichment factor evaluation classifies pollution sources as either natural or anthropogenic, some elements analyzed at the sampling site having storng natural component (Cadle et al., 1999), (Garg et al., 2000), (Schauer et al., 2006). However, those elements having strong anthropogenic pollution are known elements associted with electrical and electronic products (Tonetti, 2000).

4.5 Source Apportionment of APM

The USEPA Positive Matrix Factorization (PMF) version 5.0 modeling software was used in the source identification and apportionment of APM. In both $PM_{2.5}$ and $PM_{10-2.5}$, PMF resolved five sources for each fractions. The change in individual elements signal-to-noise ratio(S/N) can give different meaning to the model. S/N provides some indications about whether the measured concentrations are the actual concentrations or within the measurement noise level. Any calculated S/N which fall within the interval 0.2 <S/N <2.0 is considered weak (Paatero and Hopke, 2003).

Table 4.6: Summary of Elemental Concentration (ngm^{-3}) in $PM_{2.5}$

Species	**S/N**	**Min**	**25th**	**Median**	**75th**	**Max**
Species	S/N	Min	25th	Median	75th	Max
PM2.5-10	10	76.83	96.1	107.41	137.55	448.67
Na	10	1.3	2.35	2.83	3.57	15.89

Continued on next page

Table 4.6 – *Continued from previous page*

Species	**S/N**	**Min**	**25th**	**Median**	**75th**	**Max**
Mg	10	0.26	0.63	0.77	1.23	3.86
Al	10	0.89	1.42	2.5	4.32	25.39
Si	10	1.34	2.19	3.35	5.7	61.03
P	9.6	0.05	0.08	0.1	0.17	1.13
S	8.9	0.25	0.54	0.69	1.1	3.06
Cl	10	1.53	4.13	5.17	6.41	16.74
K	9.8	0.23	0.46	0.58	1.1	7.62
Ca	10	0.28	0.79	1.04	1.85	12.89
Ti	8.2	0.02	0.04	0.07	0.27	1.14
V	7.8	0	0	0	0.01	0.06
Cr	6.7	0	0.01	0.01	0.02	0.07
Mn	6.6	0	0.01	0.03	0.09	0.45
Fe	10	0.77	1.09	1.37	3.09	19.57
Ni	8.7	0	0	0.01	0.01	0.02
Cu	9	0	0	0.01	0.01	0.03
Zn	8.9	0.02	0.04	0.04	0.09	0.23
As	9.4	0.01	0.02	0.05	0.25	1.11
Se	0.1	0	0	0	0	0.01
Br	9.5	0.01	0.02	0.03	0.04	0.12

Continued on next page

Table 4.6 – *Continued from previous page*

Species	**S/N**	**Min**	**25th**	**Median**	**75th**	**Max**
Rb	9.9	0	0	0.01	0.01	0.02
Sr	8.6	0	0	0	0.01	0.03
Zr	9	0	0	0	0.01	0.02
Mo	9.4	0.03	0.04	0.04	0.05	0.1
Pd	9.9	0.02	0.03	0.04	0.05	0.07
Cd	10	0.01	0.07	0.12	0.34	0.79
Sn	10	0.83	0.99	1.22	1.76	4.02
Cs	9.4	0.03	0.08	0.16	0.42	0.92
Ba	9.9	0.01	0.11	0.25	0.75	1.46
Pt	9.7	0.02	0.09	0.19	0.52	1.04
Hg	8.7	0	0	0	0	0.01
Pb	9.2	0	0	0	0.01	0.12

Research works done in Ghana, Africa and other parts of the world mostly shown that there were likely five possible sources at most of the sampling sites (Aboh et al., 2007), (Moloi et al., 2002), (Selin Lindgren et al., 2006). These likely sources were identified as soil/dust, sea spray, industry, transport or road traffic emissions and biomass burning in both $PM_{2.5}$ and $PM_{10-2.5}$. Factor profiles are represented pictorially; blue pale bar graphs describe the concentration of each species apportioned to the particular factors, while the percentage of each species apportioned to those factors is identified as red boxes. Factor contributions to each sample is shown as time series plot for each factor. This figure 4.8 shows the typical output of the PMF, for the purpose of understanding how the ngerprint and apportionment are done, I have enlarged the portions of this picture, in order to make the explanation clearer.

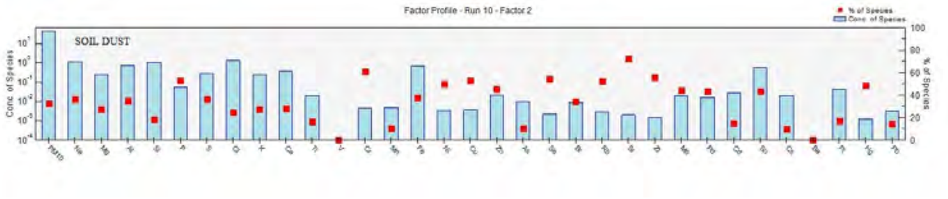

Figure 4.8: Typical Output of the PMF

4.5.1 Coarse fraction

This source figure 4.9 was identified as sea spray. Generally, fingerprint used to identify sea spray are Na, Cl, Mg and S and the samples analyzed at Agbogbloshie, these elements were identified in very concentrations and percentage contributions that clearly showed the contribution of sea spray to particulate matter at Agbogbloshie. This is because Agbogbloshie is very close to the Atlantic ocean. Simmilar works in the source apportionment have been done elswhwere which also identified sea spray with these elements (Na, Cl, Mg and S) (Guo et al., 2009), (Wu et al., 2007), (Watson and Chow, 2004).

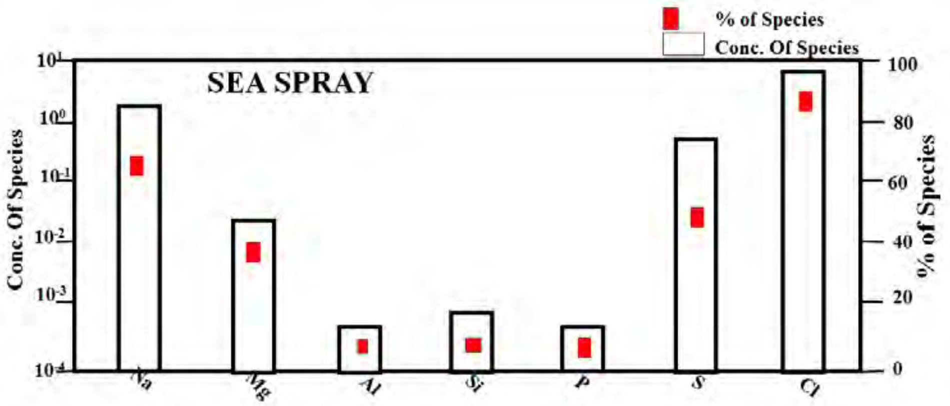

Figure 4.9: Sea spray source profile in coarse fraction

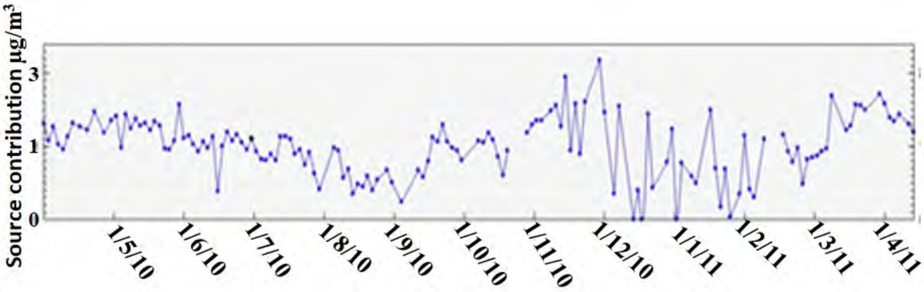

Figure 4.10: Time Series of $PM_{10-2.5}$ Source Contributions for sea spray

The second source figure 4.11 in the coarse fraction was also identified as soil dust, usually soil dust is always identified with the following fingerprint elements (Na, Mg, Al, Si, K, Ti, and Fe) (Kim and Jo, 2006), (Harrison et al., 2004) and (Ogunsola et al., 1994). The samples analyzed at Agbogbloshie, these elements were found and their contributions and percentage contributions are very high. This is because of unpaved roads at the area.

This source figure 4.13 was identify as heavy oil burning. Generally V, Ni and Cu are used to identify heavy oil burning, and these elemenst were

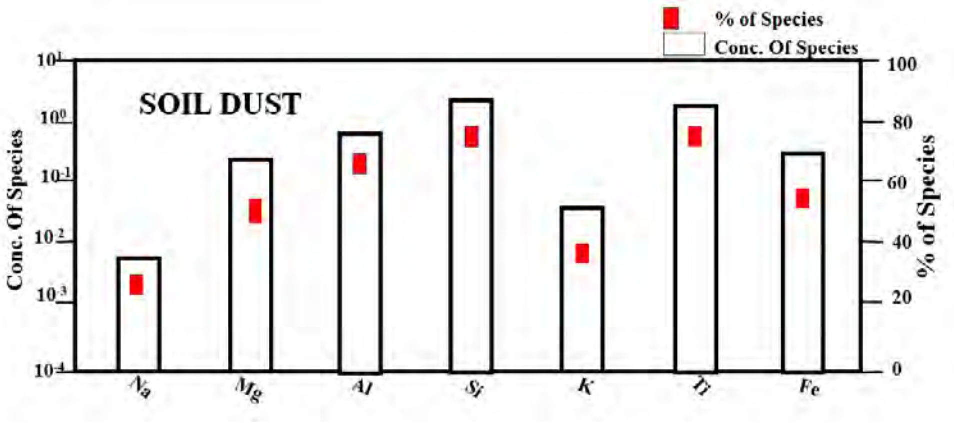

Figure 4.11: Soil dust source profile in coarse fraction

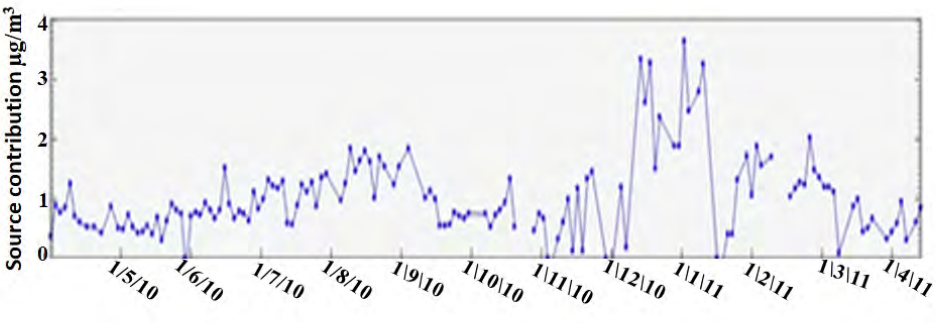

Figure 4.12: Time Series of $PM_{10-2.5}$ Source Contributions for soil dust

also found in the samples analyzed in Agbogbloshie, however all these elements were identify in high concentrations and high percentage contribution (Allen et al., 2001),(Molnar et al., 2005), (Ojanen et al., 1998).

This source figure 4.15 was identify as biomass burning and it is generally identified with the following fingerprint elements P, S, and K, however the samples analyzed at Agbogbloshie contained these elements high concentration and their percentages contribution to the fraction were also very high. This is as result of the burning of saw dust and the smoking of fish by the fishmongers not too far from the sampling site (Janssen et al., 1997),

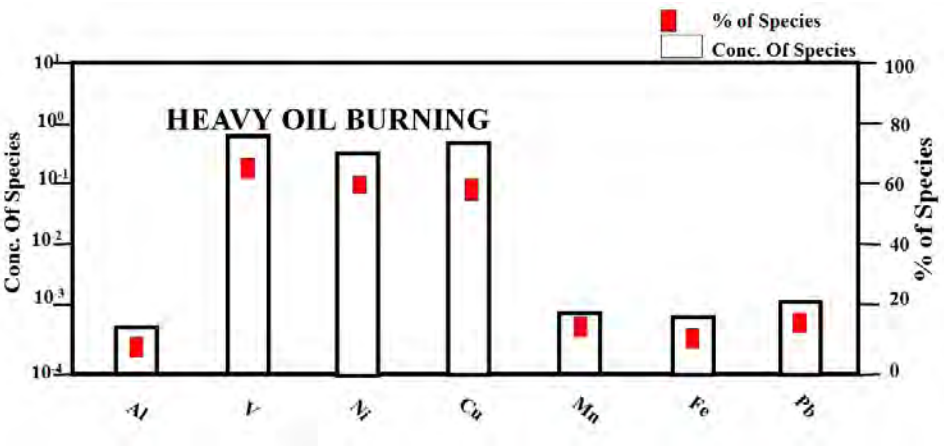

Figure 4.13: Heavy oil burning source profile in coarse fraction

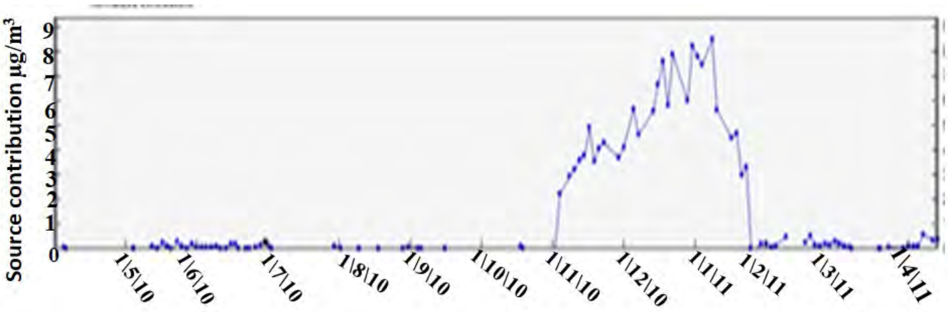

Figure 4.14: Time Series of $PM_{10-2.5}$ Source Contributions for heavy oil burning

(Song et al., 2006), (Adam, 2013).

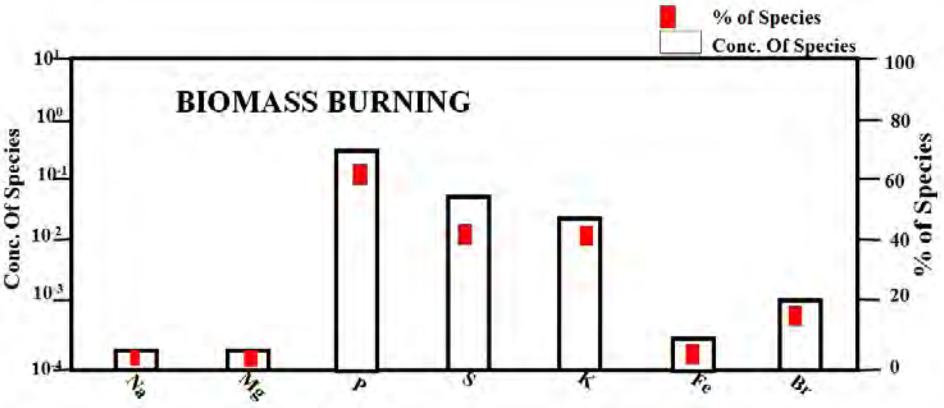

Figure 4.15: Biomass burning source profile in coarse fraction

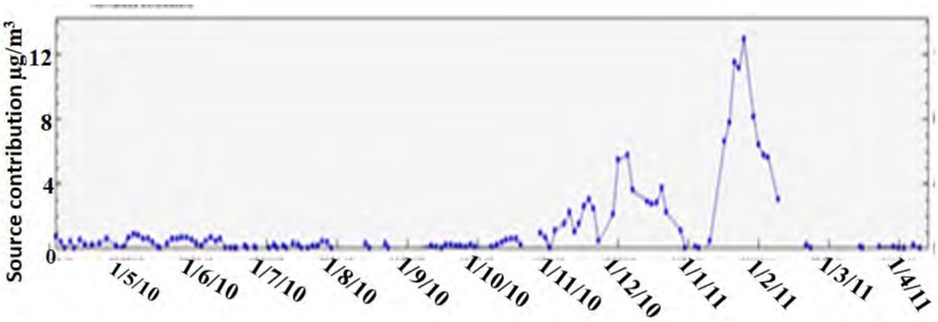

Figure 4.16: Time Series of $PM_{10-2.5}$ Source Contributions for biomass burning

The last source profile identified in the coarse was e-waste burning, this source was identified as e-waste because in EF evaluation, they are elements with EF which were associated with anthropogenic activities and they are also some known elements associated with electrical and electronic products.In addition some works have already been done looking at soil pollution, water and vegetable in Agbogbloshie close to the landfill and these elements were identified. So when the PMF was run and thses elements were picked in high concentrations and high percentage species, it is the confirmation that these are all elements coming from e-waste.

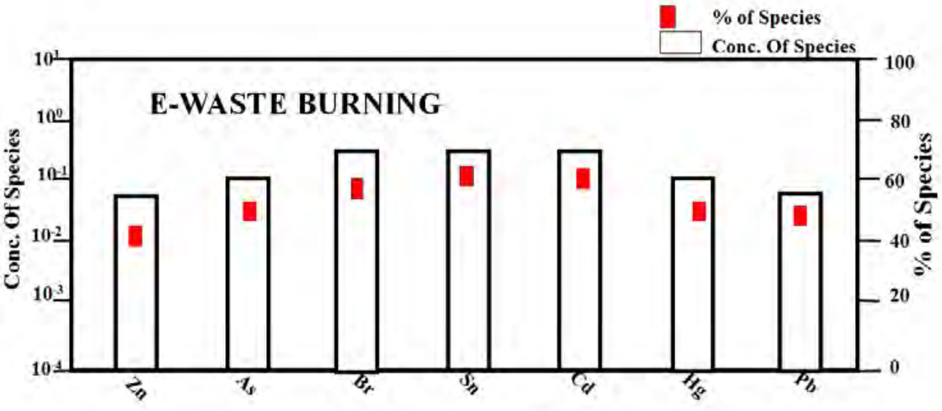

Figure 4.17: E-waste burning source profile in coarse fraction

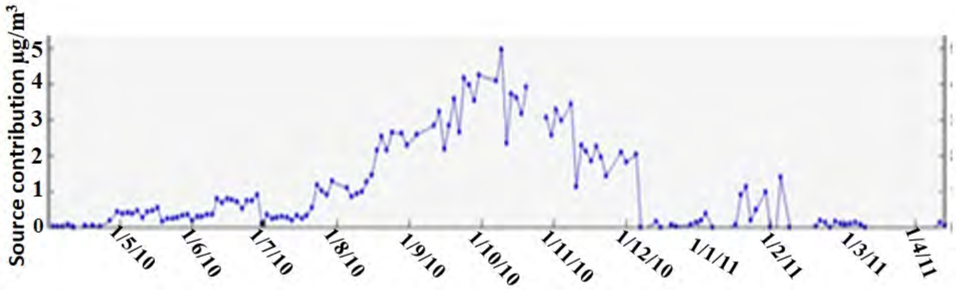

Figure 4.18: Time Series of $PM_{10-2.5}$ Source Contributions for e-waste burning

This figure 4.19 shows the contributed percentage of the species concentration to the various factors in the coarse fraction. Each factors has been colour coded for easy identification and explanation.

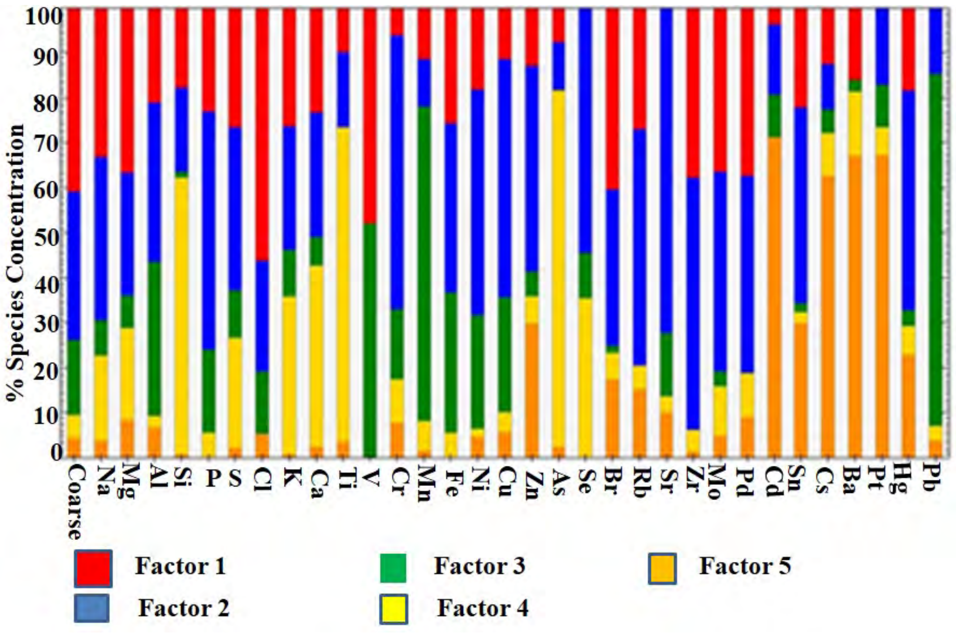

Figure 4.19: Elemental Source Profiles of $PM_{10-2.5}$

This figure 4.20 shows the percentage contribution of each identified sources in the coarse fraction. Soil dust sources contributed heavily (45%). The rest of the sources also contributed but not much, biomass burning has contribute 17%, heavy oil burning gave 16% of the contribution,12% of the total contribution came from sea spray and e-waste burning contributed 10%.

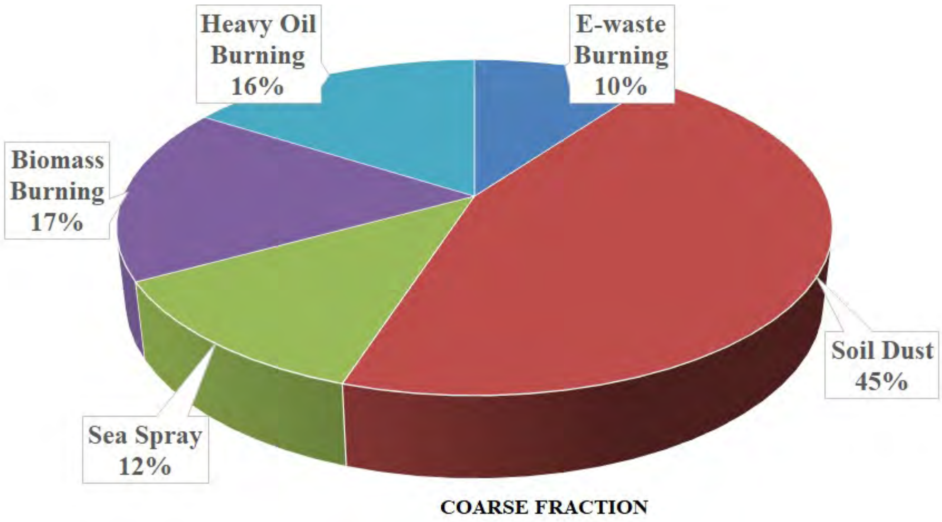

Figure 4.20: Source apportionment in coarse fraction

4.5.2 Fine fraction

In the fine fraction This source profile figure 4.21 was identified as e-waste burning, this source was identified as e-waste because in EF evaluation, they are elements with EF which were associated with anthropogenic activities and they are also some known elements associated with electrical and electronic products. In addition some works have already been done looking at soil pollution, water and vegetable in Agbogbloshie close to the landfill and these elements were identified. So when the PMF was run and thses elements were picked in high concentrations and high percentage species, it is the confirmation that these are all elements coming from e-waste.

Figure 4.21: E-waste burning source profile in fine fraction

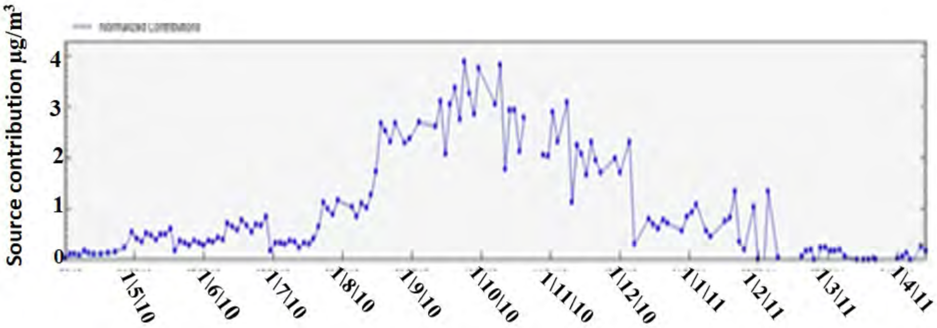

Figure 4.22: Time Series of $PM_{2.5}$ Source Contributions for e-waste burning

This source profile figure 4.23 was identified as industrial activities, generally fingerprint elements used to identify indutrial activities are V, Fe, Ni, Cu and Zn, and the samples analyzed at Agbogbloshie these elements were identified in very concentrations and percentage contributions. This is due to the presence of some many industries not to far far from the sampling area (D'Amato et al., 2010).

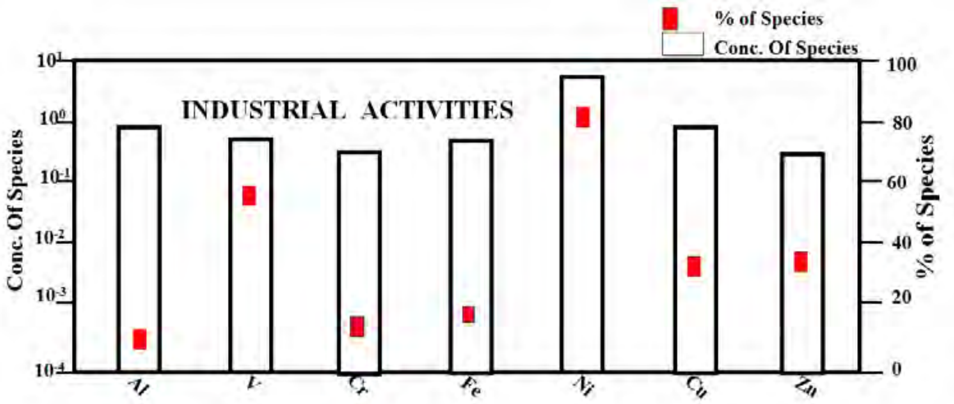

Figure 4.23: Industrial activities source profile in fine fraction

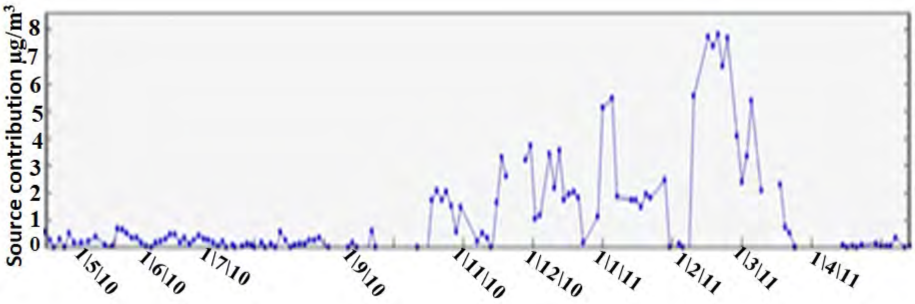

Figure 4.24: Time Series of $PM_{2.5}$ Source Contributions for industrial activities

This source profile figure 4.25 was identified as resuspended dust, generally fingerprint elements used to identify indutrial activities are Mg, Al, S, K, Ca, Ti, Mn, Fe, Zn, Pb, Sb, and the samples analyzed at Agbogbloshie these elements were identified in very concentrations and percentage contributions. This is as of lot of unpaved roads at the area (Gatari et al., 2005), (Ofosu et al., 2012).

This source figure 4.27 was identified as sea spray. Generally, fingerprint used to identify sea spray are Na, Cl, Mg and S and the samples analyzed at Agbogbloshie, these elements were identified in very concentrations and

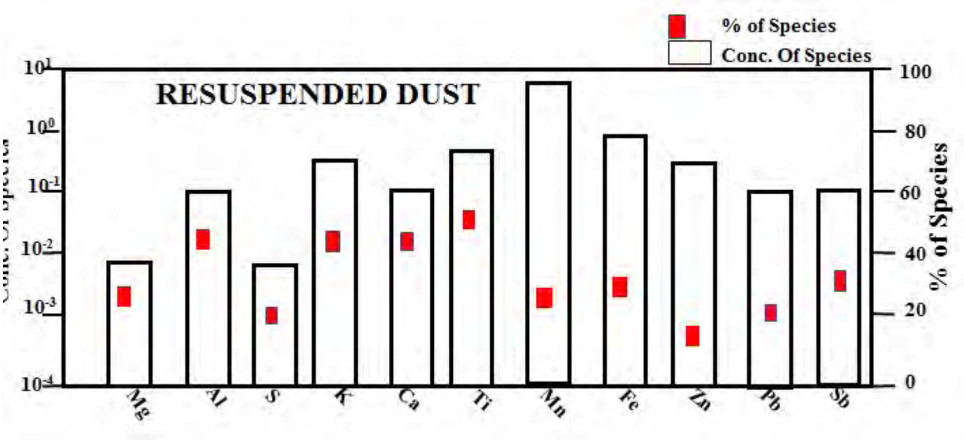

Figure 4.25: Resuspended dust source profile in fine fraction

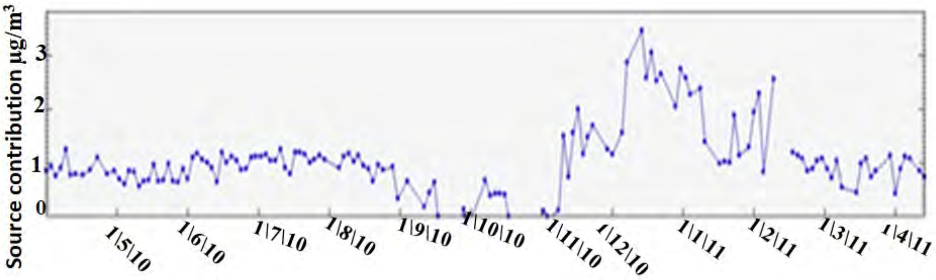

Figure 4.26: Time Series of $PM_{2.5}$ Source Contributions for resuspended dust

percentage contributions that clearly showed the contribution of sea spray to particulate matter at Agbogbloshie. This is because Agbogbloshie is very close to the Atlantic ocean. Simmilar works in the source apportionment have been done elswhwere which also identified sea spray with these elements (Na, Cl, Mg and S) (Guo et al., 2009), (Wu et al., 2007), (Watson and Chow, 2004).

This source figure 4.29 was identified as vehicular traffic. Generally, fingerprint used to identify vehicular traffic are Mn, Fe, Cu Zn (Gao et al., 2002) and the samples analyzed at Agbogbloshie, these elements were identified

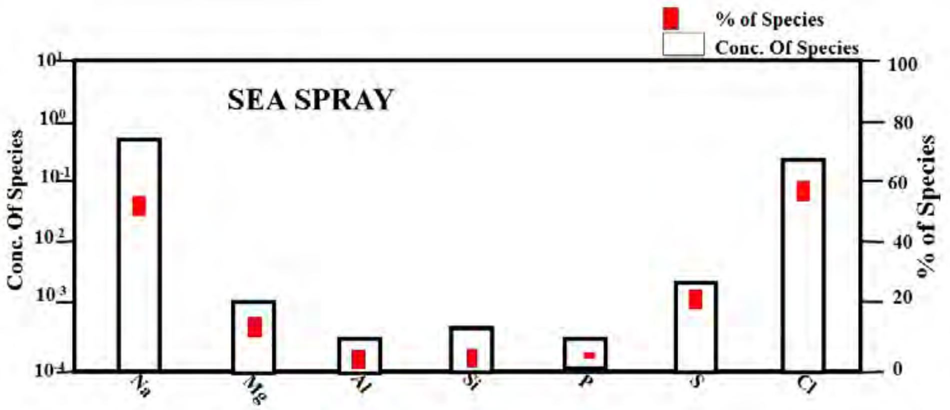

Figure 4.27: Sea spray source profile in fine fraction

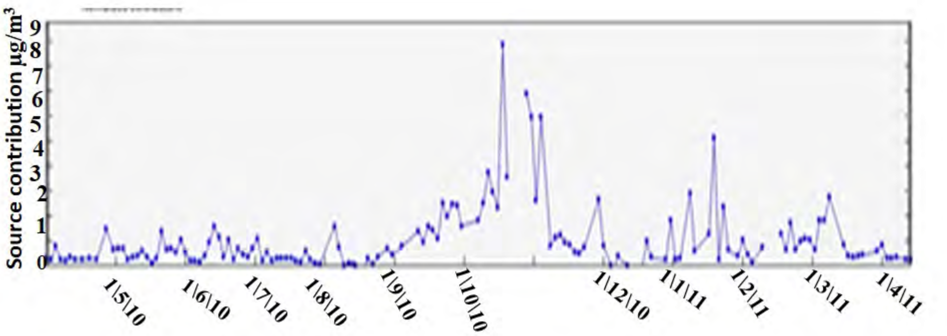

Figure 4.28: Time Series of $PM_{2.5}$ Source Contributions for Sea spray

in very concentrations and percentage contributions that clearly showed the contribution of vehicular traffic to particulate matter at Agbogbloshie. This is because Agbogbloshie is a heavy traffic area.

This figure 4.31 shows the contributed percentage of the species concentration to the various factors in the fine fraction. Each factors has been colour coded for easy identification and explanation.

This figure 4.32 shows the percentage contribution of each identified sources in the fine fraction. 49% of the total contribution in the fine fraction were

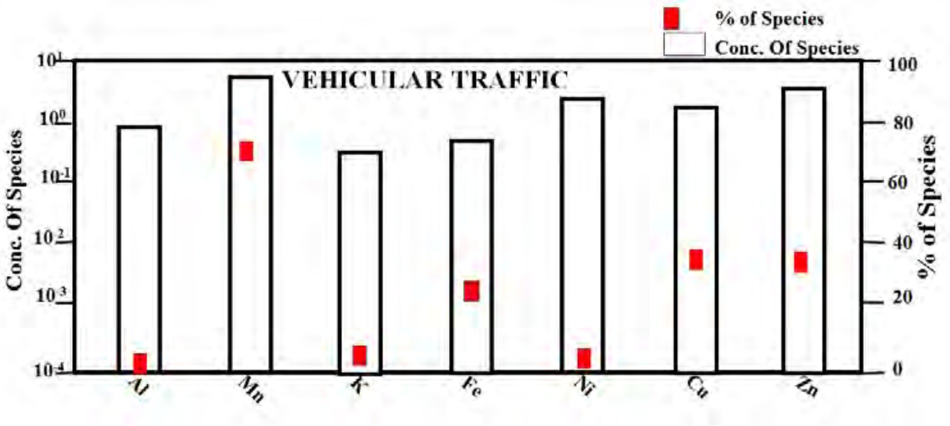

Figure 4.29: Vehicular traffic source profile in fine fraction

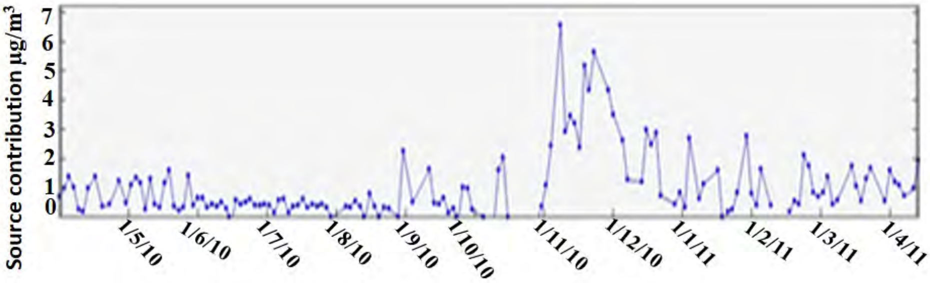

Figure 4.30: Time Series of $PM_{2.5}$ Source Contributions for vehicular traffic

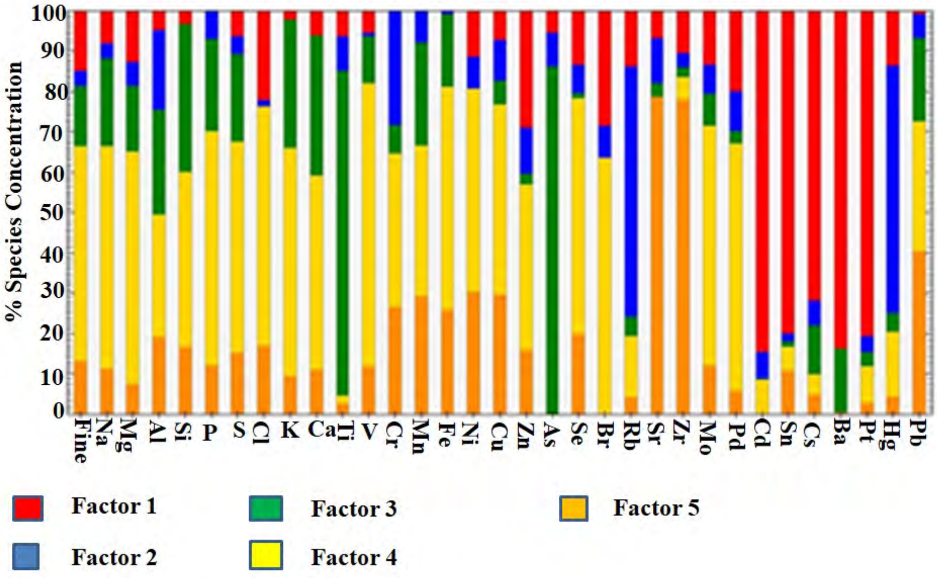

Figure 4.31: Elemental Source Profiles of $PM_{2.5}$

from e-waste burning, industrial activities contributed in total 23%, followed by 16%contribution form vehicualr traffic, resuspended dust and sea spray contributed 7% and 5% 4espectively.

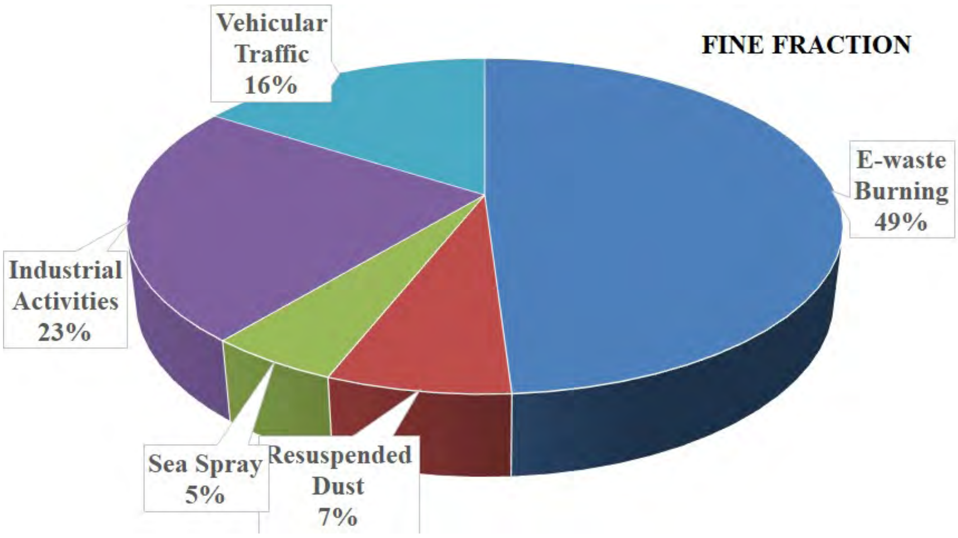

Figure 4.32: Source apportionment in fine fraction

Chapter 5

Chatper 5: Conclusions and Recommendations

5.1 Conclusions

A total of 290 samples were collected for the period of one year, from May, 2010 to April, 2011. The Gent sampler and nuclepore filters of pore sizes 0.4 µm and 8 µm receptively collect $PM_{2.5}$ and $PM_{10-2.5}$ fractions of atmospheric particulate matter (APM) at a scrap market in Agbogbloshie, Accra, Ghana. The parameters determined were particulates mass and elemental compositions. The mass of APM was obtained by gravimetric analysis and the elemental composition was determined by PIXE, PIGE and EDXRF analytical techniques.

The minimum, maximum and annual mean mass concentration values for $PM_{2.5}$ obtained for the sampling campaign were 35.43 $\mu g/m^3$, 349.68 $\mu g/m^3$ and 88.62$\mu g/m^3$ respectively. For PM_{10}, the minimum, maximum and annual mean mass concentration values were 76.83 gm3, 448.67 $\mu g/m^3$and 138.31 $\mu g/m^3$ respectively. The results obtained from this study were compared with the annual averages of some well established countries and organizations (the WHO, USEPA, EU, JAPAN EQS, UK National Air quality objective, World Bank and Canada air quality standards) in ambient air which ranged between 20 to 80 $\mu g/m^3$ for PM_{10} and $PM_{2.5}$ to 40 $\mu g/m^3$ for $PM_{2.5}$. Annual averages of 88.62 $\mu g/m^3$ for $PM_{2.5}$ and 138.31 $\mu g/m^3$forPM_{10} measured at Agbogbloshie are substantially higher. These observations are however different for both $PM_{2.5}$ and PM_{10} when the results from this work are comparable with works done in Sub-Saharan Africa. PM_{10} mass concentration levels in Addis Ababa were found to be between 10 to 100 $\mu g/m^3$, while in South Africa $PM_{2.5}$and PM_{10} levels of 86 $\mu g/m^3$ and 97 $\mu g/m^3$ respectively recorded. The average percentage ratio of $\%(PM_{2.5}/PM_{10})$ was 39.6%; this shows that the coarse fraction proportion of APM is not predominant. The fine fraction $PM_{2.5}$ was however found to dominate the APM loadings at the Agbogbloshie e-waste landfill site. A percentage ratio of 86.9% was found for $\%(PM_{2.5}/PM_{10})$, which is alarming because of the health impacts associated with high concentrations of fine fractions of APM.

Nuclear and related analytical techniques (EDXRF, PIXE and PIGE) were used to determine a total of 32 elements ranging from Na to Pb in the APM samples collected. Results from the analyses showed varying levels of concentrations with respect to dry season (harmattan) and rainy season. The average of five most abundant elements in coarse fraction $PM_{10-2.5}$ are Si: 6545.05 (range: 261.3359950.56) ngm^{-3} , Al: 3743.25 (range : 218.9424719.25) ngm^{-3} , Fe: 2464.77 (range: 182.0818982.45) ngm^{-3} , Cl: 5918.47 (range: 587.7615796.13) ngm^{-3} , Na: 4040.17 , (range: 418.2515010.32) ngm^{-3} . In the fine fraction $PM_{2.5}$ concentrations reordered were in the following order: Si: 5466.44 (range : 1339.9361029.16) ngm^{-3} , Al: 3073.44 (range: 888.7425389.05) ngm^{-3} , Fe: 1877.57 (range: 769.2819569.65) ngm^{-3} , Cl: 4972.86 (range: 1533.3616741.73) ngm^{-3} , and Na: 3163.27 (range: 1295.15 15887.22) ngm^{-3} . Coarse fractions recorded higher elemental concentrations as compare to fine fractions.

In this work, enrichment factor revealed a minimal enrichment to extremely high enrichment for some elements in the samples collected. With the exception of Cu all these elements Na, Mg, Al, Si, P ,K ,Ca, Ti, V, Cr, Mn, Fe, Ni, Cu, Rb, Sr and Zr are naturally abundant in the soil; therefore, they are associated with the natural source of pollution. Elements such as S, Zn, Br, Ba, Pb, Cl, As, Se, Mo, Cd, Sn, Cs and Hg are associated with the anthropogenic sources of pollution.

The USEPA PMF software was employed in the identification of specific sources and their contributions to the particulates collected in Agbogbloshie. With PMF five sources each were resolved for both $PM_{2.5}$ and $PM_{10-2.5}$. The following sources were identified for the $PM_{2.5}$: E-waste burning (49%), Industrial activities (23%), vehicular traffic (16%), resuspended dust (7%) and sea spray (5%). In the coarse fraction, soil dust (45%),biomass burning (17%), Heavy oil burning (16%),sea spray (12%) and e-waste burning (10%) were apportioned. Natural sources (45%) were the major contributors in the coarse fraction while anthropogenic sources(88%) were the major contributors in the fine fraction. E-waste burning contributions were identified in both fractions. In this work, the following elements (Zn, As, Br, Sn, Cd, Hg, Pb) have been identified as fingerprint for e-waste burning and this source contributed 49% of the pollutants identified in the study area.

5.2 Recommendations

From the results, discussions and conclusions of this work it is recommended that:

- The measurements should be continued at Agbogbloshie, so as to generate a larger data set for the improvement of the model and developed into a monitoring site with data spanning decades for long term trend studies.

- Permanent PM monitoring stations should be established at rural, urban and industrial areas to conduct regular monitoring of key indicator pollutants.
- Black carbon analysis should be conducted in future studies in Agbogbloshie and its surrounding neighbourhoods to understand their levels and health effects.
- For a more effective and efficient air quality situation in the country there is the need to set monitoring stations in all the capital cities and industrial cities.
- Increase community awareness and education on the effect of e-waste burning on the air quality as far as particulate matter are concerned.

References

Aboh, I. (2000). *Characterization and Sources of Air Particulate Matter at Kwabenya, Near Accra, Ghana.* PhD thesis, University of Ghana.

Aboh, I. J. K., Henriksson, D., Laursen, J., Lundin, M., Ofosu, F. G., Pind, N., Lindgren, E. S., and Wahnström, T. (2009). Identification of aerosol particle sources in semi-rural area of kwabenya, near accra, ghana, by edxrf techniques. *X-Ray Spectrometry*, 38(4):348–353.

Aboh, I. J. K., Henriksson, D., Laursen, J., Lundin, M., Pind, N., Lindgren, E. S., and Wahnström, T. (2007). Edxrf characterisation of elemental contents in pm2. 5 in a medium-sized swedish city dominated by a modern waste incineration plant. *X-Ray Spectrometry: An International Journal*, 36(2):104–110.

Adam, B. (2013). *Time and social theory.* John Wiley & Sons.

Adefolalu, D. (1984). On bioclimatological aspects of harmattan dust haze in nigeria. *Archives for meteorology, geophysics, and bioclimatology, Series B*, 33(4):387–404.

Adetunji, J., McGregor, J., and Ong, C. (1979). Harmattan haze. *Weather*, 34(11):430–436.

Afeti, G. and Resch, F. (2000). Physical characteristics of saharan dust near the gulf of guinea. *Atmospheric Environment*, 34(8):1273–1279.

Allen, A., Nemitz, E., Shi, J., Harrison, R., and Greenwood, J. (2001). Size distributions of trace metals in atmospheric aerosols in the united kingdom. *Atmospheric Environment*, 35(27):4581–4591.

Amankwaa, E. F. (2013). Livelihoods in risk: Exploring health and environmental implications of e-waste recycling as a livelihood strategy in ghana. *The Journal of Modern African Studies*, 51(4):551–575.

Angle, R. P. (2014). Industrial emissions management. In *Air Quality Management*, pages 187–202. Springer.

Annegarn, H., Cahill, T., Sellschop, J., and Zucchiatti, A. (1988). Time sequence particulate sampling and nuclear analysis. *Physica Scripta*, 37(2):282.

Aryal, R., Kim, A., Lee, B.-K., Kamruzzaman, M., and Beecham, S. (2013). Characteristics of atmospheric particulate matter and metals in industrial sites in korea. *Environment and pollution*, 2(4):10.

Atiemo, S. M., Ofosu, F. G., Aboh, I., and Kuranchie-Mensah, H. (2012). Assessing the heavy metals contamination of surface dust from waste electrical and electronic equipment (e-waste) recycling site in accra, ghana. *Res J Environ Earth Sci*, 4(5):605–611.

Ayers, G., Keywood, M., and Gras, J. (1999). Teom vs. manual gravimetric methods for determination of pm2. 5 aerosol mass concentrations. *Atmospheric Environment*, 33(22):3717–3721.

Balakrishnaiah, G., Kumar, K. R., Reddy, B., Gopal, K. R., Reddy, R., Reddy, L., Narasimhulu, K., Ahammed, Y. N., Balanarayana, C., Moorthy, K. K., et al. (2011). Characterization of pm, pm 10 and pm 2.5 mass concentrations at a tropical semi-arid station in anantapur, india. *92.60. Mt; 92.60. Sz.*

Balls, P., Hull, S., Miller, B., Pirie, J., and Proctor, W. (1997). Trace metal in scottish estuarine and coastal sediments. *Marine Pollution Bulletin*, 34(1):42–50.

Bandhu, H., Puri, S., Garg, M., Singh, B., Shahi, J., Mehta, D., Swietlicki, E., Dhawan, D., Mangal, P., and Singh, N. (2000). Elemental composition and sources of air pollution in the city of chandigarh, india, using edxrf and pixe techniques. *Nuclear Instruments and Methods* *in Physics Research Section B: Beam Interactions with Materials and Atoms*, 160(1):126–138.

Bandyopadhyay, A. (2010). Electronics waste management: Indian practices and guidelines. *International Journal of Energy & Environment*, (5).

Belis, C., Karagulian, F., Larsen, B., and Hopke, P. (2013). Critical review and meta-analysis of ambient particulate matter source apportionment using receptor models in europe. *Atmospheric Environment*, 69:94–108.

Bennet, C., Jonsson, P., and Selin Lindgren, E. (2005). Concentrations and sources of trace elements in particulate air pollution, dar es salaam, tanzania, studied by edxrf. *X-Ray Spectrometry: An International Journal*, 34(1):1–6.

Bezemer, G. (2009). Particle deposition and clearance from the respiratory tract. Master's thesis.

Boni, C., Caridi, A., Cereda, E., and Marcazzan, G. B. (1990). A pixe-pige setup for the analysis of thin samples. *Nuclear Instruments and Methods in Physics Research Section B: Beam Interactions with Materials and Atoms*, 47(2):133–142.

Braga, C., Teixeira, E., Meira, L., Wiegand, F., Yoneama, M., and Dias, J. (2005). Elemental composition of pm10 and pm2. 5 in urban environment in south brazil. *Atmospheric Environment*, 39(10):1801–1815.

Cadle, S. H., Mulawa, P. A., Hunsanger, E. C., Nelson, K., Ragazzi, R. A., Barrett, R., Gallagher, G. L., Lawson, D. R., Knapp, K. T., and Snow, R. (1999). Composition of light-duty motor vehicle exhaust particulate matter in the denver, colorado area. *Environmental Science & Technology*, 33(14):2328–2339.

Caffrey, P. F., Ondov, J. M., Zufall, M. J., and Davidson, C. I. (1998). Determination of size-dependent dry particle deposition velocities with multiple intrinsic elemental tracers. *Environmental science & technology*, 32(11):1615–1622.

Calzolai, G., Chiari, M., Lucarelli, F., Nava, S., and Portarena, S. (2010). Proton induced γ-ray emission yields for the analysis of light elements in aerosol samples in an external beam set-up. *Nuclear Instruments and Methods in Physics Research Section B: Beam Interactions with Materials and Atoms*, 268(10):1540–1545.

Canha, N., Almeida-Silva, M., Freitas, M. d. C., Almeida, S. M., and Wolterbeek, H. T. (2011). Seasonal variation of total particulate matter and children respiratory diseases at lisbon primary schools using passive methods. *Procedia Environmental Sciences*, pages 170–183.

Cao, J., Lee, S., Zheng, X., Ho, K., Zhang, X., Guo, H., Chow, J. C., and Wang, H. (2003). Characterization of dust storms to hong kong in april 1998. *Water, Air and Soil Pollution: Focus*, 3(2):213–229.

Chan, Y.-c., Hawas, O., Hawker, D., Vowles, P., Cohen, D. D., Stelcer, E., Simpson, R., Golding, G., and Christensen, E. (2011). Using multiple type composition data and wind data in pmf analysis to apportion and locate sources of air pollutants. *Atmospheric Environment*, 45(2):439–449.

Chang, T.-J., Kao, H.-M., Wu, Y.-T., and Huang, W.-H. (2009). Transport mechanisms of coarse, fine, and very fine particulate matter in urban street canopies with different building layouts. *Journal of the Air & Waste Management Association*, 59(2):196–206.

Chao, C. Y. and Wong, K. K. (2002). Residential indoor pm10 and pm2. 5 in hong kong and the elemental composition. *Atmospheric Environment*, 36(2):265–277.

Chimidza, S., Viksna, A., and Selin Lindgren, E. (2001). Edxrf and txrf analysis of aerosol particles and the mobile fraction of soil in botswana. *X-Ray Spectrometry: An International Journal*, 30(5):301–307.

Currie, L. A. (1999). Detection and quantification limits: origins and historical overview1. *Analytica Chimica Acta*, 391(2):127–134.

D'Amato, G., Cecchi, L., D'amato, M., Liccardi, G., et al. (2010). Urban air pollution and climate change as environmental risk factors of respiratory allergy: an update. *Journal of Investigational Allergology and Clinical Immunology*, 20(2):95–102.

Davidson, C. I., Lin, S. F., Osborn, J. F., Pandey, M., Rasmussen, R., and Khalil, M. (1986). Indoor and outdoor air pollution in the himalayas. *Environmental science & technology*, 20(6):561–567.

Diaz-Barriga, F. (2013). Evidence-based intervention programs to reduce childrens exposure to chemicals in e-waste sites. Discussion paper for WHO Working Meeting on e-waste and childrens health. 1–90.

Dominici, F., Peng, R. D., Barr, C. D., and Bell, M. L. (2010). Protecting human health from air pollution: shifting from a single-pollutant to a multi-pollutant approach. *Epidemiology (Cambridge, Mass.)*, 21(2):187.

Dzubay, T. G. and Barbour, R. K. (1983). A method to improve the adhesion of aerosol particles on teflon filters. *Journal of The Air Pollution Control Association*, 33(7):692–695.

El-Sharkawy, M. F. and Zaki, G. R. (2015). Effect of meteorological factors on the daily average levels of particulate matter in the eastern province of saudi arabia: A cross-sectional study. *Turkish Online Journal of Science & Technology*, 5(1).

Engelbrecht, J. P., Swanepoel, L., Chow, J. C., Watson, J. G., and Egami, R. T. (2001). Pm2. 5 and pm10 concentrations from the qalabotjha low-smoke fuels macro-scale experiment in south africa. *Environmental Monitoring and Assessment*, 69(1):1–15.

Etyemezian, V., Tesfaye, M., Yimer, A., Chow, J., Mesfin, D., Nega, T., Nikolich, G., Watson, J., and Wondmagegn, M. (2005). Results from a pilot-scale air quality study in addis ababa, ethiopia. *Atmospheric environment*, 39(40):7849–7860.

Fabretti, J.-F., Sauret, N., Gal, J.-F., Maria, P.-C., and Schärer, U. (2009). Elemental characterization and source identification of pm2. 5 using positive matrix factorization: The malraux road tunnel, nice, france. *Atmospheric Research*, 94(2):320–329.

Finlayson-Pitts, B. J. and Pitts Jr, J. N. (1986). Atmospheric chemistry. fundamentals and experimental techniques.

Finlayson-Pitts, B. J. and Pitts Jr, J. N. (1999). *Chemistry of the upper and lower atmosphere: theory, experiments, and applications*. Elsevier.

Foltescu, V. L. (1995). *Fine atmospheric particles: formation, transport and deposition.*

Fourn, L. and Fayomi, E. (2006). Pollution atmosphérique en milieu urbain à cotonou et à lokossa, bénin. *Bull Soc Pathol Exot*, 99(4):264–268.

Garg, B. D., Cadle, S. H., Mulawa, P. A., Groblicki, P. J., Laroo, C., and Parr, G. A. (2000). Brake wear particulate matter emissions. *Environmental Science & Technology*, 34(21):4463–4469.

Garman, E. F. and Grime, G. W. (2005). Elemental analysis of proteins by micropixe. *Progress in biophysics and molecular biology*, 89(2):173–205.

Gatari, M., Wagner, A., and Boman, J. (2005). Elemental composition of tropospheric aerosols in hanoi, vietnam and nairobi, kenya. *Science of the Total Environment*, 341(1-3):241–249.

Gomišček, B., Hauck, H., Stopper, S., and Preining, O. (2004). Spatial and temporal variations of pm1, pm2. 5, pm10 and particle number concentration during the auphepproject. *Atmospheric Environment*, 38(24):3917–3934.

Grover, B. D. (2006). Measurement, characterization, and source apportionment of the major chemical components of fine particulate material, including semi-volatile species.

Guerra, S. A., Lane, D. D., Marotz, G. A., Carter, R. E., Hohl, C. M., and Baldauf, R. W. (2006). Effects of wind direction on coarse and fine particulate matter concentrations in southeast kansas. *Journal of the Air & Waste Management Association*, 56(11):1525–1531.

Guo, H., Ding, A., So, K., Ayoko, G., Li, Y., and Hung, W. (2009). Receptor modeling of source apportionment of hong kong aerosols and the implication of urban and regional contribution. *Atmospheric Environment*, 43(6):1159–1169.

Habeebullah, T. M., Munir, S., AA, A. H., Morsy, E. A., Seroji, A. R., and Mohammed, A. M. (2015). The interaction between air quality and meteorological factors in an arid environment of makkah, saudi arabia. *International Journal of Environmental Science and Development*, 6(8):576.

Harrison, R. M., Jones, A. M., and Lawrence, R. G. (2004). Major component composition of pm10 and pm2. 5 from roadside and urban background sites. *Atmospheric Environment*, 38(27):4531–4538.

Harrison, R. M. and Yin, J. (2000). Particulate matter in the atmosphere: which particle properties are important for its effects on health? *Science of the total environment*, 249(1-3):85–101.

Hinds, W. C. (2012). *Aerosol technology: properties, behavior, and measurement of airborne particles*. John Wiley & Sons.

Huang, S. and Conte, M. (2009). Source/process apportionment of major and trace elements in sinking particles in the sargasso sea. *Geochimica et Cosmochimica Acta*, 73(1):65–90.

Hung, W., Cheung, C., Chan, T., Co, M., and Chan, N. (2002). Better air quality 2002: Regional workshop on better air quality in asian and pacific rim cities, hong kong: proceedings, 16-18 december 2002.

Janssen, N. A., Van Mansom, D. F., Van Der Jagt, K., Harssema, H., and Hoek, G. (1997). Mass concentration and elemental composition of airborne particulate matter at street and background locations. *Atmospheric Environment*, 31(8):1185–1193.

Jex, D., Hill, M., and Mangelson, N. (1990). Proton induced x-ray emission of spherical particles: Corrections for x-ray attenuation. *Nuclear Instruments and Methods in Physics Research Section B: Beam Interactions with Materials and Atoms*, 49(1-4):141–145.

JOHANSSON, S. A. (1992). Optimization of the sensitivity in pixe analysis. *International Journal of PIXE*, 2(01):33–46.

Johansson, S. A., Campbell, J. L., Malmqvist, K. G., Winefordner, J. D., et al. (1995). *Particle-induced X-ray emission spectrometry (PIXE)*, volume 133. John Wiley & Sons.

John, W. and Reischl, G. (1978). Measurements of the filtration efficiencies of selected filter types. *Atmospheric Environment (1967)*, 12(10):2015–2019.

Johnson, K. S., Foy, B. d., Zuberi, B., Molina, L., Molina, M. J., Xie, Y., Laskin, A., and Shutthanandan, V. (2006). Aerosol composition and source apportionment in the mexico city metropolitan area with pixe/pesa/stim and multivariate analysis. *Atmospheric Chemistry and Physics*, 6(12):4591–4600.

Kaur, S., Nieuwenhuijsen, M., and Colvile, R. (2005). Personal exposure of street canyon intersection users to pm2. 5, ultrafine particle counts and carbon monoxide in central london, uk. *Atmospheric Environment*, 39(20):3629–3641.

Kgabi, N. A. (2010). An assessment of common atmospheric particulate matter sampling and toxic metal analysis methods. *African Journal of Environmental Science and Technology*, 4(11):718–728.

Kim, M.-K. and Jo, W.-K. (2006). Elemental composition and source characterization of airborne pm 10 at residences with relative proximities to metal-industrial complex. *International archives of occupational and environmental health*, 80(1):40–50.

Kothai, P., Saradhi, I., Pandit, G., Markwitz, A., and Puranik, V. (2011). Chemical characterization and source identification of particulate matter at an urban site of navi mumbai, india. *Aerosol and Air Quality Resarch*, 11(5):560–569.

Lannefors, H., Hansson, H.-C., and Granat, L. (1983). Background aerosol composition in southern swedenfourteen micro and macro constituents measured in seven particle size intervals at one site during one year. *Atmospheric Environment (1967)*, 17(1):87–101.

Lee, B.-K. and Hieu, N. T. (2011). Seasonal variation and sources of heavy metals in atmospheric aerosols in a residential area of ulsan, korea. *Aerosol and Air Quality Resarch*, 11(6):679–688.

Leise, S., Zimmermann, F., and Matschullat, J. Regklam ergebnisbericht.

Liu, B. Y. and Lee, K. (1976). Efficiency of membrane and nuclepore filters for submicrometer aerosols. *Environmental Science & Technology*, 10(4):345–350.

Maenhaut, W., Francois, F., and Cafmeyer, J. (1994). The"gent"stacked filter unit (sfu) sampler for the collection of atmospheric aerosols in two size fractions: Description and instructions for installation and use. Technical report.

Maenhaut, W. and Raemdonck, H. (1984). Accurate calibration of a si (li) detector for pixe analysis. *Nuclear Instruments and Methods in Physics Research Section B: Beam Interactions with Materials and Atoms*, 1(1):123–136.

Maenhaut, W., Salma, I., Cafmeyer, J., Annegarn, H. J., and Andreae, M. O. (1996). Regional atmospheric aerosol composition and sources in the eastern transvaal, south africa, and impact of biomass burning. *Journal of Geophysical Research: Atmospheres*, 101(D19):23631–23650.

Marcazzan, G. B., Caruso, E., Cereda, E., Redaelli, P., Bacci, P., Ventura, A., and Lombardo, G. (1987). The cise pixe system for aerosol characterization in several italian sites. *Nuclear Instruments and Methods in Physics Research Section B: Beam Interactions with Materials and Atoms*, 22(1-3):305–314.

Maxwell, J., Campbell, J., and Teesdale, W. (1989). The guelph pixe software package. *Nuclear Instruments and Methods in Physics Research Section B: Beam Interactions with Materials and Atoms*, 43(2):218–230.

Misra, A., Jayaraman, A., and Ganguly, D. (2008). Validation of modis derived aerosol optical depth over western india. *Journal of Geophysical Research: Atmospheres*, 113(D4).

Mkoma, S. (2008). *Physico-chemical characterisation of atmospheric aerosols in Tanzania, with emphasis on the carbonaceous aerosol components and on chemical mass closure*. PhD thesis, Ghent University.

Mkoma, S., Tungaraza, C., Maenhaut, W., and Raes, N. (2010). Elemental composition and sources of atmospheric particulate matter in dar es salaam, tanzania. *Ethiopian Journal of Environmental Studies and Management*, 3(1).

Mkoma, S. L. and Mjemah, I. C. (2011). Influence of meteorology on ambient air quality in morogoro, tanzania. *International Journal of Environmental Sciences*, 1(6):1107.

Modak, P. (2010). Community-based waste management and composting for climate/co- benefits–case of bangladesh (2d) presented at the international consultative meeting on expanding waste management services in developing countries, 18-19 march 2010, tokyo, japan.

Molnar, P., Gustafson, P., Johannesson, S., Boman, J., Barregård, L., and Sällsten, G. (2005). Domestic wood burning and pm2. 5 trace elements: Personal exposures, indoor and outdoor levels. *Atmospheric Environment*, 39(14):2643–2653.

Moloi, K., Chimidza, S., Lindgren, E. S., Viksna, A., and Standzenieks, P. (2002). Black carbon, mass and elemental measurements of airborne particles in the village of serowe, botswana. *Atmospheric Environment*, 36(14):2447–2457.

Murray, K. E., Thomas, S. M., and Bodour, A. A. (2010). Prioritizing research for trace pollutants and emerging contaminants in the freshwater environment. *Environmental Pollution*, 158(12):3462–3471.

Needhidasan, S., Samuel, M., and Chidambaram, R. (2014). Electronic waste–an emerging threat to the environment of urban india. *Journal of Environmental Health Science and Engineering*, 12(1):36.

Nel, A. (2005). Air pollution-related illness: effects of particles. *Science*, 308(5723):804–806.

Norris, G. (2008). Epa positive matrix factorization (pmf) 3.0 fundamentals & user guide, us. environmental protection agency. *http://www. epa. gov/heasd/products/pmf/pmf. html*.

Oberdörster, G., Celein, R. M., Ferin, J., and Weiss, B. (1995). Association of particulate air pollution and acute mortality: involvement of ultrafine particles? *Inhalation toxicology*, 7(1):111–124.

Oberdörster, G. and Utell, M. J. (2002). Ultrafine particles in the urban air: to the respiratory tract–and beyond? *Environmental health perspectives*, 110(8):A440.

Ofosu, F. G., Aboh, I. J. K., and Bamford, S. A. Ambient air pm10 particulate levels at ashaiman near tema in ghana.

Ofosu, F. G., Hopke, P. K., Aboh, I. J., and Bamford, S. A. (2012). Characterization of fine particulate sources at ashaiman in greater accra, ghana. *Atmospheric Pollution Research*, 3(3):301–310.

Ogunsola, O., Oluwole, A., Asubiojo, O., Olaniyi, H., Akeredolu, F., Akanle, O., Spyrou, N., Ward, N., and Ruck, W. (1994). Traffic pollution: preliminary elemental characterisation of roadside dust in lagos, nigeria. *Science of the total environment*, 146:175–184.

Ojanen, C., Pakkanen, T., Aurela, M., Mäkelä, T., Meriläinen, J., Hillamo, R., et al. (1998). Hengitettävien hiukkasten kokojakauma, koostumus, ja lähteet pääkaupunkiseudulla [the size distribution of respirable particles, their composition and sources in the metropolitan area of helsinki, finland]. *Helsinki: YTV.*

Oluyemi, E. and Asubiojo, O. (2001). Ambient air particulate matter in lagos, nigeria: a study using receptor modeling with x-ray flourescence analysis. *Bulletin of the Chemical Society of Ethiopia*, 15(2):97–108.

Oren, R., Ellsworth, D. S., Johnsen, K. H., Phillips, N., Ewers, B. E., Maier, C., Schäfer, K. V., McCarthy, H., Hendrey, G., McNulty, S. G., et al. (2001). Soil fertility limits carbon sequestration by forest ecosystems in a co 2-enriched atmosphere. *Nature*, 411(6836):469.

Ostro, B., Tobias, A., Querol, X., Alastuey, A., Amato, F., Pey, J., Pérez, N., and Sunyer, J. (2011). The effects of particulate matter sources on daily mortality: a case-crossover study of barcelona, spain. *Environmental health perspectives*, 119(12):1781.

Paatero, P. (1997). Least squares formulation of robust non-negative factor analysis. *Chemometrics and intelligent laboratory systems*, 37(1):23–35.

Paatero, P. and Hopke, P. K. (2003). Discarding or downweighting high-noise variables in factor analytic models. *Analytica Chimica Acta*, 490(1-2):277–289.

Paatero, P. and Tapper, U. (1994). Positive matrix factorization: A non-negative factor model with optimal utilization of error estimates of data values. *Environmetrics*, 5(2):111–126.

Pant, P. and Harrison, R. M. (2012). Critical review of receptor modelling for particulate matter: a case study of india. *Atmospheric Environment*, 49:1–12.

Peters, A., Wichmann, H. E., Tuch, T., Heinrich, J., and Heyder, J. (1997). Respiratory effects are associated with the number of ultrafine particles. *American journal of respiratory and critical care medicine*, 155(4):1376–1383.

Polissar, A. V., Hopke, P. K., Paatero, P., Malm, W. C., and Sisler, J. F. (1998). Atmospheric aerosol over alaska: 2. elemental composition and sources. *Journal of Geophysical Research: Atmospheres*, 103(D15):19045–19057.

Pollice, A. (2011). Recent statistical issues in multivariate receptor models. *Environmetrics*, 22(1):35–41.

Pongkiatkul, P. and Oanh, N. T. K. (2012). Receptor modeling for air pollution source apportionment study. *Integrated Air Quality Management: Asian Case Studies*, 63.

Prati, P., Zucchiatti, A., Lucarelli, F., and Mando, P. (2000). Source apportionment near a steel plant in genoa (italy) by continuous aerosol sampling and pixe analysis. *Atmospheric Environment*, 34(19):3149–3157.

Rostami, A. A. (2009). Computational modeling of aerosol deposition in respiratory tract: a review. *Inhalation Toxicology*, 21(4):262–290.

Ryan, J. and Windom, H. (1988). A geochemical and statistical approach for assessing metal pollution in coastal sediments. In *Metals in coastal environments of Latin America*, pages 47–58. Springer.

Samet, J. M., Dominici, F., Curriero, F. C., Coursac, I., and Zeger, S. L. (2000). Fine particulate air pollution and mortality in 20 us cities, 1987–1994. *New England journal of medicine*, 343(24):1742–1749.

Samson, M. (2009). Refusing to be cast aside: Waste pickers organising around the world (cambridge, ma: Wiego).

Sandström, T., Nowak, D., and Van Bree, L. (2005). Health effects of coarse particles in ambient air: messages for research and decision-making.

Schauer, J. J., Lough, G. C., Shafer, M. M., Christensen, W. F., Arndt, M. F., DeMinter, J. T., and Park, J. (2006). Characterization of metals emitted from motor vehicles. *Research report (Health Effects Institute)*, (133):1–76.

Schwarze, P., Øvrevik, J., Låg, M., Refsnes, M., Nafstad, P., Hetland, R., and Dybing, E. (2006). Particulate matter properties and health effects: consistency of epidemiological and toxicological studies. *Human & experimental toxicology*, 25(10):559–579.

Seinfeld, J. H. and Pandis, S. N. (2016). *Atmospheric chemistry and physics: from air pollution to climate change*. John Wiley & Sons.

Selin Lindgren, E., Henriksson, D., Lundin, M., Therning, P., Laursen, J., and Pind, N. (2006). Possible indicators for biomass burning in a small swedish city as studied by energy dispersive x-ray fluorescence (edxrf) spectrometry. *X-Ray Spectrometry: An International Journal*, 35(1):19–26.

Sillanpää, M., Hillamo, R., Saarikoski, S., Frey, A., Pennanen, A., Makkonen, U., Spolnik, Z., Van Grieken, R., Braniš, M., Brunekreef, B., et al. (2006). Chemical composition and mass closure of particulate matter at six urban sites in europe. *Atmospheric Environment*, 40:212–223.

Sinex, S. A. and Wright, D. A. (1988). Distribution of trace metals in the sediments and biota of chesapeake bay. *Marine Pollution Bulletin*, 19(9):425–431.

Smolders, R., Koppen, G., and Schoeters, G. (2008). Translating biomonitoring data into risk management and policy implementation options for a european network on human biomonitoring. *Environmental Health*, 7(1):S2.

Song, Y., Xie, S., Zhang, Y., Zeng, L., Salmon, L. G., and Zheng, M. (2006). Source apportionment of pm2. 5 in beijing using principal component analysis/absolute principal component scores and unmix. *Science of the Total Environment*, 372(1):278–286.

Stuart, B. O. (1984). Deposition and clearance of inhaled particles. *Environmental health perspectives*, 55:369.

Sunnu, A. K. (2006). *An experimental study of the saharian dust physical characteristics and fluxes near the gulf of Guinea=[Etude expérimentale des flux et des caractéristiques physiques des poussières sahariennes dans les régions proches du golfe de Guinée]*. PhD thesis, Toulon.

Tonetti, R. (2000). Environmentally sound management of used and scrap personal computers (pcs). In *US EPA, Office of Solid Waste Second OECD Workshop on Environmentally Sound Management of Wastes Destined for Recovery Operations*, pages 28–29.

Utell, M. J. and Frampton, M. W. (2000). Acute health effects of ambient air pollution: the ultrafine particle hypothesis. *Journal of aerosol medicine*, 13(4):355–359.

Vallius, M. (2005). *Characteristics and sources of fine particulate matter in urban air*. National Public Health Institute.

Watson, J., Chow, J., and Frazier, C. (1999). X-ray fluorescence analysis of ambient air samples. *Elemental analysis of airborne particles*, 1:67–96.

Watson, J. G. (1984). Overview of receptor model principles. *Journal of the Air Pollution Control Association*, 34(6):619–623.

Watson, J. G. and Chow, J. C. (2004). 15 receptor models for air quality management.

Wedepohl, K. H. (1995). The composition of the continental crust. *Geochimica et cosmochimica Acta*, 59(7):1217–1232.

Wilson, W., Chow, J. C., Claiborn, C., Fusheng, W., Engelbrecht, J., and Watson, J. G. (2002). Monitoring of particulate matter outdoors. *Chemosphere*, 49(9):1009–1043.

Winchester, J. W., Weixiu, L., Lixin, R., Mingxing, W., and Maenhaut, W. (1981). Fine and coarse aerosol composition from a rural area in north china. *Atmospheric Environment (1967)*, 15(6):933–937.

Wu, C.-f., Larson, T. V., Wu, S.-y., Williamson, J., Westberg, H. H., and Liu, L.-J. S. (2007). Source apportionment of pm2. 5 and selected hazardous air pollutants in seattle. *Science of the total environment*, 386(1-3):42–52.

Zhang, Y.-X., Quraishi, T., and Schauer, J. J. (2008). Daily variations in sources of carbonaceous aerosol in lahore, pakistan during a high pollution spring episode. *Aerosol Air Qual. Res*, 8(2):130–146.

Zhou, Z., Dionisio, K. L., Verissimo, T. G., Kerr, A. S., Coull, B., Arku, R. E., Koutrakis, P., Spengler, J. D., Hughes, A. F., Vallarino, J., et al. (2013). Chemical composition and sources of particle pollution in affluent and poor neighborhoods of accra, ghana. *Environmental Research Letters*, 8(4):044025.

Zhou, Z., Dionisio, K. L., Verissimo, T. G., Kerr, A. S., Coull, B., Howie, S., Arku, R. E., Koutrakis, P., Spengler, J. D., Fornace, K., et al. (2014). Chemical characterization and source apportionment of household fine particulate matter in rural, peri-urban, and urban west africa. *Environmental science & technology*, 48(2):1343–1351.

Appendix

A Elemental Concentarion in Coarse Fraction

Table 1: Summary of daily Mass Concentration gcm^{-3} of APM in Agbogbloshie during the entire sampling period

Sample ID	**Na**	**Mg**	**Al**	**Si**	**P**	**S**	**Cl**	**K**	**Ca**	**Ti**
Sample ID	Na	Mg	Al	Si	P	S	Cl	K	Ca	Ti
AGB 1	2.1579	0.6163	1.197	5.5755	0.0932	0.6088	2.508	0.7313	0.7234	0.1057
AGB 2	2.6209	0.6311	1.1749	4.9006	0.1126	0.5872	2.5632	0.6077	0.8694	0.0594
AGB 3	2.3445	0.507	1.2368	4.9628	0.4011	0.701	3.0237	0.3865	2.623	0.0317
AGB 4	2.563	0.4973	1.3888	4.2714	0.0849	0.6433	4.1197	0.4507	1.1447	0.0532
AGB 5	2.4815	0.5129	1.6284	3.6502	0.0873	0.6015	4.5049	1.2558	1.5723	0.0321
AGB 6	2.8703	0.4493	1.1137	4.1322	0.1344	0.3259	3.8035	0.5826	0.9093	0.1037
AGB 7	2.7118	0.4809	1.1401	7.7922	0.0593	0.3154	4.7577	0.5401	0.8429	0.0511
AGB 8	2.2616	0.2599	0.9271	2.6882	0.0855	0.4592	4.9232	0.5121	0.8354	0.0523
AGB 9	2.4128	0.2811	0.9149	3.5424	0.1389	0.5819	2.9504	0.4274	0.7639	0.0572
AGB 10	2.4255	0.6181	1.4238	7.4276	0.1002	0.555	4.1488	0.4049	2.0856	0.0802
AGB 11	2.1058	0.572	1.6148	4.2811	0.1094	1.2641	4.2282	0.3961	0.3437	0.0555
AGB 12	2.8965	0.5394	1.1154	5.6922	0.0961	0.7803	3.9548	0.6621	0.6152	0.042
AGB 13	2.6764	0.6057	2.2677	4.5189	0.107	0.7383	4.0227	0.2263	2.2932	0.1233

Continued on next page

Table 1 – *Continued from previous page*

Sample ID	**Na**	**Mg**	**Al**	**Si**	**P**	**S**	**Cl**	**K**	**Ca**	**Ti**
AGB 14	2.4696	0.6233	1.4732	5.82	0.1053	0.7759	4.0211	0.4256	0.8481	0.1184
AGB 15	2.8839	0.7095	1.4927	4.2294	0.0897	0.7512	4.83	0.9378	1.5165	0.0962
AGB 16	2.6036	0.7665	1.4493	4.0485	0.1065	0.8924	4.5297	0.5687	0.9685	0.0753
AGB 17	2.9533	0.6902	1.4685	3.6173	0.1962	0.9162	3.9665	0.7486	1.6197	0.0767
AGB 18	2.9467	0.348	1.6665	3.7824	0.0944	0.8482	4.1069	0.6446	1.2648	0.0583
AGB 19	2.3542	0.3467	1.2633	3.355	0.1077	0.8526	2.7585	0.714	0.8145	0.0394
AGB 20	3.0052	0.5219	1.317	2.8051	0.1212	0.7351	3.6976	0.9435	0.9528	0.0257
AGB 21	1.5343	0.5795	1.5546	3.5549	0.0969	0.5766	2.0059	0.4703	1.8616	0.0517
AGB 22	3.0436	0.6507	1.2598	5.5275	0.105	0.8259	3.7	0.7733	0.8905	0.0682
AGB 23	2.1328	0.6206	1.2027	4.4209	0.1049	0.5604	4.3752	1.3795	1.0735	0.0764
AGB 24	2.8739	0.6162	1.4621	3.428	0.0857	0.6303	3.3852	0.5884	1.3083	0.0901
AGB 25	2.6121	0.507	1.1591	4.1716	0.086	0.491	3.9136	0.6351	1.0657	0.0972
AGB 26	2.4973	0.631	1.1945	3.2851	0.1135	0.8906	1.5334	0.7867	0.791	0.0625
AGB 27	2.4123	0.5359	1.0912	2.5869	0.0874	0.501	4.2964	0.5273	0.7195	0.0791
AGB 28	2.8191	0.32	1.1518	3.2212	0.0845	0.4433	4.8076	0.52	0.6246	0.0473

Continued on next page

Table 1 – *Continued from previous page*

Sample ID	**Na**	**Mg**	**Al**	**Si**	**P**	**S**	**Cl**	**K**	**Ca**	**Ti**
AGB 29	2.5408	1.042	1.0195	4.7695	0.0955	0.6087	5.1337	0.5349	0.8743	0.0638
AGB 30	2.5408	1.0122	1.1234	7.8378	0.1243	0.4244	4.8169	0.5103	1.6455	0.0863
AGB 31	2.3599	0.7268	1.261	3.3415	0.0926	0.5489	3.547	0.5531	0.9499	0.0742
AGB 32	2.1659	0.5101	0.8887	3.4895	0.0924	1.0206	5.3514	0.7574	0.7886	0.0794
AGB 33	2.3697	0.6012	1.3247	1.8738	0.118	0.9545	5.9906	0.5531	1.0404	0.0728
AGB 34	2.1394	1.3346	1.5684	1.7672	0.1239	0.6923	5.3716	0.5332	0.6435	0.0489
AGB 35	2.1766	1.176	3.1346	1.9454	0.0929	0.5815	5.5972	0.558	0.4245	0.0653
AGB 36	2.3268	0.6876	3.1036	2.183	0.12	0.4885	4.3217	0.6146	0.8239	0.0201
AGB 37	2.4478	0.9748	3.7125	2.6417	0.1067	0.5041	3.4013	0.4178	1.7354	0.045
AGB 38	2.1001	0.7522	5.1131	1.7099	0.1056	0.5048	2.2091	0.4934	2.9292	0.0275
AGB 39	2.9316	0.7812	3.3474	1.8282	0.0856	0.6062	3.3973	0.8144	0.9099	0.0421
AGB 40	4.3228	0.9277	4.0549	1.3921	0.0869	1.1047	5.9381	1.0817	1.3944	0.0537
AGB 41	3.0032	0.5226	5.2366	1.3636	0.0943	0.6179	4.0953	0.5527	0.5855	0.0451
AGB 42	3.3449	0.8313	4.0523	2.1684	0.0714	0.7189	6.3383	0.5778	0.7271	0.0219
AGB 43	2.5261	1.4091	3.4714	2.5811	0.0724	0.8056	5.168	0.4807	1.0357	0.0542

Continued on next page

Table 1 – *Continued from previous page*

Sample ID	**Na**	**Mg**	**Al**	**Si**	**P**	**S**	**Cl**	**K**	**Ca**	**Ti**
AGB 44	2.3885	0.7011	3.6017	1.7797	0.0669	0.5964	5.8809	0.4727	0.8488	0.0312
AGB 45	2.4571	0.8124	3.313	3.8724	0.0644	0.5027	6.0572	0.4483	0.9464	0.0749
AGB 46	1.9985	0.9042	2.7625	2.4186	0.0719	0.5856	4.6309	0.455	0.5617	0.0302
AGB 47	1.2952	0.5951	2.9397	2.4754	0.0808	0.6393	3.7697	0.5237	1.0663	0.1033
AGB 48	1.4762	0.5102	5.6358	2.4461	0.0755	0.7411	2.6774	0.4506	0.3184	0.0677
AGB 49	3.508	0.6757	2.1182	2.4194	0.099	1.0626	6.3581	0.4223	0.3028	0.0236
AGB 50	3.4663	0.6837	2.5725	2.8383	0.079	0.6045	5.7861	0.2859	0.6321	0.0271
AGB 51	2.9292	0.7393	4.7801	3.1815	0.078	0.6303	5.7252	0.281	0.8779	0.0484
AGB 52	3.694	0.9757	3.132	2.4404	0.0747	0.4618	7.6895	0.3855	0.5573	0.0596
AGB 53	3.5488	0.6463	3.8742	3.7703	0.0806	0.5423	6.9013	0.4572	2.1247	0.067
AGB 54	2.3146	0.6535	3.1602	4.7009	0.0868	0.5004	5.6407	0.4331	0.8199	0.067
AGB 55	3.5831	0.6675	3.8626	1.65	0.0876	0.295	4.2635	0.7247	0.8425	0.0836
AGB 56	1.4062	0.6684	1.0919	2.3827	0.0791	0.4769	4.1617	0.5233	0.8142	0.0292
AGB 57	2.8048	0.4442	1.4571	1.8146	0.1047	0.716	5.8602	0.5308	0.788	0.0285
AGB 58	2.58	0.5871	1.0837	1.8553	0.0862	0.7827	8.7962	0.5546	0.9732	0.0204

Continued on next page

Table 1 – *Continued from previous page*

Sample ID	**Na**	**Mg**	**Al**	**Si**	**P**	**S**	**Cl**	**K**	**Ca**	**Ti**
AGB 59	2.3669	1.0973	1.1903	1.7309	0.0806	0.7151	6.3563	0.531	1.0898	0.0238
AGB 60	2.1175	1.2242	1.1029	3.5069	0.1033	0.6831	7.554	0.6103	0.8305	0.0591
AGB 61	2.2828	0.6635	2.1957	3.9006	0.072	0.7902	8.5205	0.5661	1.2399	0.0282
AGB 62	1.8636	1.01	1.267	3.9628	0.0732	0.7077	4.8245	0.5652	1.4941	0.029
AGB 63	1.3636	0.7372	1.2207	3.2714	0.0676	0.6609	3.8444	0.5789	0.8492	0.0279
AGB 64	2.9798	0.8185	1.2402	2.6502	0.0978	0.6893	6.1586	0.5589	1.6984	0.1256
AGB 65	2.228	0.945	1.4601	3.5189	0.0769	0.6619	7.1165	0.4396	1.0283	0.0209
AGB 66	2.8315	0.8323	1.656	1.9522	0.0843	0.646	7.2221	0.5956	0.6265	0.0224
AGB 67	2.2667	0.9179	1.5779	2.0563	0.0614	0.7047	6.3732	0.4127	0.5657	0.0329
AGB 68	2.1774	0.772	1.1268	1.9769	0.0624	0.8335	5.7507	0.4368	1.2739	0.0298
AGB 69	3.0447	0.8889	1.3271	2.0845	0.0569	0.7572	5.5901	0.3833	0.6614	0.0662
AGB 70	2.9536	0.7374	1.2149	2.5473	0.0544	0.4257	5.5862	0.6009	0.5583	0.0437
AGB 71	3.0637	0.8218	1.4094	2.2069	0.0619	0.5173	5.6121	0.4153	0.8224	0.0281
AGB 72	2.9376	0.6144	1.5426	2.2329	0.0708	1.0878	3.0467	0.5172	0.9465	0.3186
AGB 73	2.8819	0.7666	1.4384	2.4216	0.0655	0.5348	4.4384	0.4836	1.5804	0.6058

Continued on next page

Table 1 – *Continued from previous page*

Sample ID	**Na**	**Mg**	**Al**	**Si**	**P**	**S**	**Cl**	**K**	**Ca**	**Ti**
AGB 74	3.0719	0.5827	1.5252	2.2229	0.089	0.6094	4.1791	0.505	1.5472	0.3833
AGB 75	3.0671	0.6481	7.4293	2.4114	0.069	0.452	5.1733	0.496	1.5784	0.4122
AGB 76	3.1469	0.5379	2.4989	2.0866	0.068	0.4527	6.1856	0.5292	1.272	0.5588
AGB 77	2.9956	0.8445	2.578	2.2972	0.0624	0.5066	4.6633	0.4363	0.7021	0.1537
AGB 78	3.0541	0.725	3.5326	1.9749	0.0569	0.3933	4.5889	0.3227	0.734	0.4623
AGB 79	3.0692	0.9839	3.3926	2.0277	0.0785	0.4734	4.3635	0.3322	0.8721	0.0992
AGB 80	2.5061	0.9319	3.8048	2.5424	0.0756	0.2491	5.2151	0.4164	0.6139	0.1533
AGB 81	2.7379	1.4301	3.9754	5.9276	0.0813	0.4678	5.8845	0.4728	0.5769	0.1375
AGB 82	2.7645	1.2059	5.8546	6.3042	0.0769	1.0892	7.236	0.5331	1.4566	0.0748
AGB 83	2.6911	1.1786	5.6531	3.9908	0.0731	0.6152	8.0464	0.8066	0.7555	0.3623
AGB 84	3.5182	0.8854	5.7173	4.5366	0.1601	0.8908	6.2731	0.6126	0.8083	0.8954
AGB 85	2.4054	0.7759	5.4737	2.2429	0.4356	0.6935	2.2784	0.5849	1.5577	0.4238
AGB 86	2.3538	0.8462	5.4099	4.5457	0.1655	0.655	2.2379	0.615	1.8883	0.5487
AGB 87	1.9319	0.8207	8.3576	4.3518	0.1779	1.0071	4.1074	0.6687	1.9941	1.135
AGB 88	2.262	0.7663	10.2296	1.987	0.1818	0.809	4.9243	0.6504	0.6709	0.2664

Continued on next page

Table 1 – *Continued from previous page*

Sample ID	**Na**	**Mg**	**Al**	**Si**	**P**	**S**	**Cl**	**K**	**Ca**	**Ti**
AGB 89	3.5089	1.0922	9.3165	15.111	0.6416	1.2605	5.601	0.2605	1.6614	0.2588
AGB 90	4.9999	1.0826	8.1522	7.5653	0.185	1.3452	12.0251	1.2784	1.5583	1.1096
AGB 91	4.1422	1.3089	6.2014	11.42	0.1756	1.3354	8.2549	1.2499	1.8224	0.3703
AGB 92	4.5688	1.3621	8.5121	5.0821	0.1821	1.3835	8.0057	1.279	1.9318	0.6068
AGB 93	5.1893	1.288	9.1858	5.7133	0.2146	1.5029	8.6691	1.3962	2.5804	0.2774
AGB 94	5.2108	1.4179	11.849	9.747	0.2425	1.5748	8.314	1.6315	2.5472	0.2846
AGB 95	5.4515	1.6004	4.1265	10.59	0.2187	1.5716	9.2451	1.8453	2.5784	0.2986
AGB 96	3.416	1.7314	3.3266	10.2753	1.0257	1.4482	8.962	1.7754	2.272	0.2995
AGB 97	5.666	1.7167	7.1766	9.6804	0.2032	1.4084	9.9349	1.6861	2.4566	0.0753
AGB 98	3.0788	1.6487	2.8559	8.9609	0.2084	1.6624	8.0499	1.5734	4.2254	0.2181
AGB 99	4.7076	1.5089	4.3231	20.1693	0.2362	2.0285	8.0636	2.4196	5.0612	0.7284
AGB 100	3.0798	2.0926	3.7392	25.9541	0.2804	1.761	9.3812	2.9195	4.4985	0.8553
AGB 101	4.0266	2.4301	11.6345	22.9498	0.1695	1.7859	10.7961	2.9003	3.7888	0.2946
AGB 102	7.7757	2.2059	8.25	19.2633	0.5815	1.6449	14.906	2.3556	2.7422	0.2491
AGB 103	8.4464	2.1786	25.3891	13.1252	1.1258	1.7782	6.2088	1.9166	4.3855	0.242

Continued on next page

Table 1 – *Continued from previous page*

Sample ID	**Na**	**Mg**	**Al**	**Si**	**P**	**S**	**Cl**	**K**	**Ca**	**Ti**
AGB 104	7.6375	1.9339	15.9618	19.9487	0.1708	1.7895	14.7466	2.5395	4.3981	0.2094
AGB 105	4.9733	2.0384	19.8639	23.5183	0.1754	2.0766	8.3122	3.0209	6.3695	0.2757
AGB 106	7.9032	2.1886	17.674	30.4428	0.1705	1.3824	15.3563	4.3859	1.9329	0.2934
AGB 107	12.3449	2.6166	10.3408	5.9587	0.3029	1.238	6.554	1.2998	1.5884	0.3795
AGB 108	11.5261	1.3662	15.9344	4.3364	0.2216	1.7362	7.5205	1.2458	3.1994	0.0256
AGB 109	11.3885	1.2412	9.2971	9.8032	0.4048	1.152	13.8245	1.7667	1.2536	0.0238
AGB 110	11.4571	1.6977	6.6372	3.4632	0.3104	1.2843	12.8444	1.127	1.7692	0.0565
AGB 111	12.9985	1.1687	8.1522	5.752	0.3479	1.4329	14.1586	1.3312	1.8461	0.0406
AGB 112	14.2952	1.318	4.7412	5.2955	0.2849	2.2784	15.1165	1.3591	6.3095	0.6848
AGB 113	10.0762	1.4329	4.3723	28.8219	0.2568	1.6998	6.2221	4.6853	3.5208	0.9627
AGB 114	12.508	2.7355	4.6387	15.7589	0.2554	2.8232	5.3732	2.9578	12.8929	0.8029
AGB 115	12.0798	1.7021	2.9727	61.0292	0.2012	2.545	3.7507	7.624	6.815	0.8896
AGB 116	13.0266	3.8571	3.2312	37.0827	0.2089	3.0588	12.5901	4.8589	8.0588	0.823
AGB 117	11.7757	2.8085	7.7449	44.2979	0.208	2.5933	3.5862	6.3193	7.3219	0.7932
AGB 118	12.4464	3.0954	8.348	40.5421	0.1041	1.9016	12.8245	4.6836	4.7866	0.5078

Continued on next page

Table 1 – *Continued from previous page*

Sample ID	**Na**	**Mg**	**Al**	**Si**	**P**	**S**	**Cl**	**K**	**Ca**	**Ti**
AGB 119	11.6375	2.9964	2.7391	22.595	0.1126	1.784	2.8444	2.7776	5.058	0.2912
AGB 120	13.9407	2.2674	4.0347	24.7101	0.707	1.7533	6.4426	2.0667	3.7835	0.3823
AGB 121	13.9483	1.7488	3.3283	17.5617	0.0742	1.6057	16.7417	2.0915	2.8051	1.1157
AGB 122	15.8872	2.0267	2.4982	12.0772	0.0773	1.7406	9.708	1.8957	3.4957	0.3974
AGB 123	3.8552	1.8668	2.8851	2.0134	0.1809	0.442	4.8097	2.0412	1.9464	0.4122
AGB 124	3.9666	1.9536	1.6925	1.9	0.1148	0.3329	5.2898	0.8219	1.5892	0.1366
AGB 125	4.9019	0.9777	2.1485	2.506	0.0715	0.3554	4.3773	0.4551	1.586	0.1113
AGB 126	2.9152	0.7928	1.8201	1.9301	0.0733	0.4532	5.0437	0.4971	0.9378	0.0372
AGB 127	3.37	0.7707	1.5512	1.9019	0.0724	0.3819	5.4563	0.5627	0.7038	0.0308
AGB 128	3.1696	0.6908	1.3645	1.7437	0.0772	0.455	5.7593	0.4365	0.8387	0.0225
AGB 129	3.295	0.9851	1.5549	1.8733	0.0717	0.9837	5.7119	0.4166	0.5508	0.0226
AGB 130	1.9662	0.6791	1.619	1.6045	0.0774	0.6803	4.5445	0.4715	0.4608	0.0317
AGB 131	2.4542	0.7167	1.4759	1.7827	0.07	0.6383	6.0481	0.4247	0.571	0.0239
AGB 132	2.0309	0.885	1.5106	2.039	0.0773	0.6759	4.6812	0.4528	0.6667	0.0359
AGB 133	2.3158	0.6665	1.5121	1.3399	0.0665	0.4154	2.1967	0.4299	0.2781	0.026

Continued on next page

Table 1 – *Continued from previous page*

Sample ID	**Na**	**Mg**	**Al**	**Si**	**P**	**S**	**Cl**	**K**	**Ca**	**Ti**
AGB 134	2.1178	0.674	1.6474	2.1428	0.0727	0.3592	4.5678	0.4149	0.7307	0.0467
AGB 135	2.1403	0.7714	1.5017	2.5162	0.0946	0.63	4.8849	0.3766	0.9544	0.018
AGB 136	2.1915	0.5873	1.6656	2.7059	0.0971	0.7255	5.8538	0.4125	1.0771	0.0382
AGB 137	2.438	0.6648	1.413	3.3284	0.0997	0.8388	5.6187	0.3954	1.1017	0.0218
AGB 138	2.421	0.5505	1.5243	2.7308	0.1034	0.6163	4.6381	0.5998	1.0611	0.037
AGB 139	2.0087	0.7024	1.3674	2.3283	0.0943	0.561	4.0602	0.6401	1.1097	0.0514
AGB 140	2.3863	0.759	1.9442	1.9861	0.0955	0.6754	4.7533	0.6079	0.8892	0.0438
AGB 141	2.4292	0.7417	1.5593	2.3121	0.095	0.5421	4.4399	0.5807	0.7548	0.0381
AGB 142	2.3526	0.7363	2.5224	2.3977	0.0981	0.6619	4.3357	0.6213	0.8383	0.0368
AGB 143	2.2246	0.7235	3.0367	2.2302	0.0953	0.4618	4.281	0.5798	0.7839	0.085
AGB 144	2.1609	0.7094	4.3111	1.6882	0.0941	0.295	3.9983	0.5974	0.9155	0.0306
AGB 145	2.2426	0.5394	3.045	1.7309	0.0951	0.4769	4.2308	0.5744	0.6709	0.0265

Table 2: Summary of daily Mass Concentration gcm^{-3} of APM in Agbogbloshie during the entire sampling period

Sample ID	**V**	**Cr**	**Mn**	**Fe**	**Ni**	**Cu**	**Zn**	**As**	**Se**	**Br**	**Rb**
Sample ID	V	Cr	Mn	Fe	Ni	Cu	Zn	As	Se	Br	Rb
AGB 1	0.0026	0.0097	0.0085	0.7693	0.0055	0.0067	0.0384	0.0842	0.0009	0.0201	0.0047
AGB 2	0.0041	0.0096	0.007	1.0133	0.0058	0.0054	0.0398	0.0379	0.0006	0.0237	0.0047
AGB 3	0.0025	0.0123	0.0172	2.4637	0.0057	0.0057	0.0329	0.0102	0.0006	0.0199	0.0058
AGB 4	0.0038	0.0081	0.0033	1.5787	0.0059	0.0143	0.0311	0.0488	0.0007	0.0234	0.0047
AGB 5	0.0044	0.0179	0.0036	1.9691	0.0073	0.0061	0.0637	0.0106	0.0005	0.0285	0.0047
AGB 6	0.0021	0.01	0.0065	1.7169	0.0053	0.0075	0.0363	0.0822	0.0004	0.0289	0.0047
AGB 7	0.0014	0.0117	0.0104	2.1178	0.0054	0.0156	0.0331	0.0296	0.0008	0.029	0.0047
AGB 8	0.0014	0.0098	0.0052	1.5865	0.0056	0.0059	0.0321	0.0308	0.0005	0.0261	0.0047
AGB 9	0.0015	0.0119	0.0166	1.5013	0.005	0.0105	0.0299	0.0357	0.0004	0.0212	0.0047
AGB 10	0.0009	0.0074	0.0082	1.872	0.0045	0.006	0.0311	0.0587	0.0005	0.0267	0.0048
AGB 11	0.0036	0.0096	0.0115	3.1206	0.0049	0.0059	0.0299	0.034	0.0004	0.0265	0.0066
AGB 12	0.0012	0.0164	0.0118	1.6315	0.0053	0.0065	0.0408	0.0205	0.0004	0.0297	0.0055
AGB 13	0.0013	0.0184	0.0105	1.9211	0.0053	0.0057	0.0255	0.1018	0.0004	0.0291	0.0055

Continued on next page

Table 2 – *Continued from previous page*

Sample ID	**V**	**Cr**	**Mn**	**Fe**	**Ni**	**Cu**	**Zn**	**As**	**Se**	**Br**	**Rb**
AGB 14	0.0029	0.0115	0.015	2.4208	0.0063	0.0054	0.0283	0.0969	0.0003	0.0291	0.0055
AGB 15	0.0013	0.0053	0.0121	1.3692	0.0049	0.006	0.0561	0.0747	0.0004	0.0309	0.005
AGB 16	0.0012	0.0043	0.0089	1.3839	0.0057	0.0063	0.043	0.0538	0.0003	0.0313	0.0048
AGB 17	0.0014	0.0049	0.0176	1.2082	0.0055	0.0053	0.0495	0.0552	0.0004	0.0594	0.005
AGB 18	0.002	0.0046	0.0187	1.0508	0.0049	0.0068	0.0433	0.0368	0.0003	0.0607	0.0053
AGB 19	0.0012	0.0048	0.0078	1.2693	0.0051	0.0052	0.0468	0.0179	0.0003	0.0326	0.0048
AGB 20	0.0026	0.0052	0.0329	2.0016	0.0052	0.0056	0.0808	0.0142	0.0003	0.0609	0.0047
AGB 21	0.0014	0.0047	0.0354	1.6178	0.0064	0.0061	0.0446	0.0302	0.0004	0.0326	0.0047
AGB 22	0.0015	0.0056	0.0264	1.2289	0.0069	0.0057	0.0453	0.0467	0.0005	0.0463	0.0066
AGB 23	0.006	0.0049	0.0257	1.4686	0.0056	0.0051	0.068	0.055	0.0007	0.0328	0.0055
AGB 24	0.0047	0.0048	0.0339	1.1705	0.005	0.0082	0.0459	0.0686	0.0006	0.0379	0.0053
AGB 25	0.0046	0.0044	0.0294	0.9322	0.0049	0.0073	0.0457	0.0757	0.0004	0.0335	0.0054
AGB 26	0.0048	0.0069	0.0302	1.2439	0.005	0.0076	0.0549	0.041	0.0005	0.0311	0.0061
AGB 27	0.0042	0.0043	0.0283	1.7802	0.0051	0.0053	0.0443	0.0576	0.0007	0.0337	0.0053
AGB 28	0.0131	0.0069	0.0268	4.0449	0.0063	0.0048	0.0435	0.0258	0.0013	0.0278	0.0048

Continued on next page

Table 2 – *Continued from previous page*

Sample ID	**V**	**Cr**	**Mn**	**Fe**	**Ni**	**Cu**	**Zn**	**As**	**Se**	**Br**	**Rb**
AGB 29	0.011	0.0048	0.0274	1.1893	0.0048	0.0041	0.0421	0.0423	0.0008	0.0462	0.0047
AGB 30	0.0114	0.0046	0.0332	1.2059	0.0052	0.0038	0.045	0.0648	0.0011	0.0448	0.0047
AGB 31	0.01	0.0055	0.0269	1.0064	0.0048	0.0044	0.0421	0.0527	0.0008	0.0336	0.0051
AGB 32	0.0183	0.006	0.0278	0.9727	0.0045	0.0045	0.0533	0.0579	0.0008	0.0245	0.0063
AGB 33	0.0093	0.0057	0.0254	1.072	0.0048	0.0047	0.0456	0.0513	0.0008	0.0298	0.0071
AGB 34	0.0115	0.0045	0.0312	1.1353	0.0055	0.0041	0.0432	0.0274	0.0008	0.0549	0.0062
AGB 35	0.0145	0.0052	0.0289	1.2248	0.0052	0.0043	0.0474	0.0438	0.0094	0.0287	0.0051
AGB 36	0.0132	0.006	0.0046	0.9566	0.0062	0.0037	0.043	0.0086	0.0084	0.0323	0.0061
AGB 37	0.0029	0.0062	0.0206	0.9889	0.0051	0.004	0.0412	0.0235	0.0007	0.0273	0.0049
AGB 38	0.0034	0.0055	0.0242	0.8471	0.005	0.004	0.0436	0.0084	0.001	0.0294	0.0055
AGB 39	0.0036	0.0072	0.0609	0.8348	0.0052	0.004	0.0558	0.0206	0.0026	0.0304	0.0051
AGB 40	0.0035	0.0049	0.0194	1.1352	0.005	0.0039	0.0592	0.0322	0.0009	0.0249	0.0052
AGB 41	0.0086	0.0042	0.0487	1.2412	0.0054	0.0052	0.0459	0.0237	0.0008	0.0254	0.0055
AGB 42	0.0031	0.0043	0.0131	0.9514	0.0052	0.004	0.046	0.02	0.0011	0.0186	0.0063
AGB 43	0.0042	0.0067	0.0175	1.6069	0.0051	0.0042	0.0422	0.0327	0.0006	0.0279	0.0047

Continued on next page

Table 2 – *Continued from previous page*

Sample ID	**V**	**Cr**	**Mn**	**Fe**	**Ni**	**Cu**	**Zn**	**As**	**Se**	**Br**	**Rb**
AGB 44	0.0084	0.0049	0.0175	1.1366	0.0052	0.004	0.0429	0.0097	0.0008	0.0384	0.0053
AGB 45	0.0052	0.0048	0.0267	1.1646	0.0049	0.0045	0.0422	0.0258	0.0008	0.0153	0.0047
AGB 46	0.0059	0.0051	0.0189	1.1527	0.0201	0.0046	0.0433	0.0087	0.0008	0.029	0.0048
AGB 47	0.0078	0.0056	0.0109	1.1583	0.0056	0.0046	0.0449	0.0818	0.001	0.0192	0.0047
AGB 48	0.0077	0.0038	0.021	1.2661	0.0047	0.0042	0.0385	0.0462	0.001	0.0182	0.0047
AGB 49	0.0076	0.0049	0.0417	1.3679	0.0047	0.0049	0.0437	0.0367	0.0008	0.0521	0.005
AGB 50	0.0065	0.0047	0.013	1.2007	0.0049	0.0048	0.0442	0.0313	0.001	0.0122	0.0047
AGB 51	0.0074	0.0055	0.0132	1.7963	0.0055	0.0186	0.0417	0.0269	0.0009	0.0186	0.0048
AGB 52	0.0047	0.0035	0.0168	1.9863	0.0047	0.0053	0.0405	0.0382	0.0006	0.039	0.0056
AGB 53	0.0058	0.0041	0.012	0.9481	0.0045	0.0053	0.0448	0.0455	0.001	0.0187	0.0051
AGB 54	0.0059	0.0041	0.0107	1.1828	0.005	0.0041	0.0398	0.0455	0.0008	0.0262	0.0047
AGB 55	0.008	0.0078	0.0102	0.9917	0.0047	0.004	0.0545	0.0621	0.0012	0.0293	0.0048
AGB 56	0.0037	0.0097	0.0056	0.9882	0.0043	0.0048	0.0409	0.0077	0.0015	0.0501	0.0076
AGB 57	0.0061	0.0064	0.0098	0.9617	0.0045	0.0039	0.0398	0.007	0.0014	0.0402	0.0057
AGB 58	0.0048	0.0184	0.0181	1.5977	0.0045	0.0038	0.0424	0.0089	0.0007	0.0386	0.0047

Continued on next page

Table 2 – *Continued from previous page*

Sample ID	**V**	**Cr**	**Mn**	**Fe**	**Ni**	**Cu**	**Zn**	**As**	**Se**	**Br**	**Rb**
AGB 59	0.0041	0.0203	0.0134	1.0583	0.0047	0.0044	0.0404	0.0223	0.0005	0.0415	0.0047
AGB 60	0.0064	0.0043	0.0093	1.0522	0.0045	0.0037	0.0428	0.0376	0.0005	0.0366	0.0049
AGB 61	0.0078	0.0045	0.0101	1.217	0.0044	0.0037	0.0447	0.014	0.0006	0.0415	0.0048
AGB 62	0.0067	0.0039	0.0095	1.0448	0.0046	0.0038	0.0391	0.0075	0.001	0.0405	0.0047
AGB 63	0.0047	0.0036	0.0048	0.9977	0.0061	0.0049	0.0447	0.0108	0.0008	0.0396	0.0054
AGB 64	0.0046	0.0038	0.0176	1.2324	0.0065	0.0036	0.0467	0.1041	0.0007	0.0354	0.0052
AGB 65	0.0049	0.0042	0.0282	1.0397	0.0059	0.004	0.0424	0.01	0.0008	0.0327	0.0057
AGB 66	0.0047	0.0067	0.0629	1.0025	0.0147	0.0051	0.0489	0.0259	0.0005	0.0214	0.006
AGB 67	0.0037	0.004	0.0169	0.9448	0.0055	0.0054	0.0388	0.0114	0.0006	0.0225	0.0057
AGB 68	0.0075	0.0025	0.0134	1.0352	0.0059	0.0059	0.0384	0.0183	0.0005	0.0218	0.0067
AGB 69	0.0111	0.0043	0.0078	0.9015	0.0063	0.0058	0.0379	0.0447	0.0005	0.0205	0.0079
AGB 70	0.0042	0.0043	0.006	0.8922	0.0109	0.0047	0.0483	0.0222	0.0005	0.0197	0.0069
AGB 71	0.0046	0.0048	0.0108	1.1939	0.0063	0.0046	0.0386	0.0815	0.0009	0.0188	0.0082
AGB 72	0.0015	0.0053	0.0124	1.6802	0.0055	0.0047	0.0375	0.2971	0.0007	0.0173	0.0074
AGB 73	0.0014	0.0103	0.0149	3.6449	0.0053	0.0051	0.0411	0.5843	0.0007	0.1076	0.007

Continued on next page

Table 2 – *Continued from previous page*

Sample ID	**V**	**Cr**	**Mn**	**Fe**	**Ni**	**Cu**	**Zn**	**As**	**Se**	**Br**	**Rb**
AGB 74	0.0014	0.0092	0.0124	1.0893	0.0059	0.0077	0.0362	0.3618	0.001	0.0889	0.0093
AGB 75	0.0016	0.0104	0.0068	1.0059	0.006	0.0068	0.0946	0.3907	0.0007	0.0929	0.0083
AGB 76	0.0028	0.0091	0.005	0.9064	0.0043	0.0049	0.1025	0.5373	0.0006	0.0998	0.0086
AGB 77	0.002	0.0113	0.0089	0.8927	0.0045	0.0046	0.0974	0.1322	0.0015	0.0925	0.0085
AGB 78	0.0021	0.0104	0.0114	0.992	0.0042	0.0051	0.0948	0.4408	0.0007	0.091	0.0074
AGB 79	0.0019	0.0095	0.0079	1.1053	0.0046	0.0054	0.0983	0.0777	0.0009	0.0513	0.0077
AGB 80	0.0011	0.0246	0.0069	1.1948	0.0046	0.0078	0.1079	0.1319	0.0019	0.0506	0.0089
AGB 81	0.002	0.0163	0.0072	0.9066	0.0053	0.0097	0.1272	0.116	0.0004	0.0483	0.0102
AGB 82	0.0022	0.0183	0.0263	0.9989	0.0054	0.0067	0.1155	0.0533	0.0009	0.0367	0.0103
AGB 83	0.0025	0.0183	0.0285	0.9595	0.0054	0.0053	0.1156	0.3409	0.001	0.0402	0.0083
AGB 84	0.0053	0.017	0.0968	1.0616	0.005	0.0048	0.1206	0.8739	0.0007	0.0359	0.0167
AGB 85	0.002	0.0148	0.0924	0.8131	0.0056	0.0047	0.1259	0.4023	0.0008	0.0503	0.0093
AGB 86	0.002	0.0179	0.1048	1.135	0.0056	0.0079	0.1302	0.5272	0.0014	0.0411	0.0154
AGB 87	0.0031	0.0179	0.1012	1.2121	0.0058	0.0058	0.1316	1.1135	0.0004	0.0446	0.0134
AGB 88	0.0021	0.0222	0.1131	1.3032	0.0051	0.0063	0.1338	0.245	0.0007	0.0947	0.0087

Continued on next page

Table 2 – *Continued from previous page*

Sample ID	**V**	**Cr**	**Mn**	**Fe**	**Ni**	**Cu**	**Zn**	**As**	**Se**	**Br**	**Rb**
AGB 89	0.0122	0.0163	0.1085	2.0712	0.0128	0.0125	0.1325	0.2373	0.0016	0.0201	0.016
AGB 90	0.0153	0.016	0.1047	2.0045	0.012	0.0328	0.1215	1.0881	0.0015	0.0396	0.0072
AGB 91	0.0127	0.0182	0.1086	2.2698	0.0123	0.0125	0.1424	0.3488	0.0018	0.0378	0.007
AGB 92	0.0144	0.0178	0.1183	2.4526	0.0121	0.0134	0.1574	0.5853	0.0017	0.0389	0.0074
AGB 93	0.0194	0.0195	0.1331	3.4688	0.013	0.0147	0.1496	0.2559	0.002	0.0439	0.0071
AGB 94	0.0161	0.0178	0.1365	3.4296	0.0136	0.0136	0.148	0.2631	0.0015	0.0533	0.0069
AGB 95	0.0146	0.0195	0.1366	3.4773	0.0127	0.0149	0.1274	0.2771	0.0025	0.0492	0.0068
AGB 96	0.0186	0.0199	0.1355	3.3525	0.013	0.0141	0.1373	0.278	0.0018	0.0433	0.0065
AGB 97	0.0187	0.0199	0.1318	3.489	0.0132	0.0137	0.1335	0.0538	0.0028	0.0307	0.0071
AGB 98	0.016	0.023	0.1756	5.5507	0.0148	0.016	0.1587	0.1966	0.0023	0.0302	0.0105
AGB 99	0.0298	0.0149	0.1976	6.7912	0.0149	0.015	0.1459	0.7069	0.0029	0.035	0.0071
AGB 100	0.0282	0.0145	0.1913	6.104	0.017	0.0153	0.1504	0.8338	0.0033	0.0388	0.0059
AGB 101	0.0204	0.0127	0.1758	5.295	0.0157	0.0152	0.2291	0.2731	0.0017	0.0388	0.006
AGB 102	0.0206	0.0099	0.1447	3.9176	0.0142	0.0141	0.1874	0.2276	0.0017	0.0584	0.0056
AGB 103	0.0306	0.0088	0.1891	5.7018	0.0148	0.0145	0.2264	0.2205	0.0032	0.0461	0.0054

Continued on next page

Table 2 – *Continued from previous page*

Sample ID	**V**	**Cr**	**Mn**	**Fe**	**Ni**	**Cu**	**Zn**	**As**	**Se**	**Br**	**Rb**
AGB 104	0.0231	0.0096	0.1887	6.2218	0.0162	0.0157	0.1782	0.1879	0.0016	0.0441	0.0056
AGB 105	0.0233	0.0204	0.2428	8.3531	0.0163	0.0169	0.1393	0.2542	0.0033	0.046	0.0072
AGB 106	0.0353	0.0104	0.227	8.0475	0.0177	0.0171	0.1873	0.2719	0.0047	0.0468	0.0059
AGB 107	0.0251	0.0172	0.1643	5.526	0.0135	0.015	0.1291	0.358	0.0017	0.0495	0.0055
AGB 108	0.0608	0.0212	0.4518	19.5697	0.023	0.0234	0.123	0.0141	0.0025	0.0532	0.0084
AGB 109	0.0326	0.0223	0.2724	10.8873	0.0188	0.016	0.1266	0.0123	0.0036	0.0523	0.0056
AGB 110	0.0574	0.0307	0.3173	14.0553	0.0178	0.0221	0.0415	0.0351	0.0082	0.0534	0.0059
AGB 111	0.037	0.0271	0.2769	11.4835	0.0239	0.0201	0.0372	0.0191	0.0045	0.0285	0.0145
AGB 112	0.0228	0.0093	0.1611	6.2974	0.0143	0.0154	0.035	0.6634	0.0009	0.0212	0.0063
AGB 113	0.0136	0.0677	0.1745	7.8735	0.022	0.0227	0.0393	0.9412	0.0007	0.0172	0.0077
AGB 114	0.0209	0.0144	0.1491	5.5588	0.0142	0.0139	0.0452	0.7814	0.0007	0.0228	0.0158
AGB 115	0.0142	0.0117	0.1565	4.0518	0.0128	0.0137	0.052	0.8681	0.0021	0.0238	0.0061
AGB 116	0.0188	0.0117	0.1565	4.8008	0.0141	0.0141	0.0457	0.8015	0.0009	0.0392	0.0107
AGB 117	0.0052	0.0257	0.0886	2.385	0.0048	0.0054	0.0476	0.7717	0.0016	0.0383	0.0062
AGB 118	0.005	0.0232	0.0342	2.0134	0.0042	0.0052	0.0696	0.4863	0.0009	0.0284	0.0061

Continued on next page

Table 2 – *Continued from previous page*

Sample ID	**V**	**Cr**	**Mn**	**Fe**	**Ni**	**Cu**	**Zn**	**As**	**Se**	**Br**	**Rb**
AGB 119	0.0084	0.0224	0.0335	2.1235	0.0041	0.0051	0.0448	0.2697	0.0011	0.0361	0.0067
AGB 120	0.0049	0.0199	0.0254	1.2382	0.0038	0.0048	0.0473	0.3608	0.0009	0.0356	0.0059
AGB 121	0.0038	0.0225	0.0288	1.4083	0.0039	0.0053	0.0441	1.0942	0.0008	0.0409	0.0057
AGB 122	0.0153	0.0282	0.0641	3.92	0.0068	0.0088	0.1137	0.3759	0.0009	0.046	0.0062
AGB 123	0.0024	0.0247	0.0332	1.7753	0.0038	0.0054	0.0915	0.3907	0.0025	0.047	0.0065
AGB 124	0.0063	0.0217	0.034	1.6032	0.0046	0.0042	0.0368	0.1151	0.0075	0.0452	0.0055
AGB 125	0.0074	0.0237	0.0329	1.6114	0.0036	0.0043	0.0357	0.0898	0.0016	0.0424	0.0071
AGB 126	0.0086	0.0199	0.1306	1.3163	0.0039	0.0038	0.0347	0.0157	0.0021	0.0428	0.0055
AGB 127	0.007	0.0193	0.0259	1.1366	0.0039	0.0036	0.0248	0.0093	0.0014	0.0405	0.0058
AGB 128	0.0048	0.0226	0.0274	1.4151	0.0046	0.0039	0.0157	0.011	0.0007	0.0913	0.0063
AGB 129	0.0053	0.0229	0.0379	2.8432	0.0046	0.0055	0.0176	0.0111	0.0004	0.1249	0.006
AGB 130	0.0052	0.0211	0.0158	1.1227	0.0032	0.0042	0.0191	0.0102	0.0011	0.0147	0.0053
AGB 131	0.0034	0.0192	0.023	1.2626	0.0041	0.0038	0.0177	0.0124	0.0007	0.0105	0.0084
AGB 132	0.004	0.0413	0.0344	1.0849	0.006	0.0069	0.0163	0.0145	0.0006	0.0167	0.0075
AGB 133	0.007	0.0127	0.0401	1.2817	0.0056	0.0062	0.0165	0.0145	0.0016	0.0176	0.0078

Continued on next page

Table 2 – *Continued from previous page*

Sample ID	**V**	**Cr**	**Mn**	**Fe**	**Ni**	**Cu**	**Zn**	**As**	**Se**	**Br**	**Rb**
AGB 134	0.0087	0.012	0.0111	1.201	0.0056	0.0062	0.0267	0.0252	0.0009	0.0204	0.0055
AGB 135	0.0074	0.0109	0.008	1.2151	0.0137	0.005	0.0249	0.0165	0.0009	0.0285	0.005
AGB 136	0.0014	0.0114	0.0099	3.6972	0.0113	0.0147	0.0258	0.0144	0.0006	0.0147	0.0047
AGB 137	0.0022	0.012	0.0064	2.7122	0.0102	0.0109	0.0245	0.0103	0.0007	0.0144	0.0048
AGB 138	0.0058	0.0137	0.0119	3.3734	0.0103	0.011	0.0213	0.0256	0.0085	0.0147	0.005
AGB 139	0.0038	0.0137	0.0082	4.0883	0.0107	0.0111	0.0371	0.0299	0.0081	0.0137	0.0052
AGB 140	0.0038	0.0204	0.0092	3.5938	0.01	0.011	0.0376	0.0223	0.0084	0.0093	0.0053
AGB 141	0.0038	0.011	0.1106	3.3541	0.0101	0.0106	0.0404	0.0166	0.0084	0.0124	0.0047
AGB 142	0.0038	0.011	0.0863	3.0622	0.0101	0.0116	0.04	0.0153	0.0086	0.027	0.0049
AGB 143	0.0038	0.0141	0.0934	3.2076	0.0107	0.0118	0.0377	0.0635	0.0084	0.0287	0.0047
AGB 144	0.0038	0.0105	0.0998	4.5547	0.0112	0.0143	0.0369	0.0091	0.0092	0.0165	0.0047
AGB 145	0.0037	0.0122	0.0906	4.4551	0.0104	0.0145	0.0349	0.015	0.0089	0.0139	0.0047

Table 3: Summary of daily Mass Concentration gcm^{-3} of APM in Agbogbloshie during the entire sampling period

Sample ID	**Sr**	**Zr**	**Mo**	**Pd**	**Cd**	**Sn**	**Cs**	**Ba**	**Pt**	**Hg**	**Pb**
Sample ID	Sr	Zr	Mo	Pd	Cd	Sn	Cs	Ba	Pt	Hg	Pb
AGB 1	0.0028	0.0039	0.0298	0.0341	0.0384	0.8473	0.0307	0.0437	0.0789	0.0018	0.0037
AGB 2	0.0035	0.0071	0.0327	0.0331	0.0592	0.8724	0.0591	0.0951	0.045	0.0018	0.0092
AGB 3	0.0047	0.0052	0.0285	0.0276	0.0395	0.9292	0.0439	0.0721	0.0527	0.0027	0.0044
AGB 4	0.0094	0.0049	0.0402	0.0266	0.0395	0.8331	0.0548	0.0798	0.08	0.0018	0.003
AGB 5	0.0016	0.0069	0.0289	0.0276	0.0374	0.9413	0.0635	0.0918	0.0505	0.0019	0.006
AGB 6	0.0016	0.0063	0.0318	0.0312	0.0603	0.8648	0.0493	0.0601	0.0745	0.0018	0.005
AGB 7	0.0031	0.0073	0.0298	0.0218	0.0308	0.9871	0.0428	0.0732	0.0406	0.0019	0.0032
AGB 8	0.0063	0.0053	0.035	0.0238	0.0428	0.8998	0.0384	0.0787	0.0658	0.0019	0.0033
AGB 9	0.0031	0.0018	0.0318	0.0284	0.0374	0.8823	0.046	0.0667	0.0669	0.0018	0.0029
AGB 10	0.0046	0.0021	0.0348	0.0339	0.045	1.0046	0.046	0.0929	0.0647	0.0018	0.0028
AGB 11	0.0065	0.0044	0.0378	0.0349	0.0874	0.9502	0.0634	0.0976	0.185	0.0035	0.0031
AGB 12	0.0024	0.0061	0.0318	0.0288	0.1392	1.0129	0.1343	0.2257	0.1005	0.0024	0.0036
AGB 13	0.0035	0.0073	0.0321	0.0282	0.0902	1.1546	0.0961	0.1685	0.1196	0.0024	0.0032

Continued on next page

Table 3 – *Continued from previous page*

Sample ID	**Sr**	**Zr**	**Mo**	**Pd**	**Cd**	**Sn**	**Cs**	**Ba**	**Pt**	**Hg**	**Pb**
AGB 14	0.0081	0.0052	0.0343	0.0299	0.0902	0.9148	0.1234	0.1876	0.1877	0.0024	0.0037
AGB 15	0.0044	0.0042	0.0353	0.0315	0.0847	1.1846	0.1452	0.2175	0.1142	0.0019	0.0046
AGB 16	0.0024	0.0017	0.0363	0.0287	0.142	0.9938	0.1097	0.1385	0.1741	0.0019	0.0044
AGB 17	0.0074	0.0041	0.0326	0.0331	0.0684	1.2991	0.0934	0.1712	0.0896	0.0019	0.0047
AGB 18	0.0055	0.0022	0.0322	0.0294	0.0983	1.081	0.0825	0.1848	0.1523	0.0022	0.0061
AGB 19	0.002	0.002	0.0309	0.0347	0.0847	1.0374	0.1016	0.1549	0.155	0.0018	0.0054
AGB 20	0.0036	0.0072	0.0348	0.0321	0.1038	1.3427	0.1016	0.2203	0.1496	0.0019	0.0076
AGB 21	0.0052	0.0087	0.0324	0.0282	0.0686	0.9107	0.0509	0.0769	0.1442	0.0019	0.0044
AGB 22	0.0022	0.0028	0.0325	0.0287	0.1085	0.9589	0.1054	0.1755	0.0792	0.0036	0.0045
AGB 23	0.0018	0.0085	0.0321	0.0344	0.0707	1.068	0.076	0.1315	0.0939	0.0025	0.0124
AGB 24	0.01	0.002	0.0319	0.0287	0.0707	0.8834	0.097	0.1461	0.1463	0.0022	0.0045
AGB 25	0.0047	0.0069	0.0318	0.0345	0.0665	1.0911	0.1138	0.1692	0.0897	0.0023	0.0046
AGB 26	0.0023	0.0055	0.0325	0.0355	0.1106	0.9442	0.0865	0.1084	0.1358	0.003	0.0072
AGB 27	0.0026	0.0036	0.035	0.0456	0.0539	1.1792	0.0739	0.1336	0.0708	0.0022	0.0053
AGB 28	0.0026	0.0032	0.0478	0.0382	0.077	1.0114	0.0655	0.1441	0.1191	0.0019	0.0044

Continued on next page

Table 3 – *Continued from previous page*

Sample ID	**Sr**	**Zr**	**Mo**	**Pd**	**Cd**	**Sn**	**Cs**	**Ba**	**Pt**	**Hg**	**Pb**
AGB 29	0.0024	0.0019	0.0437	0.0401	0.0665	0.9778	0.0802	0.121	0.1212	0.0019	0.0055
AGB 30	0.0024	0.0023	0.0453	0.0406	0.0812	1.2128	0.0802	0.1713	0.117	0.0018	0.0051
AGB 31	0.0024	0.002	0.033	0.0405	0.1122	1.0022	0.0799	0.1248	0.2386	0.002	0.0054
AGB 32	0.0027	0.003	0.0469	0.0463	0.1796	1.0838	0.1722	0.2917	0.1286	0.0032	0.0053
AGB 33	0.0022	0.0036	0.035	0.0369	0.1157	1.2684	0.1225	0.2172	0.1534	0.004	0.0042
AGB 34	0.0011	0.0034	0.0501	0.0389	0.1157	0.956	0.158	0.242	0.2422	0.0031	0.0043
AGB 35	0.0025	0.0035	0.0469	0.043	0.1086	1.3075	0.1864	0.2811	0.1463	0.002	0.0064
AGB 36	0.0023	0.0038	0.0499	0.0433	0.1832	1.059	0.1403	0.1781	0.2244	0.003	0.0043
AGB 37	0.0023	0.0028	0.0529	0.0431	0.0873	1.4566	0.119	0.2207	0.1144	0.0018	0.0041
AGB 38	0.0026	0.0038	0.0369	0.042	0.1264	1.1726	0.1048	0.2385	0.196	0.0024	0.0043
AGB 39	0.0023	0.0022	0.0372	0.0334	0.1086	1.1158	0.1296	0.1994	0.1996	0.002	0.005
AGB 40	0.0022	0.0025	0.0375	0.035	0.1335	1.5134	0.1296	0.2846	0.1925	0.0021	0.0063
AGB 41	0.0022	0.0041	0.0404	0.0389	0.0638	0.9005	0.0476	0.0716	0.1337	0.0024	0.0068
AGB 42	0.0023	0.0027	0.0429	0.043	0.1006	0.945	0.098	0.1626	0.0737	0.0032	0.0043
AGB 43	0.0015	0.0042	0.0413	0.0398	0.0657	1.0457	0.0709	0.1219	0.0873	0.0018	0.0016

Continued on next page

Table 3 – *Continued from previous page*

Sample ID	**Sr**	**Zr**	**Mo**	**Pd**	**Cd**	**Sn**	**Cs**	**Ba**	**Pt**	**Hg**	**Pb**
AGB 44	0.0025	0.0037	0.0381	0.0498	0.0657	0.8753	0.0902	0.1355	0.1357	0.0022	0.0015
AGB 45	0.0025	0.003	0.0352	0.0414	0.0618	1.067	0.1057	0.1568	0.0834	0.0018	0.0017
AGB 46	0.0015	0.009	0.0439	0.0388	0.1025	0.9315	0.0806	0.1006	0.126	0.0019	0.0017
AGB 47	0.0027	0.0019	0.0397	0.0349	0.0502	1.1484	0.0689	0.1239	0.066	0.0044	0.0018
AGB 48	0.0023	0.0021	0.0407	0.043	0.0715	0.9935	0.0612	0.1336	0.1105	0.0018	0.0016
AGB 49	0.0024	0.005	0.0365	0.0411	0.0618	0.9625	0.0747	0.1123	0.1124	0.0019	0.0022
AGB 50	0.0021	0.0019	0.0445	0.0433	0.0754	1.1794	0.0747	0.1587	0.1086	0.0018	0.0024
AGB 51	0.0021	0.0085	0.0433	0.0412	0.1558	1.0937	0.109	0.1728	0.333	0.0018	0.0015
AGB 52	0.0023	0.0026	0.0403	0.0422	0.2508	1.2087	0.239	0.4079	0.178	0.0025	0.0016
AGB 53	0.0025	0.0024	0.0383	0.0372	0.1608	1.4689	0.169	0.3028	0.213	0.002	0.0018
AGB 54	0.0023	0.0021	0.0423	0.0398	0.1608	1.0286	0.219	0.3379	0.338	0.0019	0.0016
AGB 55	0.0012	0.002	0.0445	0.0417	0.1508	1.5239	0.259	0.3929	0.203	0.0018	0.0045
AGB 56	0.0024	0.0041	0.0347	0.0414	0.2558	1.1737	0.194	0.2478	0.313	0.0046	0.002
AGB 57	0.0021	0.0083	0.0349	0.0413	0.1207	1.734	0.164	0.3078	0.1579	0.0026	0.0014
AGB 58	0.0024	0.0046	0.0396	0.0471	0.1758	1.3338	0.144	0.3329	0.273	0.0018	0.0025

Continued on next page

Table 3 – *Continued from previous page*

Sample ID	**Sr**	**Zr**	**Mo**	**Pd**	**Cd**	**Sn**	**Cs**	**Ba**	**Pt**	**Hg**	**Pb**
AGB 59	0.0024	0.0022	0.0376	0.0278	0.1508	1.2537	0.179	0.2778	0.278	0.0019	0.0023
AGB 60	0.0011	0.0032	0.0394	0.0298	0.1858	1.814	0.179	0.3979	0.268	0.0018	0.0018
AGB 61	0.0029	0.0061	0.0378	0.0344	0.3785	1.5613	0.2574	0.4177	0.8155	0.0018	0.0018
AGB 62	0.0023	0.0028	0.0386	0.0355	0.6145	1.8471	0.5805	1.0018	0.4303	0.0018	0.0031
AGB 63	0.0016	0.0054	0.0381	0.0356	0.3909	2.4933	0.4065	0.7408	0.5173	0.0024	0.0019
AGB 64	0.0046	0.0026	0.0378	0.0429	0.3909	1.3998	0.5308	0.8278	0.828	0.0022	0.0024
AGB 65	0.0053	0.0025	0.0381	0.0342	0.366	2.63	0.6302	0.9645	0.4925	0.0026	0.0018
AGB 66	0.0064	0.0018	0.0384	0.0358	0.627	1.7601	0.4687	0.6041	0.7658	0.0029	0.0039
AGB 67	0.0071	0.0091	0.0388	0.0374	0.2915	3.1518	0.3941	0.7532	0.3806	0.0027	0.0045
AGB 68	0.0053	0.003	0.0368	0.0423	0.4282	2.1578	0.3444	0.8154	0.6664	0.0036	0.0032
AGB 69	0.0073	0.0068	0.0437	0.0392	0.366	1.959	0.4314	0.6787	0.6789	0.0048	0.0034
AGB 70	0.0063	0.0029	0.0396	0.0492	0.453	3.3507	0.4314	0.9769	0.654	0.0038	0.0053
AGB 71	0.0027	0.0042	0.0395	0.0408	0.4753	1.7647	0.322	0.5243	1.0253	0.0051	0.0042
AGB 72	0.0072	0.0039	0.0374	0.0482	0.7727	2.1247	0.729	1.26	0.5401	0.0043	0.0036
AGB 73	0.0045	0.0025	0.039	0.0344	0.4909	2.9387	0.5098	0.9312	0.6497	0.0039	0.005

Continued on next page

Table 3 – *Continued from previous page*

Sample ID	**Sr**	**Zr**	**Mo**	**Pd**	**Cd**	**Sn**	**Cs**	**Ba**	**Pt**	**Hg**	**Pb**
AGB 74	0.0084	0.003	0.0377	0.0424	0.4909	1.5612	0.6663	1.0408	1.041	0.0062	0.0035
AGB 75	0.0021	0.0045	0.0416	0.0406	0.4596	3.1109	0.7916	1.213	0.6183	0.0052	0.0034
AGB 76	0.0051	0.0061	0.0392	0.0428	0.7883	2.0151	0.5881	0.7591	0.9627	0.0055	0.0052
AGB 77	0.0049	0.0047	0.0393	0.0407	0.3657	3.7683	0.4942	0.9469	0.4775	0.0054	0.0055
AGB 78	0.0028	0.0037	0.0375	0.0416	0.5379	2.516	0.4315	1.0252	0.8375	0.0043	0.0048
AGB 79	0.006	0.0018	0.0364	0.0372	0.4596	2.2656	0.5411	0.853	0.8531	0.0046	0.0049
AGB 80	0.0022	0.002	0.0393	0.0398	0.5692	4.0187	0.5411	1.2287	0.8218	0.0058	0.0048
AGB 81	0.0057	0.0086	0.0451	0.0343	0.4075	1.6223	0.2768	0.4497	0.8785	0.0071	0.0048
AGB 82	0.0075	0.0078	0.0368	0.0421	0.662	1.9304	0.625	1.0792	0.4633	0.0072	0.006
AGB 83	0.0058	0.0018	0.0395	0.042	0.4209	2.6269	0.4375	0.7979	0.557	0.0052	0.0051
AGB 84	0.0052	0.0022	0.0379	0.0478	0.4209	1.4482	0.5715	0.8917	0.8919	0.0136	0.0056
AGB 85	0.0058	0.0019	0.0367	0.0339	0.3941	2.7742	0.6786	1.039	0.5302	0.0062	0.0049
AGB 86	0.0032	0.0023	0.0382	0.0341	0.6754	1.8366	0.5045	0.6506	0.8249	0.0123	0.0049
AGB 87	0.0054	0.0032	0.0379	0.0356	0.3137	3.3368	0.4241	0.8113	0.4097	0.0103	0.0049
AGB 88	0.0045	0.0085	0.0382	0.0362	0.4611	2.2652	0.3705	0.8783	0.7178	0.0056	0.0049

Continued on next page

Table 3 – *Continued from previous page*

Sample ID	**Sr**	**Zr**	**Mo**	**Pd**	**Cd**	**Sn**	**Cs**	**Ba**	**Pt**	**Hg**	**Pb**
AGB 89	0.0077	0.0087	0.0444	0.0363	0.3941	2.0509	0.4643	0.731	0.7311	0.0129	0.099
AGB 90	0.0294	0.0159	0.0633	0.0444	0.4879	3.5511	0.4643	1.0524	0.7044	0.0041	0.1004
AGB 91	0.0158	0.0075	0.0663	0.0429	0.3494	1.5003	0.2381	0.3858	0.7526	0.0039	0.0988
AGB 92	0.0175	0.0089	0.0703	0.0373	0.5671	1.7639	0.536	0.9243	0.3974	0.0043	0.1003
AGB 93	0.0291	0.0089	0.0506	0.0712	0.3609	2.3597	0.3755	0.6837	0.4776	0.004	0.1016
AGB 94	0.0131	0.0069	0.0911	0.0438	0.3609	1.3514	0.4901	0.7639	0.7641	0.0039	0.1012
AGB 95	0.0129	0.0149	0.054	0.0458	0.3379	2.4857	0.5818	0.8899	0.4547	0.0037	0.0999
AGB 96	0.0116	0.0131	0.0765	0.0505	0.5786	1.6837	0.4328	0.5577	0.7068	0.0035	0.1004
AGB 97	0.0124	0.0165	0.0749	0.046	0.2692	2.9669	0.3641	0.6951	0.3516	0.004	0.1019
AGB 98	0.0126	0.0122	0.0716	0.0496	0.3952	2.0503	0.3183	0.7524	0.6151	0.0074	0.1035
AGB 99	0.0092	0.0127	0.0587	0.059	0.3379	1.867	0.3985	0.6264	0.6266	0.004	0.1133
AGB 100	0.0067	0.0149	0.0975	0.0538	0.4182	3.1502	0.3985	0.9014	0.6037	0.0028	0.1049
AGB 101	0.004	0.0202	0.0733	0.0619	0.1606	1.1038	0.1122	0.1781	0.3435	0.003	0.1063
AGB 102	0.0037	0.0064	0.0757	0.0576	0.2587	1.2226	0.2464	0.4208	0.1834	0.0025	0.1063
AGB 103	0.0091	0.0089	0.0715	0.0574	0.1658	1.4911	0.1741	0.3124	0.2196	0.0023	0.1043

Continued on next page

Table 3 – *Continued from previous page*

Sample ID	Sr	Zr	Mo	Pd	Cd	Sn	Cs	Ba	Pt	Hg	Pb
AGB 104	0.0071	0.0089	0.0653	0.0575	0.1658	1.0367	0.2258	0.3485	0.3487	0.0025	0.1122
AGB 105	0.0079	0.0094	0.0682	0.063	0.1554	1.5479	0.2671	0.4053	0.2093	0.0042	0.1105
AGB 106	0.0079	0.0033	0.054	0.052	0.2639	1.1865	0.2	0.2556	0.3229	0.0028	0.1139
AGB 107	0.0044	0.0024	0.0556	0.0465	0.1245	1.7648	0.169	0.3175	0.1628	0.0024	0.1096
AGB 108	0.0061	0.0036	0.0734	0.0475	0.1813	1.3517	0.1483	0.3433	0.2816	0.0053	0.1101
AGB 109	0.0021	0.0023	0.0573	0.0465	0.1554	1.2691	0.1845	0.2865	0.2867	0.0025	0.1123
AGB 110	0.0084	0.0078	0.0653	0.05	0.1916	1.8474	0.1845	0.4105	0.2764	0.0028	0.1176
AGB 111	0.0039	0.0031	0.0605	0.0462	0.1235	2.0503	0.5021	1.4551	0.2327	0.0114	0.1038
AGB 112	0.0038	0.009	0.0573	0.0464	0.1292	1.6632	0.3844	0.7887	0.1173	0.0032	0.1063
AGB 113	0.0052	0.0078	0.0931	0.0544	0.1653	3.4958	0.3445	0.9738	0.2089	0.0046	0.1063
AGB 114	0.0044	0.0018	0.056	0.0534	0.1621	1.5038	0.3648	0.7753	0.854	0.0127	0.1068
AGB 115	0.0023	0.0032	0.0785	0.0544	0.1837	1.6226	0.4985	0.7697	0.5876	0.0031	0.1007
AGB 116	0.0037	0.0026	0.0769	0.0464	0.0951	1.6911	0.2192	0.8399	0.7356	0.0076	0.0998
AGB 117	0.0044	0.0048	0.0737	0.0574	0.0841	0.9367	0.7633	1.0043	0.865	0.0031	0.005
AGB 118	0.0095	0.0088	0.0608	0.0572	0.1224	1.6479	0.6614	0.8823	0.7178	0.0031	0.0126

Continued on next page

Table 3 – *Continued from previous page*

Sample ID	**Sr**	**Zr**	**Mo**	**Pd**	**Cd**	**Sn**	**Cs**	**Ba**	**Pt**	**Hg**	**Pb**
AGB 119	0.0031	0.0043	0.0995	0.0732	0.0155	1.2865	0.8969	0.7823	0.6224	0.0037	0.0128
AGB 120	0.0121	0.0024	0.0753	0.0582	0.0147	2.6417	0.5909	0.6948	0.0826	0.0028	0.01
AGB 121	0.0055	0.0085	0.0763	0.0578	0.1566	1.3517	0.9157	0.8772	0.5401	0.0026	0.0096
AGB 122	0.0024	0.0027	0.0721	0.0588	0.1038	1.3843	0.77	0.1118	0.0867	0.0032	0.0112
AGB 123	0.0019	0.0022	0.0454	0.0314	0.1052	1.468	0.6799	0.5208	0.0391	0.0034	0.0097
AGB 124	0.0066	0.0025	0.0483	0.0178	0.0522	0.8761	0.0399	0.0828	0.0777	0.0024	0.0091
AGB 125	0.0103	0.0024	0.0441	0.0339	0.0816	0.9117	0.0802	0.1316	0.0605	0.004	0.005
AGB 126	0.0082	0.0073	0.0457	0.032	0.0537	0.9923	0.0585	0.0991	0.0714	0.0024	0.0051
AGB 127	0.0057	0.0076	0.0435	0.0341	0.0537	0.856	0.074	0.1099	0.0181	0.0027	0.0053
AGB 128	0.0036	0.0035	0.0473	0.0344	0.0506	1.0093	0.0864	0.127	0.0683	0.0033	0.005
AGB 129	0.0029	0.0065	0.0376	0.0332	0.0831	0.9009	0.0662	0.0821	0.1024	0.0029	0.006
AGB 130	0.0028	0.0075	0.0431	0.0333	0.0413	1.0744	0.0569	0.1006	0.0543	0.0022	0.007
AGB 131	0.0049	0.0076	0.0473	0.0362	0.0584	0.9505	0.0507	0.0884	0.09	0.0053	0.0043
AGB 132	0.0038	0.0022	0.0503	0.0318	0.0506	0.9257	0.0616	0.0913	0.0915	0.0044	0.0036
AGB 133	0.0031	0.0034	0.0533	0.0307	0.0614	1.0992	0.0762	0.0161	0.0884	0.0048	0.0034

Continued on next page

Table 3 – *Continued from previous page*

Sample ID	**Sr**	**Zr**	**Mo**	**Pd**	**Cd**	**Sn**	**Cs**	**Ba**	**Pt**	**Hg**	**Pb**
AGB 134	0.0045	0.0099	0.046	0.0326	0.0147	0.9569	0.0592	0.0132	0.0673	0.0025	0.0036
AGB 135	0.0042	0.0036	0.0363	0.0303	0.0178	1.3117	0.0655	0.0108	0.0886	0.002	0.0036
AGB 136	0.0035	0.0021	0.0466	0.0342	0.0958	1.2195	0.0822	0.013	0.054	0.0018	0.0047
AGB 137	0.0037	0.0056	0.0395	0.0268	0.1152	1.1311	0.0867	0.0128	0.0876	0.0018	0.0046
AGB 138	0.0068	0.0046	0.0405	0.0288	0.0472	0.9943	0.0841	0.0116	0.0451	0.0019	0.0049
AGB 139	0.0059	0.0022	0.0389	0.0329	0.0766	1.0729	0.0722	0.0124	0.0736	0.0021	0.0058
AGB 140	0.0048	0.0053	0.0364	0.0289	0.0459	0.9581	0.145	0.0161	0.1051	0.0022	0.0059
AGB 141	0.0042	0.0036	0.0351	0.0299	0.0469	0.9417	0.2	0.0287	0.0693	0.0018	0.0048
AGB 142	0.0041	0.0035	0.039	0.0319	0.0549	1.0105	0.1602	0.0497	0.0548	0.0019	0.0047
AGB 143	0.0042	0.0025	0.0366	0.0332	0.0803	0.8843	0.1225	0.0148	0.0601	0.0018	0.0108
AGB 144	0.0032	0.0037	0.0352	0.0348	0.042	1.068	0.1667	0.0979	0.0867	0.0018	0.0094
AGB 145	0.0063	0.0037	0.0397	0.0287	0.0335	0.9795	0.1567	0.0954	0.0844	0.0018	0.0086